FATE OF SILVER NANOPARTICLES IN SURFACE WATER ENVIRONMENTS

DISSERTATION

Presented in Partial Fulfillment of the Requirements for the Degree Doctor of Philosophy in the Graduate School of The Ohio State University

By

Xuan Li

Graduate Program in Civil Engineering

The Ohio State University

2011

Dissertation Committee:

Professor John J. Lenhart, Advisor

Professor Harold W. Walker

Professor Linda K. Weavers

Professor Nicholas T. Basta

Abstract

The widespread use of nanomaterials has the potential to adversely affect human and ecosystem health. Silver nanoparticles, as the most mass produced and utilized nanomaterials, may be released from the washing of silver-containing fabrics and food through sewage systems to natural waters. However, the fate of silver nanoparticles after entering the water environment is not clearly known. The objectives of the research were to: 1) evaluate how water chemistry, particularly concentration and valence of electrolyte, and dissolved natural organic matter affect the aggregation of silver nanoparticles, 2) elucidate how the physical and chemical properties of the silver nanoparticles, altered through the addition of different capping layers, affects their aggregation, and 3) investigate how aggregation, capping layer and environmentally-related factors, mainly sunlight irradiation affect silver release from silver nanoparticles in natural water.

To meet these objectives, a systematic investigation of the aggregation behavior and silver release of a suite of silver nanoparticles in a controlled laboratory setting was conducted. The early stage aggregation kinetics of bare silver nanoparticles (*ca.* 82 nm in diameter), as well as particles coated with a suite of stabilizing agents (Citrate, SDS and Tween) were investigated over a range of electrolyte types (NaCl, $NaNO_3$ and $CaCl_2$) and concentrations by monitoring time-rate of change of the particle hydrodynamic radius using dynamic light scattering (DLS). The electrophoretic mobility and morphologies of particles and aggregates were evaluated. Experiments were also carried out in the

presence of Nordic aquatic fulvic acid to investigate the effect of NOM on the stability of silver nanoparticles. To investigate silver release from silver nanoparticles under environmentally relevant conditions, batch experiments were conducted with bare and coated silver nanoparticles in a natural water in the presence and absence of synthetic sunlight irradiation.

The aggregation kinetic results of uncoated silver nanoparticles were consistent with classical Derjaguin-Landau-Verwey-Overbeek (DLVO) theory, although immediate dissolutions of particles were observed in all three electrolyte solutions. Critical Coagulation Concentration values were identified as 30 mM, 40 mM, and 2 mM for $NaNO_3$, NaCl, and $CaCl_2$, respectively. The dissolution of the silver nanoparticles was highly dependent on the electrolyte type and concentration. For example, the particle size was as low as ca. 40 nm in 100 mM NaCl because of instant dissolution. At the same $NaNO_3$ concentration, however, the particle size was *ca*. 50 nm. Secondary AgCl precipitates formed within the chloride-containing systems as the particles dissolved during aggregation. Aggregation of the silver nanoparticles was also examined in the presence of 10 mg l^{-1} Nordic aquatic fulvic acid and was little changed compared to that evaluated under identical fulvic acid-free conditions.

Electrophoretic mobilities of all the coated particles were less negative relative to that of bare particles, indicating a reduced electrostatic repulsion. However, the aggregation of citrate-coated particles and SDS-coated particles were very similar to that for the uncoated particles, and even that the higher concentration of SDS showed stabilizing effects to limited extent. The non-ionic steric stabilizer, Tween, significantly enhanced

stability. Critical Coagulation Concentration values were 500 mM NaCl and 700 mM $CaCl_2$ for Tween-coated particles. The dissolution of the silver nanoparticles was inhibited by the SDS and Tween coatings, but not by the citrate coating. The behavior of the Tween-coated silver nanoparticles also exhibited a dependence on electrolyte type, as its stability was greater and dissolution was lower in $NaNO_3$ than in NaCl.

In the natural water system investigated, Tween-coated particles released silver quicker than did bare- and citrate-coated particles, which rapidly aggregated. A silver concentration of 40 µg/L was reached after just 6 hours by Tween-coated particles, accounting for *ca*. 3 % of the total silver. Silver release of Tween-coated particles remained steady until Day-5, when it dropped to a plateau of *ca*. 30 µg/L. The similar levels of silver concentrations were reached in uncoated and Citrate-coated systems at the end of the 15 days, before which time they showed a steady increase from the closed to zero values at the beginning of the period of 15 days. The presence of synthetic sun light and citrate impart significant morphological changes to the particles, however, aggregation seems the controlling process in this study.

Dedication

This document is dedicated to my family.

Acknowledgments

I am heartily thankful to my supervisor, Dr. John Lenhart, for his guidance and support throughout the last three years. Without his continuous encouragement and invaluable advice, I could never finish my pursuit in three years. His forgiveness and magnanimous are the most precious lessons I have learned from him.

I would like to thank my dissertation committee members: Dr. Harold Walker, Dr. Linda Weavers, and Dr. Nicholas Basta for their helpful advice and suggestions during the years of my research projects and graduate studies. And I thank Dr. Yu-Ping Chin for his insightful guidance to my research.

My special thanks go to Mr. Richard Montione and Brian Kemmenoe at Campus Microscopy & Imaging Facility for their support on the TEM/SEM imaging, and Dr. Yun Wu at Nanotech West for her assistance on the Zeta potential analysis in this research. My appreciation also goes to my previous advisors, Dr. Guibai Li and Guoren Xu at Harbin Institute of Technology. They led me to the door, showing a whole new world to me. I also thank Dr. Jun Ma, Nanqi Ren, Shuili Yu, Yongpeng Xu, Mingren Sun, Lixin Sun, Chunmei Lv at Harbin Institute of Technology for their support during my graduate study.

I would also like to thank former and current lab-mates (Jung Ju Lee, Ziqi He, Yu Sik Hwang, Jason Cheng, Dong Chen, Ping Sun, Limei Yang, Mengling Stuckman, Qianheng Wang, Ruiyang Xiao, Rachael Pasini, Yuan Gao, and Qing Ye, Zongsu Wei,

Tingting Yin, Andrea Mobley, Brittnee Halpin, Chenyi Yuan, David Diaz-rivera, Jnq Tan, Kamau Mbalia, Lauren Corrigan, Lauren Czaplicki, Maryam Ansari, Matthew Noerpel, Meiqiang Cai, Michael Brooker, Russell Stech, Shuai Liu, Xiaoying Song, Yen-Ling Liu, Yingying He, Zuzana Bohrerova, Katie Kinstedt, Maureen Langlois, Alex Anderson) for their friendship and the wonderful time we had together in the lab and office. My gratitude extends to my friends at the Ohio State University: Nengmou Wang, Chongtao Ge, Qin Wu, Ming Sheng, Zeng Zhang, Xiaojia Zhao, Junkun Wan, Hao Wang, Tian Luo, Gang Wang, Li Zhou, Charlie Maxwell, Anh-Minh Nguyen, Aya Aho Matsuda, Greg Roth, Patrick McAloon, Haixin He, Yang Xing, Yang Yang, Di You, Yan Liu, Qingpeng Niu, Guangdong Liu; my colleagues Peng Yi at John Hopkins University, Renzun Zhao at Virginia Tech, Yuanyuan Liu at UIUC, Jie Ma at Rice University, Hong Luo at Arizona State University, Rong Yu at Clemson University, Xianyu Meng at Utah State University, Dr. Kai Li at Stanford University, Dr. Zhen Li at U.S.EPA, Dr. Yi Wang at ZymaX Forensics Isotope, Yunzhou Chai at Dow, Huifeng Shan at CH2M Hill, Jing Zhou at AECOM, Phil Tang at Vironex, Yinan Qi at Black&Veatch; my best friends Lei Yang, Xi Chen, Yunhui Chen, Saifeng Chen, Jianyu Wang, Xue Wang, in China, and those who are not listed here, for their friendship. My life in Columbus has been joyful and rich through getting to know them.

Last but not least, I would like to express my sincere appreciation to my parents. I do not think that I can compensate my absence for such a long time. Thanks to their love and selfless support, I could pursue my dream. You are my world. And, I especially thank my

girlfriend, who never appeared in the past three years. So I can concentrate on my research and finish my degree so soon.

This research has been supported by the U.S. National Oceanic and Atmospheric Administration through its Ohio Sea Grant College Program. Support from the Thomas Ewing French Fellowship Fund for me is also gratefully acknowledged.

Vita

2001.....B.S. Water Supply and Drainage Engineering, Harbin Institute of Technology

2007.....M.S. Municipal Engineering, Harbin Institute of Technology

2008 to present.....Graduate Researching Associate, The Ohio State University

Publications

Li, X.; Lenhart, J.J. "Ion Release Kinetics and Stability of Coated Silver Nanoparticles in Surface Water" (Manuscript in Preparation)

Li, X.; Lenhart, J.J.; Walker, W.W. "Aggregation Kinetics and Dissolution of Coated Silver Nanoparticles", Langmuir (In Press)

Li, X.; Lenhart, J.J.; Walker, W.W. "Dissolution-Accompanied Aggregation Kinetics of Silver Nanoparticles", Langmuir, 2010, 26 (22), 16690

Fields of Study

Major Field: Civil Engineering

Table of Contents

List of Tables

List of Figures

Chapter 1. Introduction and Background

1.1 Problem Statement and Motivation

Nanoscience and nanotechnology involve the synthesis, assembly, manipulation and application of materials on the nanometer-scale level that spans approximately 1 to 100 nm at two- or three-dimensions [1-2]. The rapid development of the nanotechnology industry has introduced nanomaterials into many aspects of our daily life [3-4]. Manufactured nanoparticles are utilized more than any other nanomaterial in a variety of areas including pharmaceuticals, cosmetics, electronics, optical devices, environmental remediation, catalysis chemistry and material sciences due to the relative ease with which they can be prepared [5-7]. Nanoparticles are distinguished from compositionally-identical material of larger-size by not only their high surface area but also their unique and high reactivity, tunable electronic and optical properties, broad-spectrum antibacterial properties, and, most important, their ability to be manipulated at near atomic scales [8-10]. Nanoparticles are produced by a huge range of methods [4] that can generally be ascribed to two categories, top-down approaches, such as milling or attrition, repeated quenching and photolithography, and bottom-up approaches, such as chemical reactions, nucleation and growth processes [11]. The chemical composition of nanoparticles is as varied as their manufacturing methods. In general, nanoparticles are categorized into carbon-based materials such as fullerenes and carbon nanotubes and inorganic nanoparticles including the ones based on metal oxides (e.g., zinc oxide, iron

oxide, titanium dioxide and cerium oxide), metals (gold, silver and iron) and quantum dots (cadmium sulfide and cadmium selenide) [12]. Of these, metallic nanoparticles are of particular interest because of their potential function in sensing, catalysis, transport, and other applications in biological and medical sciences [12].

Although the promise of nanotechnology to improve our quality of life seems bright and unlimited, it is inevitable that some portion of these manufactured materials will be introduced into the environment [3, 13-14]. Nanomaterials may enter and accumulate in air, water, soil, or organisms from point sources such as factories or landfills, as well as from nonpoint sources, such as wet deposition from the atmosphere, storm-water runoff, and attrition from nanomaterial-containing products [13-14]. Among the likely route of discharge of nanomaterials into the environment, the release of commercial nanoparticles into natural waters through the discharge of treated municipal sewage attracts the most concern [15]. After entering a water body, the fate of these nanomaterials depends upon transport (aggregation, deposition, adsorption, bioaccumulation) and transformation (oxidation, reduction, dissolution, bio- and UV-degradation) processes. The impact of these processes on determining nanomaterial fate is currently poorly understood. In addition, the risk posed by such materials to human health and the environment is unclear, although preliminary evidence exists to suggest certain nanomaterials may harm people, organisms or the environment [14, 16]. Thus, there is a critical need for laboratory based studies addressing ecotoxicological effects and environmental transport of nanomatierials.

Among the commonly used nanomaterials currently raising public concerns to environmental and human health risks, metallic silver nanoparticles (Ag(0)) are given special attention because of their fast application in more commercial products than any other nanomaterial [17-18]. Silver nanoparticles are being mass produced and utilized in hundreds of commercially available products (e.g., biomedical devices, water and air filters, foodware, electronic appliances, cosmetics, clothing, and numerous household products) due to their broad-spectrum antimicrobial properties and lower propensity to induce microbial resistance than other antibiotics[4, 19]. In addition to products exploiting their antimicrobial properties, silver nanoparticles are also widely used in catalysis, optics and other areas due to their unique size-dependent optical, electrical and magnetic properties [20].

The widespread use of silver nanomaterials has the potential to adversely affect human and ecosystem health. Silver nanoparticles may be released to the environment directly from products containing silver nanoparticles, such as colloidal silver medicine [21]. The discharge of silver nanoparticles into sewage systems from the washing of silver-containing fabrics and food containers has been experimentally confirmed [15] and could be a significant source should nanosilver-containing products see widespread commercial success. Their potential introduction and predicted environmental concentrations (PEC) in the wastewater and subsequently surface waters and drink water systems have been estimated based on probabilistic materials flow analysis from a life-time perspective of nanosilver-containing products. Those predicted environmental concentrations have been confirmed as risks to aquatic organisms when compared to toxic levels reported in similar

ecotoxicological studies [22-23]. However, the fate of silver nanoparticles after entering the natural environment is not clearly known. How silver nanoparticles behave in the natural environment and how this behavior poses a risk to human and ecosystem health has become an urgent issue that needs to be tackled.

1.1.1 Toxicity of silver nanoparticles

Although specific knowledge of the toxicity of silver nanoparticles to humans and ecosystems is lacking, many are concerned that widespread utilization of silver nanoparticles represents a potential human and ecosystem hazard [22-23]. What is known is that silver nanoparticles are effective biocides against a wide range of bacteria, fungi and viruses [15]. Toxicity of silver nanoparticles to cells from higher-order life such as zebra fish, clams, rats, and even humans has been reported [16]. The only negative effect reported for humans is skin discoloration [24].

Publications investigating the toxic effects of silver nanoparticles are numberless. However, no consistent agreement about the antimicrobial mechanism of silver nanoparticles has been reached, and contradictory findings are routinely reported [20]. Among the commonly proposed mechanisms resulting in the antimicrobial ability of nanosilver are [25]: (1) uptake of the released silver ions from silver nanoparticles, (2) generated reactive oxygen species (ROS) from silver nanoparticles and silver ions, and (3) cell membrane damage caused by direct interaction of silver nanoparticles.

The oxidative dissolution of silver nanoparticles releases free silver ions into solution. The amount of the silver ion released varies from 3 % of the total silver content to complete dissolution, depending on the solution chemistry [26-31]. Uptake of silver ions

and its following interaction with respiratory and transport proteins disrupts these critical pathways due to the high affinity of Ag^+ with thiol (-SH) groups present in the corresponding proteins [32-35]. The link between the toxicity of silver nanoparticles and the released silver ions has been investigated in several studies [19, 36], in which Ag^+ binding ligands (e.g., Cl^- and cysteine,) were used to complex released silver ions from silver nanoparticles. The toxicity of silver nanoparticles in the presence of Cl^- or cysteine is lower, suggesting the silver ion is the major cause of their antimicrobial activity.

Reactive oxygen species (ROS) produce oxidative stress resulting in membrane lipid and DNA damage [37]. While the source of ROS is unclear, it could result from impairment of the antioxidant defenses of the cells and subsequent accumulation of metabolism-generated ROS, or from directly generated ROS from silver nanoparticles and silver ions [25, 27, 38-42]. Either way, the result is that the escalated concentration of intracellular EOS results in membrane protein damage and/or DNA damage. Silver nanoparticles can attach to bacterial cell membranes and, depending upon particle size, can subsequently penetrate directly into the cells [25, 27, 36, 42-44]. Once inside the cell, damage can occur via ROS generation or ionic silver via the mechanisms previously described.

1.1.2 Environmental fate of silver nanoparticles

It is currently unclear how the chemical and physical processes that control the fate of silver nanoparticles after discharge into the natural environment also affect their toxicity. Although the literature investigating the antimicrobial effects of silver and nanosilver are numerous, only recently have studies attempting to characterize the fate of silver nanoparticles in the natural environment been published[31, 45-50]. A table summarizing

these studies, highlighting the investigated system, including the type of silver nanoparticles and the matrix, as well as major reached conclusions are summarized in Table 1.1.

Table 1.1 Recent advances in environmental fate studies of silver nanoparticles

Source(s)	Silver nanoparticles	Matrix	Phenomenon investigated	Key aspects
Li et al.[45-46]*	Bare, citrate-, SDS-, Tween-coated	Simple electrolyte solution	Aggregation kinetics	Aggregation of bare particles is consistent with DLVO theory.
El Badawy et al.[47]	Bare, citrate-, PVP-, BPEI-coated	Simple electrolyte solution	Aggregation stabilities	Sterically stabilized particles possess the best stability in simple electrolyte solution.
Huynh and Chen[49]	Citrate-, PVP-coated	Simple electrolyte solution, humic acid	Aggregation kinetics	Humic acid and PVP coatings can stabilize particles sterically.
Liu and Hurt[31]	Citrate-coated	Deoxygenated DI water, simple electrolyte solution, humic and fulvic acid, sea water	Silver ion release	High pH, electrolyte-induced aggregation and presence of NOM can decrease the silver ion release.
Jin et al.[48]	Manufactured	Complicated synthetic fresh water	Aggregation stabilities and toxicity	Aggregation stability and toxicity of silver nanoparticles highly depends on electrolyte composition.
Liu et al.[50]	Gum Arabic- and PVP-coated	DI water	Aggregation stabilities under sunlight exposure	Sunlight exposure can induce aggregation of sterically stabilized particles without precipitation occurred.
Scheckel et al. [51]	Bare and unknown organic coating**	Simple electrolyte solution with Kaolin	Speciation and chemical transformation on the water-kaolin interface	Silver nanoparticles remain unchanged in $NaNO_3$ but AgCl formed in the presence of NaCl

*The second and third chapters of this dissertation

**Detailed information about the organic coating was not released because of commercial confidentiality

After entering the water system, the transport of nanoparticles highly depends on whether they remain suspended in, or removed by the processes, such as aggregation, precipitation, adsorption and dissolution, from the water column [52-53]. Of all the processes examined (Table 1.1), aggregation of silver nanoparticles appears to strongly influence other processes, including precipitation, adsorption and dissolution, and thus is particularly important in determining the transport of the particles in aquatic systems. Knowledge of the aggregation stability of manufactured nanoparticles (e.g., silver nanoparticles) is primarily based on extensive studies and established theory for natural colloids, (i.e., mineral, organic or biological particles with size ranging from about 1 nm to 1 μm) [54-59]. These studies utilize particle size change rates for mono-dispersed colloid systems aggregating in solutions of simple electrolytes in order to characterize aggregation stabilities [59]. To interpret these results, the classic Derjaguin-Landau-Verwey-Overbeek (DLVO) theory [57-58] of colloidal stability is often adopted. This theory describes the force between surfaces of charged particles interacting in a liquid medium as a combination of van der Waals attraction, the sum of the forces resulting from the interaction of adjacent dipoles, and electrostatic repulsion of the double layer of counterions. The surface of metal oxide develops a charge as surface groups dissociate in the presence of water. This results in the subsequent development of a surface potential, which is balanced by the layer of counterions. Summing this electrostatic double layer force and the van der Waals attraction force allows for an estimation of the interaction energy. In a dilute system, particles of like charge are electrostatically stabilized as an energy barrier is formed when the repulsive electrostatic interactions are in excess of the

attractive van der Waals interactions. Under this condition, aggregation is confined or limited to very slow rate and the particles in the system stay suspended for a relatively long term. This energy barrier is disrupted by adding electrolytes into the system which screen the surface charge and decrease the surface potential of particles, subsequently increasing the probability that interacting particles can attach [59]. When sufficient electrolyte is present to eliminate the energy barrier, rapid aggregation occurs with the particle size change with time nearly independent of the electrolyte concentration.

In addition to van der Waals attraction and electrostatic repulsion, additional interfacial forces that influence colloid stability originate from the use of an engineered coating layer or adsorbed natural organic matter (NOM). Coating layers are adopted to protect the nanoparticles from aggregation during their synthesis and application [60]. These capping layers enhance particle stability mainly via the introduction of steric forces imparted by the presence of molecules extending from the paticles' surface or electrostatic repulsion imparted by the attachment of molecules with highly charged functional groups. Typical capping agents adopted to stabilize nanoparticles can be small ionic molecules, surfactants or polymers. Adsorbed small ionic molecules can form a charged layer that increases repulsive electrostatic interactions between particles. Adsorbed surfactant and polymer molecules impart extra stability through steric repulsion, as well as electrostatic repulsion if they are ionic. The molecules comprising the coating layers can be designed with a high charge density or increased steric interaction and thus nanoparticles with such coating layers can be stabilized in aquatic environment longer than bare particles, ranging from 24 hours to greater than 30 days [61].

Natural organic matter (NOM), which is ubiquitous in natural water systems, comes from the degradation of plants and animals in the environment. NOM, such as humic acid and fulvic acid are large polymeric molecules with phenolic and carboxylic groups, providing the molecules with a negative charge when dissolved in water. NOM molecules adsorb to the surface of nanoparticles and enhance their stability through either increased electrostatic repulsion or steric repulsion [62-65]. The extra stability resulting from the adsorption of NOM molecules to the particles' surface facilitates their dispersion allowing them to remain longer in the water system without being removed.

1.1.3 Environmental conditions affecting the toxicity of silver nanoparticles

The aggregation behavior of silver nanoparticles not only affects their stability in the natural waters, it also affects their toxicity [44, 66]. Several factors influence silver nanoparticle toxicity including particle size, shape, crystallinity, surface chemistry, and coating layers, as well as environmental factors such as pH, ionic strength, and the presence of complexing agents and NOM [26-27, 44, 66-67]. These factors can be classified into three categories: 1) factors associated with the properties of the particle itself that decide the silver ion release rate, such as particle size, shape, crystallinity and surface chemistry; 2) factors that influence the silver release and direct contact of particles with target microorganisms through influencing their aggregation state, such as pH, ionic strength, NOM and coating layers; and 3) factors that influence the concentration of released silver ion, such as complexing agents and other ligands that can associate with free silver ions in natural waters. In addition to the factors listed above, morphological changes in silver nanoparticles via the photochemical reduction of silver

ions by sunlight irradiation also contributes to affect their stability and subsequently their toxicity [50, 68-73].

Over the past few decades, the aggregation behavior of a variety of nanoparticles with/without coating layers has been extensively investigated in systems with monovalent electrolytes, divalent electrolytes, and natural organic matter [62-63, 74-77]. However, comparable studies investigating the aggregation behavior of silver nanoparticles are limited [45-47, 49, 66]. Of those publications, only one case investigated the aggregation kinetics of silver nanoparticles [49]. One of the key mechanisms for silver nanoparticles to exert biocidal activity has been confirmed to be due to the release of silver ions. Water chemistry factors that affect the silver ion release from silver nanoparticles, such as pH, dissolved oxygen, complexing agents and natural organic matter have been studied under specific experimental conditions [19, 26, 78-79]. However, research investigating the link between the aggregation state of silver nanoparticles and silver ion release in complex environmental conditions is limited [31].

1.2. Research Objectives

The results of previous studies clearly indicate that aggregation behavior of silver nanoparticles may be similar to that for other nano-sized colloid systems. Extra electrostatic repulsion and steric repulsion can be imparted to stabilize the silver nanoparticles by including engineered capping agents or dissolved natural organic matter, such as humic acid and fulvic acid. Silver release through partial oxidation and dissolution is considered a major pathway for silver nanoparticles to exert bactericidal

effects, however, the relationship between environmentally relevant factors and silver release remain unclear.

Based on this, the objectives of the research were to:

1) Evaluate how water chemistry, mainly concentration and valence of electrolyte, as well as dissolved natural organic matter affect the aggregation of silver nanoparticles.

2) Elucidate how the physical and chemical properties of the silver nanoparticles, altered through the addition of different capping layers, affects their aggregation.

3) Investigate how aggregation, capping layer and environmentally-related factors, mainly sunlight irradiation affect silver release from silver nanoparticles in natural water.

To meet these objectives, a systematic investigation of the aggregation kinetics of a suite of silver nanoparticles in a controlled laboratory setting was conducted. The silver nanoparticles used in this research were synthesized following the protocol described by Kvítek et al. [66]. The early stage aggregation kinetics of bare silver nanoparticles, as well as particles coated with a suite of stabilizing agents were investigated over a range of electrolyte types and concentrations by monitoring time-rate of change of the particle hydrodynamic radius using dynamic light scattering (DLS). The electrophoretic mobility of the particles through the same processes was also measured. Morphologies of particles and aggregates were evaluated using transmission electron microscopy (TEM). Experiments were also carried out in the presence of Nordic aquatic fulvic acid to investigate the effect of NOM on the stability of silver nanoparticles. To investigate silver release from silver nanoparticles under environmentally relevant conditions, batch

experiments were conducted with bare and coated silver nanoparticles in a natural water in the presence and absence of synthetic sunlight irradiation.

1.3. Dissertation Overview

The dissertation has three main chapters, three of which are manuscripts published or accepted in peer reviewed journals (Chapters 2 and 3) and in preparation for submittal to a peer reviewed journal (Chapter 4). The dissertation thus contains 5 chapters including the introduction and background (Chapter 1) and conclusions and further work (Chapter 5).

Chapter 2 is entitled "Dissolution-Accompanied Aggregation Kinetics of Silver Nanoparticles". It was published in *Langmuir* (2010) volume 22 by Xuan Li, with co-authors John J. Lenhart and Harold W. Walker. The manuscript describes experimental results conducted to evaluate the early stage aggregation kinetics of bare silver nanoparticles over a range of electrolyte types (NaCl, $NaNO_3$ and $CaCl_2$) and concentrations. Effects of natural organic matter to this process were also investigated by introducing Nordic aquatic fulvic acid to the system. Dr. Harold W. Walker in the Department of Civil and Environmental Engineering and Geodetic Science at Ohio State University contributed with the important editorial suggestions to the theoretical concept of DLVO theory and aggregation kinetics in the final manuscript.

Chapter 3, "Aggregation Kinetics and Dissolution of Coated Silver Nanoparticles" was accepted by *Langmuir* and is authored by Xuan Li, John J. Lenhart and Harold W.

Walker. As an extension of the first manuscript, this manuscript further investigated aggregation kinetics of silver nanoparticles coated with several types of representative capping agents under the same aquatic chemistry condition. The aggregation rates of coated particles were normalized by that of bare particles to evaluate the extra stabilization effects of capping agents.

Chapter 4, "Ion Release Kinetics and Stability of Coated Silver Nanoparticles in Surface Water" is in preparation for submittal to *Environmental Science and Technology* by Xuan Li and John J. Lenhart. The chapter describes the significance of capping agents and aggregation status in affecting the silver release of silver nanoparticles. Natural water from the Olentangy River was selected as the matrix to conduct the batch experiment for 15 days. Daily synthetic sunlight irradiation of eight hours was provided by a Xe ozone-free lamp to investigate effects of sunlight to silver release. Aggregation behavior was interpreted by both dynamic light scattering (DLS) data and transmission electron microscopy (TEM) images collected from the systems.

Finally, the conclusions of this study and recommendations for future work are summarized in Chapter 5.

References

[1] Rotello, V.M., *Nanoparticles : building blocks for nanotechnology*. 2004, New York: Kluwer Academic/Plenum Publishers. 284 p.

[2] Rosi, N.L. and C.A. Mirkin, *Nanostructures in Biodiagnostics.* Chemical Reviews, 2005. **105**(4): p. 1547-1562.

[3] Colvin, V.L., *The potential environmental impact of engineered nanomaterials.* Nature Biotechnology, 2003. **21**(10): p. 1166-1170.

[4] Maynard, A., et al., *Safe handling of nanotechnology.* Nature, 2006. **444**(7117): p. 267-269.

[5] Niemeyer, C.M., *Nanoparticles, proteins, and nucleic acids: Biotechnology meets materials science.* Angewandte Chemie-International Edition, 2001. **40**(22): p. 4128-4158.

[6] Poole, C.P. and F.J. Owens, *Introduction to nanotechnology*. 2003, Hoboken, NJ: J. Wiley. xii, 388 p.

[7] Schmid, G., *Nanoparticles : from theory to application*. 2nd ed. 2010, Weinheim: Wiley-VCH. xiii, 522 p.

[8] Banfield, J.F. and H.Z. Zhang, *Nanoparticles in the environment.* Nanoparticles and the Environment, 2001. **44**: p. 1-58.

[9] Guzman, K.A.D., M.R. Taylor, and J.F. Banfield, *Environmental risks of nanotechnology: National nanotechnology initiative funding, 2000-2004.* Environmental Science & Technology, 2006. **40**(5): p. 1401-1407.

[10] Sweet, L. and B. Strohm, *Nanotechnology - Life-cycle risk management.* Human and Ecological Risk Assessment, 2006. **12**(3): p. 528-551.

[11] Cao, G., *Nanostructures & nanomaterials : synthesis, properties & applications*. 2004, London: Imperial College Press. xiv, 433 p.

[12] Ju-Nam, Y. and J.R. Lead, *Manufactured nanoparticles: An overview of their chemistry, interactions and potential environmental implications.* Science of the Total Environment, 2008. **400**(1-3): p. 396-414.

[13] Wiesner, M.R. *Responsible development of nanotechnologies for water and wastewater treatment*. in *3rd IWA Leading-Edge Conference Water and Wastewater Treatment Technologies*. 2005. Sapporo, Japan.

[14] Wiesner, M., et al., *Assessing the risks of manufactured nanomaterials.* Environmental Science & Technology, 2006. **40**(14): p. 4336-4345.

[15] Benn, T.M. and P. Westerhoff, *Nanoparticle silver released into water from commercially available sock fabrics.* Environmental Science & Technology, 2008. **42**(11): p. 4133-4139.

[16] Hussain, S., et al., *In vitro toxicity of nanoparticles in BRL 3A rat liver cells.* Toxicology in Vitro, 2005. **19**(7): p. 975-983.

[17] Kim, J.S., et al., *Antimicrobial effects of silver nanoparticles.* Nanomedicine-Nanotechnology Biology and Medicine, 2007. **3**(1): p. 95-101.

[18] Tolaymat, T.M., et al., *An evidence-based environmental perspective of manufactured silver nanoparticle in syntheses and applications: A systematic review and*

critical appraisal of peer-reviewed scientific papers. Science of the Total Environment, 2010. **408**(5): p. 999-1006.

[19] Navarro, E., et al., *Toxicity of Silver Nanoparticles to Chlamydomonas reinhardtii.* Environmental Science & Technology, 2008. **42**(23): p. 8959-8964.

[20] Marambio-Jones, C. and E.M.V. Hoek, *A review of the antibacterial effects of silver nanomaterials and potential implications for human health and the environment.* Journal of Nanoparticle Research, 2010. **12**(5): p. 1531-1551.

[21] Rejeski, D., *Nanotechnology and consumer products.* 2009; Available from: http://www.nanotechproject.org/publications/archive/nanotechnology_consumer_products/.

[22] Mueller, N.C. and B. Nowack, *Exposure modeling of engineered nanoparticles in the environment.* Environmental Science & Technology, 2008. **42**(12): p. 4447-4453.

[23] Gottschalk, F., et al., *Modeled Environmental Concentrations of Engineered Nanomaterials (TiO2, ZnO, Ag, CNT, Fullerenes) for Different Regions.* Environmental Science & Technology, 2009. **43**(24): p. 9216-9222.

[24] Brandt, D., et al., *Argyria secondary to ingestion of homemade silver solution.* Journal of the American Academy of Dermatology, 2005. **53**(2, Supplement): p. S105-S107.

[25] Hwang, E.T., et al., *Analysis of the Toxic Mode of Action of Silver Nanoparticles Using Stress-Specific Bioluminescent Bacteria.* Small, 2008. **4**(6): p. 746-750.

[26] Lok, C.N., et al., *Silver nanoparticles: partial oxidation and antibacterial activities.* Journal of Biological Inorganic Chemistry, 2007. **12**(4): p. 527-534.

[27] Choi, O., et al., *The inhibitory effects of silver nanoparticles, silver ions, and silver chloride colloids on microbial growth.* Water Research, 2008. **42**(12): p. 3066-3074.

[28] Blaser, S.A., *Environmental risk analysis for silver-containing nanofunctionalized products* 2006, Swiss Federal Institute of Technology (ETHZ): Zurich.

[29] Blaser, S.A., et al., *Estimation of cumulative aquatic exposure and risk due to silver: Contribution of nano-functionalized plastics and textiles.* Science of the Total Environment, 2008. **390**(2-3): p. 396-409.

[30] Kumar, R., S. Howdle, and H. Munstedt, *Polyamide/silver antimicrobials: Effect of filler types on the silver ion release.* Journal of Biomedical Materials Research Part B-Applied Biomaterials, 2005. **75B**(2): p. 311-319.

[31] Liu, J.Y. and R.H. Hurt, *Ion Release Kinetics and Particle Persistence in Aqueous Nano-Silver Colloids.* Environmental Science & Technology, 2010. **44**(6): p. 2169-2175.

[32] Ratte, H., *Bioaccumulation and toxicity of silver compounds: A review.* Environmental Toxicology and Chemistry, 1999. **18**(1): p. 89-108.

[33] Hiriart-Baer, V.P., et al., *Toxicity of silver to two freshwater algae, Chlamydomonas reinhardtii and Pseudokirchneriella subcapitata, grown under continuous culture conditions: Influence of thiosulphate.* Aquatic Toxicology, 2006. **78**(2): p. 136-148.

[34] Wood, C.M., R.C. Playle, and C. Hogstrand, *Physiology and modeling of mechanisms of silver uptake and toxicity in fish.* Environmental Toxicology and Chemistry, 1999. **18**(1): p. 71-83.

[35] Liau, S.Y., et al., *Interaction of silver nitrate with readily identifiable groups: relationship to the antibacterial action of silver ions.* Letters in Applied Microbiology, 1997. **25**(4): p. 279-283.

[36] Smetana, A.B., et al., *Biocidal Activity of Nanocrystalline Silver Powders and Particles.* Langmuir, 2008. **24**(14): p. 7457-7464.

[37] Kim, S.K., et al., *Investigation of jumbo squid (Dosidicus gigas) skin gelatin peptides for their in vitro antioxidant effects.* Life Sciences, 2005. **77**(17): p. 2166-2178.

[38] Carlson, C., et al., *Unique Cellular Interaction of Silver Nanoparticles: Size-Dependent Generation of Reactive Oxygen Species.* The Journal of Physical Chemistry B, 2008. **112**(43): p. 13608-13619.

[39] Yoon, J., et al., *Silver-ion-mediated reactive oxygen species generation affecting bactericidal activity.* Water Research, 2009. **43**(4): p. 1027-1032.

[40] Inoue, Y., et al., *Bactericidal activity of Ag–zeolite mediated by reactive oxygen species under aerated conditions.* Journal of Inorganic Biochemistry, 2002. **92**(1): p. 37-42.

[41] Yoon, K.Y., et al., *Antimicrobial Effect of Silver Particles on Bacterial Contamination of Activated Carbon Fibers.* Environmental Science & Technology, 2008. **42**(4): p. 1251-1255.

[42] Choi, O. and Z.Q. Hu, *Size dependent and reactive oxygen species related nanosilver toxicity to nitrifying bacteria.* Environmental Science & Technology, 2008. **42**(12): p. 4583-4588.

[43] Sondi, I. and B. Salopek-Sondi, *Silver nanoparticles as antimicrobial agent: a case study on E-coli as a model for Gram-negative bacteria.* Journal of Colloid and Interface Science, 2004. **275**(1): p. 177-182.

[44] Morones, J.R., et al., *The bactericidal effect of silver nanoparticles.* Nanotechnology, 2005. **16**(10): p. 2346-2353.

[45] Li, X.A., J.J. Lenhart, and H.W. Walker, *Aggregation Kinetics and Dissolution of Coated Silver Nanoparticles.* Langmuir, (In Press).

[46] Li, X.A., J.J. Lenhart, and H.W. Walker, *Dissolution-Accompanied Aggregation Kinetics of Silver Nanoparticles.* Langmuir, 2010. **26**(22): p. 16690-16698.

[47] El Badawy, A., et al., *Impact of Environmental Conditions (pH, Ionic Strength, and Electrolyte Type) on the Surface Charge and Aggregation of Silver Nanoparticles Suspensions.* Environmental Science & Technology, 2010: p. 1260-1266.

[48] Jin, X., et al., *High-Throughput Screening of Silver Nanoparticle Stability and Bacterial Inactivation in Aquatic Media: Influence of Specific Ions.* Environmental Science & Technology, 2010. **44**(19): p. 7321-7328.

[49] Huynh, K.A. and K.L. Chen, *Aggregation Kinetics of Citrate and Polyvinylpyrrolidone Coated Silver Nanoparticles in Monovalent and Divalent Electrolyte Solutions.* Environmental Science & Technology, 2011: p. null-null.

[50] Liu, J., et al., *Toxicity Reduction of Polymer-Stabilized Silver Nanoparticles by Sunlight.* Journal of Physical Chemistry C, 2011. **115**(11): p. 4425-4432.

[51] Scheckel, K.G., et al., *Synchrotron Speciation of Silver and Zinc Oxide Nanoparticles Aged in a Kaolin Suspension.* Environmental Science & Technology, 2010. **44**(4): p. 1307-1312.

[52] Klaine, S.J., et al., *Nanomaterials in the environment: Behavior, fate, bioavailability, and effects.* Environmental Toxicology and Chemistry, 2008. **27**(9): p. 1825-1851.

[53] Barcelo, D., et al., *Fate and toxicity of emerging pollutants, their metabolites and transformation products in the aquatic environment.* Trac-Trends in Analytical Chemistry, 2008. **27**(11): p. 991-1007.

[54] Omelia, C.R., *Particle Particle Interactions in Aquatic Systems.* Colloids and Surfaces, 1989. **39**(1-3): p. 255-271.

[55] Stumm, W., L. Sigg, and B. Sulzberger, *Chemistry of the solid-water interface : processes at the mineral-water and particle-water interface in natural systems*. 1992, New York: Wiley. x, 428 p.

[56] Buffle, J., et al., *A generalized description of aquatic colloidal interactions: The three-colloidal component approach.* Environmental Science & Technology, 1998. **32**(19): p. 2887-2899.

[57] Derjaguin B. V., L., L. D., *Theory of the stability of strongly charged lyophobic sols and of the adhesion of strongly charged particles in solutions of electrolytes.* Acta Physiconchim, 1941. **14**: p. 733-762.

[58] Verwey E. J. W., O.J.T.G., *Theory of the stability of lyophobic colloids*. 1948, Amsterdam: Elsevier.

[59] Elimelech, M.G., J.; Jia, X.; Williams, R. J., *Particle Deposition & Aggregation: Measurement, Modelling and Simulation*. 1995, Oxford: Butterworth-Heinemann.

[60] Cushing, B.L., V.L. Kolesnichenko, and C.J. O'Connor, *Recent advances in the liquid-phase syntheses of inorganic nanoparticles.* Chemical Reviews, 2004. **104**(9): p. 3893-3946.

[61] Pal, T., T.K. Sau, and N.R. Jana, *Reversible formation and dissolution of silver nanoparticles in aqueous surfactant media.* Langmuir, 1997. **13**(6): p. 1481-1485.

[62] Chen, K.L., S.E. Mylon, and M. Elimelech, *Aggregation kinetics of alginate-coated hematite nanoparticles in monovalent and divalent electrolytes.* Environmental Science & Technology, 2006. **40**(5): p. 1516-1523.

[63] Chen, K.L. and M. Elimelech, *Influence of humic acid on the aggregation kinetics of fullerene (C-60) nanoparticles in monovalent and divalent electrolyte solutions.* Journal of Colloid and Interface Science, 2007. **309**(1): p. 126-134.

[64] Chen, K.L., S.E. Mylon, and M. Elimelech, *Enhanced aggregation of alginate-coated iron oxide (hematite) nanoparticles in the presence of calcium, strontium, and barium cations.* Langmuir, 2007. **23**(11): p. 5920-5928.

[65] Mylon, S.E., K.L. Chen, and M. Elimelech, *Influence of natural organic matter and ionic composition on the kinetics and structure of hematite colloid aggregation: Implications to iron depletion in estuaries.* Langmuir, 2004. **20**(21): p. 9000-9006.

[66] Kvitek, L., et al., *Effect of surfactants and polymers on stability and antibacterial activity of silver nanoparticles (NPs).* Journal of Physical Chemistry C, 2008. **112**(15): p. 5825-5834.

[67] Pal, S., Y.K. Tak, and J.M. Song, *Does the antibacterial activity of silver nanoparticles depend on the shape of the nanoparticle? A study of the gram-negative bacterium Escherichia coli.* Applied and Environmental Microbiology, 2007. **73**(6): p. 1712-1720.

[68] Wodka, D., et al., *Photocatalytic activity of titanium dioxide modified by silver nanoparticles.* ACS Appl Mater Interfaces, 2010. **2**(7): p. 1945-53.

[69] Callegari, A., D. Tonti, and M. Chergui, *Photochemically grown silver nanoparticles with wavelength-controlled size and shape.* Nano Letters, 2003. **3**(11): p. 1565-1568.

[70] Torigoe, K. and K. Esumi, *Preparation of Bimetallic Ag-Pd Colloids from Silver(I) Bis(Oxalato)Palladate(Ii).* Langmuir, 1993. **9**(7): p. 1664-1667.

[71] Shahverdi, A.R., et al., *A sunlight-induced method for rapid biosynthesis of silver nanoparticles using an Andrachnea chordifolia ethanol extract.* Applied Physics a-Materials Science & Processing, 2011. **103**(2): p. 349-353.

[72] Maillard, M., P.R. Huang, and L. Brus, *Silver nanodisk growth by surface plasmon enhanced photoreduction of adsorbed [Ag+]*. Nano Letters, 2003. **3**(11): p. 1611-1615.

[73] Ahern, A.M. and R.L. Garrell, *Insitu Photoreduced Silver-Nitrate as a Substrate for Surface-Enhanced Raman-Spectroscopy.* Analytical Chemistry, 1987. **59**(23): p. 2813-2816.

[74] Lecoanet, H.F., J.Y. Bottero, and M.R. Wiesner, *Laboratory assessment of the mobility of nanomaterials in porous media.* Environmental Science & Technology, 2004. **38**(19): p. 5164-5169.

[75] Lecoanet, H.F. and M.R. Wiesner, *Velocity effects on fullerene and oxide nanoparticle deposition in porous media.* Environmental Science & Technology, 2004. **38**(16): p. 4377-4382.

[76] Brant, J., H. Lecoanet, and M.R. Wiesner, *Aggregation and deposition characteristics of fullerene nanoparticles in aqueous systems.* Journal of Nanoparticle Research, 2005. **7**(4-5): p. 545-553.

[77] Hyung, H., et al., *Natural organic matter stabilizes carbon nanotubes in the aqueous phase.* Environmental Science & Technology, 2007. **41**(1): p. 179-184.

[78] Fabrega, J., et al., *Silver Nanoparticle Impact on Bacterial Growth: Effect of pH, Concentration, and Organic Matter.* Environmental Science & Technology, 2009. **43**(19): p. 7285-7290.

[79] Damm, C. and H. Munstedt, *Kinetic aspects of the silver ion release from antimicrobial polyamide/silver nanocomposites.* Applied Physics a-Materials Science & Processing, 2008. **91**(3): p. 479-486.

Chapter 2. Dissolution-Accompanied Aggregation Kinetics of Silver Nanoparticles

(Langmuir, 2010, **26**(22): p. 16690-16698)

Abstract

In this study, bare silver nanoparticles with diameters of 82±1.3 nm were synthesized by the reduction of the $Ag(NH_3)_2^+$ complex with D-maltose and their morphology, crystalline structure, UV-vis spectrum and electrophoretic mobilities were determined. Dynamic Light Scattering was employed to assess early-stage aggregation kinetics by measuring the change in the average hydrodynamic diameter of the nanoparticles with time over a range of electrolyte types (NaCl, $NaNO_3$ and $CaCl_2$) and concentrations. From this the Critical Coagulation Concentration values were identified as 30 mM, 40 mM, and 2 mM for $NaNO_3$, NaCl, and $CaCl_2$, respectively. Although the silver nanoparticles were observed to dissolve in all three electrolyte solutions, the aggregation results were still consistent with classical Derjaguin-Landau-Verwey-Overbeek (DLVO) theory. The dissolution of the silver nanoparticles, which were coated with a layer of Ag_2O, was highly dependent on the electrolyte type and concentration. In systems with Cl^- a secondary precipitate, likely AgCl, also formed and produced a coating layer that incorporated the silver nanoparticles. Aggregation of the silver nanoparticles was also examined in the presence of Nordic aquatic fulvic acid and was little changed compared to that evaluated under identical fulvic acid-free conditions. These results provide a

fundamental basis for further studies evaluating the environmental fate of silver nanoparticles in natural aquatic systems.

2.1. Introduction

Nanomaterials have been introduced into our daily activities and while the promise of nanotechnology to improve our quality of life seems unlimited, at the same time it is inevitable that some portion of these manufactured materials will be introduced into the environment [1-3]. One of the likely routes of introduction will occur as commercial nanomaterials are released into natural waters as a waste stream component. Nanoparticulate silver, for example, is increasingly being used in a variety of commercial settings [4], many of which could result in the release of nanosilver [5]. After entering an aquatic system, its fate, like other particles, depends upon whether it remains suspended in solution, or whether processes that effect particle aggregation or dissolution remove it from the water column. The risk posed by such materials to human health and the environment is currently unclear, but preliminary evidence exists to suggest certain nanomaterials such as nano-silver may harm people, organisms or the environment [3, 6-8].

Although there exists many potentially harmful nano-materials [8-9] nano-silver is unique in that it is already widely employed in a host of commercially available products such as textiles, food containers, home appliances, and even dietary supplements, within which the well known anti-microbial effect of silver is exploited [4, 10]. This effect is thought to result from the dissolution of the silver, which releases Ag^{+} ions at a rate that

depends on solution chemistry [8-9, 11]. Toxicity of ionic silver to microorganisms and higher aquatic life forms has been extensively studied with the mode of toxic effect related to cell inactivation resulting from the interaction of Ag^+ ions with proteins and enzymes through specific cell-membrane functional groups like thiol (-SH) [12-15]. Toxicity of the silver nanoparticles to bacteria has also recently been investigated, but it isn't clear whether the mechanism can be attributed to a property specific to nano-silver or just to the effects of Ag^+ ions [16-22]. For example, silver nanoparticles were recently shown to be toxic to the freshwater algae, *Chlamydomonas reinhardtii* [10]. Toxicity resulting from ionic silver produced by the dissolving nano-silver was implicated, but by itself it could not account for all of the toxic effects [10]. Since the uptake of dissolved silver by bacteria and other aquatic organisms is greatly affected by silver speciation (e.g., free ion or complex) [23-24], it is therefore critically important to know not only the behavior and the fate of silver nanoparticles themselves, but also the species that evolve from the aggregation, dissolution and aqueous reactions that occur after the particles are discharged to natural water environments.

The aggregation and deposition kinetics of a variety of nanoparticles have been extensively studied in systems with monovalent electrolytes, divalent electrolytes, and natural organic matter [25-30]. In most cases, the classic Derjaguin-Landau-Verwey-Overbeek (DLVO) theory of colloidal stability [31-32] has been satisfactorily applied to explain the aggregation behavior of these nanoparticles in the presence of simple electrolytes, which induce aggregation by screening the surface charge [33]. Natural organic matter (NOM), which is ubiquitous in natural waters has been shown to adsorb to

the surface of nanoparticles, enhancing their stability via either steric or electrostatic repulsion [28-29, 34-35]. Enhanced aggregation is also reported in certain systems when intermolecular bridging of humic acid macromolecules occurs in the presence of multivalent cations such as Ca^{2+} [34]. Among the extensive literature describing colloid aggregation kinetics, however, there is little information regarding silver nanoparticles, with only a few recent papers evaluating their fate in surface water [36-37].

The objective of this study was to investigate the early stage aggregation kinetics of silver nanoparticles in the presence of common electrolytes at neutral pH. This was done by measuring the rate of change of the particle hydrodynamic radius using Dynamic Light Scattering (DLS) over a range of electrolyte types (NaCl, $NaNO_3$ and $CaCl_2$) and concentrations. The effects of fulvic acid, which is often the most significant class of natural organic matter in surface waters [38], on aggregation were also investigated. Aggregate structure and morphology was evaluated using transmission electron microscopy (TEM). For all three electrolytes, our results indicate that particle aggregation, accompanied by dissolution and for NaCl the formation of a secondary precipitate, occurred at environmentally-relevant electrolyte concentrations. The existence of adsorbed fulvic acid was found to have no obvious effects on aggregation as little change was observed in the CCC.

2.2. Experimental Section

2.2.1 Materials.

$AgNO_3$ (99.8%) and D-maltose (99%) were purchased from Sigma-Aldrich as powder and were used without further purification. Ammonium hydroxide (trace metal grade)

was purchased from Fisher Scientific. All other reagents were analytical grade or better. The electrolyte solutions (NaCl, $NaNO_3$ and $CaCl_2$), buffer solution ($NaHCO_3$), and reagents employed were prepared using deionized water (Milli-Q, Millipore) with a resistivity of 18.2 MΩ·cm. Solutions were filtered through 0.1 μm cellulose ester membranes (Millipore) before use. Experiments with fulvic acid used a standard Nordic aquatic fulvic acid purchased from the International Humic Substance Society (IHSS). All labware and glassware were thoroughly cleaned before use with 10% nitric acid, followed by a thorough rinse with deionized water and oven-drying under dust-free conditions.

2.2.2 Synthesis and dialysis of silver nanoparticles.

Silver nanoparticles were synthesized by the reduction of the $[Ag(NH_3)_2]^+$ complex with D-maltose following the method described by Kvítek et al. [39]. In short, 2 mL of 0.01 mol L^{-1} silver nitrate was pipetted into a 50 mL glass beaker. To this 10 mL of a 0.02 mol L^{-1} ammonia solution was added and the solution was subsequently stirred with a magnetic stir bar. 250 μl of 0.1 mol L^{-1} sodium hydroxide was then added to adjust the solution pH value to 11.5, after which 8 mL of 0.025 mol L^{-1} D-maltose was introduced into the system to reduce the formed $Ag(NH_3)_2^+$ complex to form metallic silver nanoparticles. The synthesis process required 15 minutes and was conducted in the dark at a room temperature of 22 ± 1 °C.

The freshly synthesized, orange-colored silver nanoparticle suspension was dialyzed using cellulose ester membranes (Spectra/Por® Biotech) with a molecular weight cut off (MWCO) of 8-10 kDa and deionized water as the dialysate solvent over a period of 24

hours. The deionized water dialysate was periodically changed (typically a minimum of 4 times) and its conductivity and total organic carbon (TOC) content were measured to ensure that residual ions and D-maltose were removed. The TOC concentration and conductivity were measured using a TOC analyzer (TOC-5000A, Shimadzu Corp.) and zeta potential analyzer (ZetaPALS, Brookhaven Instruments Corp.), respectively. For the aggregation and electrophoretic mobility determinations, five such batches of silver nanoparticles were synthesized and combined to form a 100 mL stock suspension, which was stored in a polypropylene bottle in the dark at 4 °C. The concentration of this stock suspension was determined by gravimetric analyses to be 31.6 mg L^{-1}. The aggregation and electrophoretic mobility studies were conducted within one week after the synthesis of this silver nanoparticle stock suspension. Loss of particles during this time was on the order of 1 – 2 percent. Before each analysis, the working solutions were sonicated for 5 seconds in an ultrasonic water bath.

The size, morphology, crystallinity, and UV-vis absorbance of the silver nanoparticles were characterized. The hydrodynamic diameter and UV-vis analyses were conducted on a sample prepared by diluting an aliquot of the stock suspension 25 times in a sodium bicarbonate – sodium chloride buffer solution that fixed the final solution pH at 7.0 ± 0.3 and ionic strength at 1 mM. The hydrodynamic diameter was measured using Dynamic Light Scattering (DLS) (90Plus, Brookhaven Instruments Corp., Holtsville, NY). UV-vis absorption spectra were collected over a wavelength range of 200 to 700 nm using a Shimadzu UV-4201PC UV-vis spectrophotometer. The crystalline nature of the particles

was evaluated using a Philips CM-200 TEM equipped with a light element EDS X-ray detector.

2.2.3 Aggregation Kinetics.

For all aggregation experiments, the silver nanoparticle stock suspension was diluted 25 times in a 5.0×10^{-2} mM sodium bicarbonate buffer at pH 7.0 ± 0.3 and the resulting suspension was briefly sonicated in an ultrasonic water bath. Three mL of this silver nanoparticle solution was introduced into a disposable acrylic cuvette which was thoroughly rinsed with deionized water. A pre-calculated amount of electrolyte solution was then added into the cuvette to obtain the desired electrolyte concentration. Finally, the cuvette was covered with a plastic lid and quickly hand-shaken before being inserted into the DLS sample holder. Measurements were started immediately and the change in the average hydrodynamic diameter was recorded over 15 minutes at a time interval of 90 seconds. The initial particle size during the aggregation experiments was determined based upon a backwards extrapolation (to time zero) of the linearly increasing trend in particle size with time. All aggregation experiments were conducted at a temperature of 22 ± 0.5 °C.

The initial change in the average hydrodynamic radius of the silver nanoparticles with time (dr/dt) induced by the different electrolyte solutions was calculated and related to the experimental aggregation rate constant (k_{exp}) using the following expression [40]:

$$k_{exp} = \frac{1}{\alpha N r_0} \cdot \frac{dr}{dt} \quad (1)$$

where N is the initial particle concentration, r_0 is the initial particle radius, and α is an optical factor. The value of k_{exp} was calculated by conducting a linear least squares regression analysis to the initial change in hydrodynamic radius with time (dr/dt). The aggregation kinetics were characterized by determining the inverse stability ratio "1/W", which was calculated by dividing the rate of change in the hydrodynamic radius for a given experiment condition (k_{exp}) to the rate of change for rapid aggregation (k_{rapid}), or diffusion-limited aggregation, which is independent of the electrolyte concentration:

$$\frac{1}{W} = \frac{k_{\mathrm{exp}}}{k_{\mathrm{rapid}}} \tag{2}$$

The initial particle concentration N, and initial particle radius r_0 in both the given experimental condition and diffusion-limited aggregation were the same and thus cancelled out. Values used for k_{rapid} were determined for each electrolyte system from the average value of the k_{exp} values in the diffusion-limited aggregation regime.

2.2.4 Electrophoretic Mobilities.

The electrophoretic mobility of the silver nanoparticles was measured at a temperature of 22 ± 0.5 °C across the pH range 4.0 to 10.0 in 1 mM NaCl with a Brookhaven Instrument Corp. ZetaPALS Instrument. Measurements were also collected across the range of electrolyte concentrations employed in the aggregation experiments. Error estimates were based on ten measurements conducted on five separate samples for each solution condition.

2.2.5 Effect of Fulvic Acid on the Stability of Silver Nanoparticles.

A 100 mg L^{-1} fulvic acid stock solution was prepared by dissolving 100 mg of the Nordic fulvic acid into one liter of deionized water. To ensure dissolution, the solution was

stirred overnight. The fulvic acid solution was subsequently filtered with a 0.2 μm PTFE membrane (Millipore). The resulting solution had a TOC concentration of 44.5 mg C L^{-1} and was stored in the dark at 4 °C with an unadjusted pH value of 5.5.

Fulvic acid coated silver nanoparticles were prepared by equilibrating 1 mL of the fulvic acid stock solution with 9 mL of the silver nanoparticle stock suspension in 50 mL polycarbonate ultracentrifuge tubes. Sodium chloride and sodium hydroxide were added as needed to achieve an ionic strength of 1 mM and pH of 7.0 ± 0.3, respectively. The tubes were sealed and slowly shaken for 24 hours in the dark at room temperature. The resulting suspensions were analyzed using the same procedures described above, except a different dilution was adopted in order to obtain the same initial particle concentration as that studied in the absence of fulvic acid. The fulvic acid adsorption density of 15 mg-C/g-nanoparticle was determined upon analyzing the TOC concentration in the supernatant collected after centrifuging (Legend^{TM} RT, Kendro Laboratory Products) a parallel set of samples at 16,000g for 40 min.

2.2.6 Transmission Electron Microscopy.

The size and morphology of dispersed and aggregated silver nanoparticles were observed by transmission electron microscopy using a Technai G2 Spirit TEM at 120 kV. Samples were prepared and equilibrated for 15 minutes in a glass bottle on undiluted stock solutions of the silver nanoparticles at the same solution condition as those employed in the aggregation experiments. One drop of resulting suspension was transferred onto a 100 mesh copper grid and dried within 10 minutes under blowing nitrogen. Images were collected using a digital camera at magnifications that ranged from 71,000 to 144,000.

We did not make an effort to preserve the aggregates and thus the sizes of those imaged were not necessarily representative of those found in the suspensions. Nevertheless, the particle morphology should be preserved.

2.3. Results and Discussion

2.3.1 Characterization of Silver Nanoparticles.

The hydrodynamic particle diameter measured from DLS was 82.0 ± 1.3 nm. TEM images verified the spherical and monodisperse nature of the silver nanoparticles and confirmed the size, with a mean diameter of *ca*. 82 nm resulting from the average of visual measurements of the particles captured in a representative TEM image (Figure 2.1a). Based on this size, the measured suspension concentration (31.6 mg L^{-1}) and a density of metallic silver (10.5 g cm^{-3}), the particle concentration of the silver nanoparticle stock suspension was calculated as 1.1×10^{10} particles mL^{-1}. Based on the 25 times dilution, suspensions utilized in the aggregation tests had a particle concentration of 4.4×10^{8} particles mL^{-1}. The electron diffraction pattern (inset to Figure 2.1a) was consistent with that expected for metallic silver.

The UV-vis absorption spectrum (Figure 2.1b) of the suspension showed a maximum absorption peak at a wavelength of 446 nm, consistent with the reported location of the surface plasmon absorption band of silver nanoparticles synthesized in this manner [20]. The position and width of the plasmon band in the UV-vis absorption spectrum of the silver nanoparticles depends on the size and polydispersity of the particles as well as the presence on the surface of the particles of adsorbed substances or an oxidation layer [41-45]. In general, mono-dispersed silver nanoparticles under 100 nm in size with no

adsorbed substances (i.e. ions and/or surfactants) or oxidized surface layer have a narrow surface plasmon adsorption peak at a wavelength of 390 to 450 nm that varies with particle size. The existence of an oxidized surface layer on the particle results in a red-shift in the position and a broadening of the peak [43, 45-48]. No procedures were undertaken to control the atmosphere during particle synthesis or dialysis and therefore the resulting silver nanoparticles likely had an oxidized surface layer particularly since UV-vis results presented in the literature for non-oxidized 82 nm silver nanoparticles lie at lower wavelength [44, 47], which is consistent with classical Mie theory [49-50]. Thus, we attribute the observed red-shift and breadth of the UV-vis absorption peak relative to that expected for uncoated metallic silver nanoparticles to the existence of an oxidized layer on the surface of our particles.

2.3.2 Aggregation of Silver Nanoparticles in the Presence of Sodium Chloride.

The aggregation rates of silver nanoparticles in NaCl exhibit DLVO-type behavior (Figure 2.2a). At low NaCl concentrations (10, 20 and 40 mM), each increase in the electrolyte leads to a corresponding increase in the aggregation rate until a concentration of 40 mM NaCl was reached. Above this concentration, the aggregation rate only slightly increased as the maximum aggregation rate was attained.

Evident in the aggregation profile was a decrease in the initial particle size at the beginning of the aggregation process, which is defined here as the value determined at time equal to zero based upon a linear fit to the time-rate of change of the hydrodynamic diameter measured during each aggregation kinetics experiment. This decrease in particle size likely reflects dissolution of the silver nanoparticles in the presence of Cl^-. For

example, within 15 min after the addition of NaCl, the particle diameter in the presence of very low concentration of NaCl (e.g., 10 mM NaCl, see Figure 2.2) remains at *ca.* 82 nm, equal to the average particle diameter measured in the absence of electrolyte. At 20 mM NaCl, however, the initial particle diameter decreased to 73.5 nm and over time it slightly increased as aggregation occurred. Further increases in NaCl concentration lead to a smaller initial particle and at 100 mM NaCl a minimum initial particle diameter of 40 nm was observed (see Figure 2.3). Above this concentration, the initial size stabilized or slightly increased. It should be noted that before starting the DLS measurements that approximately 10 seconds were required to mix the silver nanoparticle suspension and electrolyte solution after they were transferred into the cuvette. Considering how quickly the change in size occurred, slight differences in the timing of this mixing procedure likely produced differences in the measured initial particle size. The classical approach to calculate the inverse stability ratio using equation (2) relies on a constant initial particle radius r_0, which was not observed for our systems. Thus, even though the initial particle size in some systems decreased from that observed in the stock suspension, we still adopt equation (3) and fix r_0 at 82 nm in order to calculate nominal k_{exp} and $1/W$.

Despite the decreased initial size of the silver nanoparticles, a typical stability profile characterized by two regimes consistent with DLVO colloidal theory was observed (Figure 2.4). Within the reaction-limited regime at low NaCl concentrations ($1/W < 1$) the stability of the particles decreased with increasing NaCl. Under these conditions, increasing the electrolyte concentration leads to a corresponding increase in aggregation rate by diminishing the electrostatic energy barrier to aggregation that exists between the

negatively charged silver nanoparticles. When the electrolyte concentration reaches and exceeds the critical coagulation concentration (CCC) at $1/W$ of 1 sufficient electrolyte was present to eliminate the energy barrier resulting in rapid aggregation. Above the CCC, diffusion-limited aggregation occurs and the rate of change of the hydrodynamic radius was nearly independent of the electrolyte concentration. The CCC was determined as approximate 40 mM NaCl for our silver nanoparticles at pH 7.0 (see Figure 2.4).

2.3.3 Dissolution of Silver Nanoparticles in the Presence of Sodium Chloride.

As stated earlier, elemental silver is sensitive to the presence of oxidants and under oxygenated conditions Ag^0 at the nanoparticle surface can be oxidized to Ag_2O

$$2Ag^0 + 1/2O_2 = Ag_2O(s) \quad (4)$$

which forms an oxidized layer surrounding the particle [8, 43, 45, 48, 51]. Evidence of the oxide layer exists in the UV-vis spectrum of our particles shown in Figure 2.1b and it dissolves to release ionic silver as follows:

$$Ag_2O(s) + H_2O = 2Ag^+ + 2OH^- \quad (5)$$

In a dilute aqueous suspension of silver nanoparticles at equilibrium with atmospheric oxygen, but lacking other electrolytes, dissolution of the surface layer of Ag_2O is hindered due to the adsorption and accumulation of Ag^+ at the particle surface [41, 46-

47]. Consistent with this was our observation of little change measured in the size of the stock silver nanoparticles for periods approaching 2 weeks (Figure A.S1).

The observed decrease in the initial size of the silver nanoparticles in the presence of sodium chloride, which averaged *ca.* 20%, occurred soon after the addition of NaCl (Figure 2.2a). This rapid dissolution likely reflects a shift in the dissolution of Ag_2O described in equation (5) due to changing ionic strength as well as a redistribution in the adsorbed Ag^+. However, the potential for Cl^- to catalyze oxidative corrosion of the silver particles as described by Henglein and co-workers [41, 43, 46-47] cannot be ruled out.

Released Ag^+ ions from the silver nanoparticles can react with Cl^- ions, forming AgCl(s):

$$Ag^+ + Cl^- \rightarrow AgCl(s) \qquad (6)$$

Although the concentration of released Ag^+ ions was not measured, we estimate the potential for formation of solid AgCl as high based upon its reported solubility constant ($K_{sp} = 1.77 \times 10^{-11}$) [52] and the relatively high Cl^- concentration of 0.02 M present when the obvious size decrease was first observed. The precipitated AgCl can form on or deposit to the nanosilver particles and it appears to dramatically alter the particle morphology as TEM images for samples with high concentrations of NaCl (Figure 2.5a) depict partially dissolved silver nanoparticles adhered to each other and forming aggregates of irregular shape and size. The smooth surface of the adhered nanoparticles can be attributed to the AgCl precipitate and throughout the imaged sample no distinct separation was observed between the particles or within the aggregates. Evidence exists

in a similar system in which the formation of AgCl precipitate on the surface of silver nanoparticles in the presence of NaCl was confirmed by X-ray diffraction [36]. Thus, in the presence of NaCl dissolution and aggregation of the silver nanoparticles appears to occur simultaneously with the formation of AgCl precipitate.

2.3.4 Aggregation of Silver Nanoparticles in the Presence of Sodium Nitrate.

Aggregation was also evaluated in $NaNO_3$, which should not produce a secondary precipitate under the conditions studied. Similar to the results obtained in systems with NaCl, $NaNO_3$-induced aggregation also shows dominant DLVO-type tendencies (Figure 2.2b). A decrease in the initial particle size was also observed for $NaNO_3$, to an extent that exceeded that observed in NaCl. This was particularly evident at electrolyte concentrations lower than 50 mM (Figure 2.3). For example, the average particle size in 10 mM $NaNO_3$ was approximately 5 nm lower than that observed in 10 mM NaCl. As in systems with Cl^-, this decrease in particle size likely results from the dissolution of Ag_2O upon perturbation of the solution chemistry as well as nitrate-promoted oxidative corrosion. The trend reversed at electrolyte concentrations above 50 mM, however, where the initial particle size in the presence of $NaNO_3$ was significantly larger than that in the presence of NaCl.

In the presence of $NaNO_3$, the aggregated silver nanoparticles exhibited an open fractal structure (Figure 2.5b) characteristic of aggregates formed under favorable conditions. This is consistent with previous observations for other nano-sized metal and metal-oxide particles like gold and hematite [28, 53] (Figure 2.5b). The average diameter of 73 nm, estimated from the TEM image, confirmed that the dissolution of the silver nanoparticles

also occurred in the presence of $NaNO_3$. The amorphous features observed in systems with NaCl, likely formed of precipitated AgCl, was not observed as the silver nanoparticles showed a relatively uniform size and shape with no evidence of secondary precipitates.

Interestingly, the distinct differences in the systems observed in the TEM images for the NaCl and $NaNO_3$ systems brought no obvious changes to the aggregation kinetics. As shown in Figure 2.4, typical two-regime, DLVO-type aggregation kinetics was observed in the relationship of $1/W$ with $NaNO_3$ concentration. The CCC for the silver nanoparticles in $NaNO_3$ was approximately 30 mM at pH 7.0, which was only slightly lower than the value of 40 mM observed in NaCl (Figure 2.4).

2.3.5 Aggregation of Silver Nanoparticles in the Presence of Calcium Chloride.

The aggregation of silver nanoparticles was examined in systems with calcium chloride ranging from 0.5 mM to 10 mM. Stability followed trends observed with NaCl and $NaNO_3$ (Figure 2.4) and as expected, the CCC in $CaCl_2$ was lower (2 mM). This was consistent with the Schulze-Hardy rule [33] which predicts a ratio of CCC_{Na}/CCC_{Ca} of z^6 for particles with large zeta potentials, where z is the valence of the calcium counterion (i.e., z=2), and CCC_{Na}/CCC_{Ca} of z^2 for particles with small zeta potentials [54]. Our data showed a ratio of 20, proportional to $z^{4.32}$ which is an appropriate value when compared to similar studies employing nano-sized iron oxide particles [34-35] and reflects a modification of the surface due to the adsorption of cations. Particle dissolution was also observed in $CaCl_2$ as evident in the decrease in the initial particle size (Figure 2.3) and it occurred at lower concentrations than that observed in systems with monovalent

electrolytes. In this case, an initial particle size of 54.8 nm was observed even at a low $CaCl_2$ concentration of 1.5 mM (Figure A.S2). This suggests that Ca^{2+} might have exchanged with Ag^+. Since Ag^+ is believed to inhibit dissolution [46], the presence of excess Ca^{2+} at the interface appears to allow dissolution of the oxide-coated particle at lower electrolyte concentrations. Similar processes involving the adsorption of multivalent cations are thought to be responsible for controlling mineral dissolution in natural systems [55].

2.3.6 Changes in Electrophoretic Mobility of Silver Nanoparticles Induced by Electrolytes.

Theoretically, oxide-layer free bare silver nanoparticles suspended in deionized water should have a surface charge of zero. The observed negative potential and mobility of silver nanoparticles in previous studies reflects the presence of the oxidized layer [56-58]. Furthermore, the adsorption of hydroxide and/or other anions also imparts a negative surface charge that varies with pH and electrolyte concentration. The resulting electrostatic force can stabilize the particles and prevents aggregation. Added electrolytes balance and screen this surface charge and induce destabilization and aggregation.

Zeta potentials of the silver nanoparticles were measured at different pH values and electrophoretic mobility values were measured across a wide range of electrolyte concentrations. The zeta potential of silver nanoparticles at neutral and high pH values (6.0 - 10.0) remained unchanged at -45.8 ± 0.9 mV (Figure 2.6a), consistent with results reported for particles synthesized in this manner [59]. With decreasing pH, the zeta potential increases, but even at pH 4.0 it remained negative.

The electrophoretic mobilities of the particles across a range of electrolyte concentrations at pH=7.0±0.3 are presented in Figure 2.6b. The electrophoretic mobilities at NaCl concentrations lower than the CCC (40 mM NaCl) were near -4.70×10^{-8} m^2/V-s and slowly increase to less negative values with increasing NaCl concentration. Above the CCC, the electrophoretic mobility increases with increasing NaCl concentration from approximately -4.70×10^{-8} m^2/V-s at 40 mM NaCl to -1.50×10^{-8} m^2/V-s at 300 mM NaCl. This behavior differs from that reported for nano-sized metal oxides, such as hematite or carbon-based nanomaterials such as fullerene (C_{60}), in which a continuous increase in the electrophoretic mobility (or zeta potential) with increasing electrolyte concentration is reported at electrolyte concentrations lower than the CCC [35, 60]. A similar trend was observed when $NaNO_3$ was used as the electrolyte, although the average electrophoretic mobilities were approximately 20% less negative. The zeta potential of AgCl is more negative than nanosilver [36] and thus the lower mobility values in systems with NaCl may reflect the presence of AgCl precipitates on the particle surfaces. Consistent with the results presented by Chen et al. [60] for hematite, $CaCl_2$ sharply increased the electrophoretic mobility of the silver nanoparticles, presumably due to the adsorption of Ca^{2+} at the nanoparticle surface [33].

2.3.7 Effects of Fulvic Acid on the Aggregation and Electrophoretic Mobility of Silver Nanoparticles.

The addition of 10 mg/L of fulvic acid had no noticeable effect on the aggregation kinetics of the silver nanoparticles (Figure 2.7). This corresponds to a TOC concentration of about 4.5 mg L, which is typical of natural waters [61]. The particles did adsorb

approximately 15 mg fulvic acid as C per gram of nanoparticle, however, the CCC values in NaCl, $NaNO_3$ and $CaCl_2$ were 40, 30 and 1.5 mM (Figure 2.7), which was very similar to the CCCs observed in the absence of fulvic acid. This result differs from other studies in which the stabilizing effect of adsorbed NOM and consequent increase in CCC was observed in systems with hematite, magnetite, latex, and clay particles [33, 35, 62-65].

The average size of the silver nanoparticles in the presence of fulvic acid and little added electrolyte remained at 82 nm. This was the same value as that for the particles in the absence of fulvic acid as any increase in the hydrodynamic size of the silver nanoparticles due to the adsorbed fulvic acid macromolecules is difficult to detect by DLS [35, 66]. Figure 2.8a shows a TEM image of the silver nanoparticles in the presence of fulvic acid with 1 mM NaCl. Similar to the DLS measurements, no change in the particle size was observed. In most instances the images showed discrete particles, however, in some instances the particles merged into larger structures, suggesting portions of the fulvic acid could have promoted dissolution in a manner analogous to that observed with chloride. This seems reasonable since fulvic acids are complex and heterogeneous mixtures of molecules [67], and some of these molecules could likely promote catalyzed oxidation and particle dissolution.

Upon the addition of electrolyte (NaCl, $NaNO_3$ or $CaCl_2$), the silver nanoparticles underwent an initial decrease in particle size prior to aggregation (Figure 2.9) similar to the extent of that observed in the absence of fulvic acid (Figure 2.3). Comparing results in Figure 2.3 and 2.9 did not provide evidence of any significant influence of fulvic acid

on the initial particle size across the range of electrolyte types and concentrations examined, but some slight differences were evident.

The electrophoretic mobility of the silver nanoparticles with increasing NaCl or $NaNO_3$ in the presence of fulvic acid is compared with those obtained in the absence of fulvic acid in Figure 2.10. For both NaCl and $NaNO_3$ fulvic acid produced a slight increase in particle mobility. This differs with reported trends where fulvic acid coated particles typically show a more negative electrophoretic mobility value [63, 65, 68]. For most research working on magnetite, hematite and TiO_2 nanoparticles with circum-neutral to slightly basic values of pH_{pzc}, the electrophoretic mobility at pH 7 decreases from positive to negative after adsorption of NOM [35, 62-64], stabilizing the particles through the resulting electrostatic repulsive force. However, in the present research, the particle mobility resulting after the adsorption of the fulvic acid was less negative than that of the bare silver nanoparticles (Figure 2.10). Pelley and Tufenkji [69] report a similar result for latex microspheres in the presence of Suwannee River humic acid and attribute it to a moderation of the surface potential to one that approximates that of the adsorbed organic matter. Similar results showing that particle mobility is dominated by adsorbed organic matter is reported by Beckett and Le [70]. It is also possible upon adsorption that the fulvic acid disrupts the oxide layer and therefore alters the particle electrophoretic mobility. Nevertheless, in the presence of adsorbed fulvic acid, substantial electrostatic repulsive interactions remain and little change was observed in the particle stability. Similar results evaluating particle stability or transport indicate that the small size of fulvic acid results in little impact on particle stability or transport. Larger molecular

weight humic acids, however, appear to have more of an impact on particle stability [71-72].

The introduction of fulvic acid into systems with NaCl introduced nebulous features near or around the particles (Figure 2.8b). These features likely represent fulvic acid-AgCl precipitates formed from the dissolution of silver nanoparticles, since these features were not observed in systems with $NaNO_3$ and fulvic acid (Figure A.S3). Extensive dissolution of the silver nanoparticles occurred in 100 mM NaCl and the resulting aggregates appeared semi-transparent due to more extensive contributions from the AgCl-fulvic acid precipitates (Figure 2.8c). In 200 mM NaCl, further dissolution of the particles was observed (Figure 2.8d). The resulting particles and aggregates were sensitive to exposure to the TEM electron source and over time they would fade from view. For example, the image in 200 mM NaCl (Figure 2.8d) was digitally recorded 20 seconds after the electron source was directed onto the target area and upon continued exposure the features gradually vanished.

2.4. Conclusion

Mono-dispersed silver nanoparticles were synthesized with a negatively charged oxide layer. Their early stage aggregation kinetics induced by common electrolytes at neutral pH in the absence and presence of fulvic acid was investigated. A dissolution-accompanied aggregation was observed in the presence of NaCl, $NaNO_3$ and $CaCl_2$. Although the initial particle size decreased because of dissolution immediately after the addition of the electrolyte, the increase in hydrodynamic radius over time followed expected trends for early-stage aggregation in the presence of electrolytes. The

dissolution of silver nanoparticles likely results from electrolyte-induced perturbations in the concentration of adsorbed Ag^+ which seems to inhibit dissolution of the surface oxide layer. Despite the decrease of the particle size at the beginning of the aggregation caused by dissolution, the aggregation behavior of silver nanoparticles was consistent with classical DLVO theory. The CCC for silver nanoparticles was determined as 40 mM NaCl, 30 mM $NaNO_3$ and 2 mM $CaCl_2$. AgCl precipitates formed within the chloride-containing systems as the particles dissolved during aggregation. The resulting particles and aggregates were characterized by having smooth continuous surfaces with little evidence of separate particles. The absence of a comparable precipitate in systems with $NaNO_3$ resulted in aggregates and particles of a discrete nature.

The presence of fulvic acid was found to have no obvious effects on the aggregation kinetics, as the CCC values were little changed. The dissolution of the silver nanoparticles in systems with fulvic acid and NaCl was somewhat enhanced and a small increase was measured in the electrophoretic mobilities of the particles with fulvic acid. However, neither change was sufficient in magnitude to alter the stability of the particles.

Acknowledgments

This research has been supported by the U.S. National Oceanic and Atmospheric Administration through its Ohio Sea Grant College Program. Support from the Thomas Ewing French Fellowship Fund for X.L. is also gratefully acknowledged. The authors would like to acknowledge the help of Dr. Yun Wu at The Ohio State University's Nanotech West Laboratory for her help with DLS measurements.

References

[1] Colvin, V.L., *The potential environmental impact of engineered nanomaterials.* Nature Biotechnology, 2003. **21**(10): p. 1166-1170.

[2] Wiesner, M.R. *Responsible development of nanotechnologies for water and wastewater treatment*. in *3rd IWA Leading-Edge Conference Water and Wastewater Treatment Technologies*. 2005. Sapporo, JAPAN.

[3] Wiesner, M., et al., *Assessing the risks of manufactured nanomaterials.* Environmental Science & Technology, 2006. **40**(14): p. 4336-4345.

[4] Maynard, A., et al., *Safe handling of nanotechnology.* Nature, 2006. **444**(7117): p. 267-269.

[5] Benn, T.M. and P. Westerhoff, *Nanoparticle silver released into water from commercially available sock fabrics.* Environmental Science & Technology, 2008. **42**(11): p. 4133-4139.

[6] Hussain, S., et al., *In vitro toxicity of nanoparticles in BRL 3A rat liver cells.* Toxicology in Vitro, 2005. **19**(7): p. 975-983.

[7] Gao, J., et al., *Dispersion and Toxicity of Selected Manufactured Nanomaterials in Natural River Water Samples: Effects of Water Chemical Composition.* Environmental Science & Technology, 2009. **43**(9): p. 3322-3328.

[8] Blaser, S.A., et al., *Estimation of cumulative aquatic exposure and risk due to silver: Contribution of nano-functionalized plastics and textiles.* Science of the Total Environment, 2008. **390**(2-3): p. 396-409.

[9] Blaser, S.A., *Environmental risk analysis for silver-containing nanofunctionalized products* 2006, Swiss Federal Institute of Technology (ETHZ): Zurich.

[10] Navarro, E., et al., *Toxicity of Silver Nanoparticles to Chlamydomonas reinhardtii.* Environmental Science & Technology, 2008. **42**(23): p. 8959-8964.

[11] Kumar, R., S. Howdle, and H. Munstedt, *Polyamide/silver antimicrobials: Effect of filler types on the silver ion release.* Journal of Biomedical Materials Research Part B-Applied Biomaterials, 2005. **75B**(2): p. 311-319.

[12] Ratte, H., *Bioaccumulation and toxicity of silver compounds: A review.* Environmental Toxicology and Chemistry, 1999. **18**(1): p. 89-108.

[13] Hiriart-Baer, V.P., et al., *Toxicity of silver to two freshwater algae, Chlamydomonas reinhardtii and Pseudokirchneriella subcapitata, grown under continuous culture conditions: Influence of thiosulphate.* Aquatic Toxicology, 2006. **78**(2): p. 136-148.

[14] Wood, C.M., R.C. Playle, and C. Hogstrand, *Physiology and modeling of mechanisms of silver uptake and toxicity in fish.* Environmental Toxicology and Chemistry, 1999. **18**(1): p. 71-83.

[15] Liau, S.Y., et al., *Interaction of silver nitrate with readily identifiable groups: relationship to the antibacterial action of silver ions.* Letters in Applied Microbiology, 1997. **25**(4): p. 279-283.

[16] Kim, J.S., et al., *Antimicrobial effects of silver nanoparticles.* Nanomedicine-Nanotechnology Biology and Medicine, 2007. **3**(1): p. 95-101.

[17] Lee, H.Y., et al., *A practical procedure for producing silver nanocoated fabric and its antibacterial evaluation for biomedical applications.* Chemical Communications, 2007(28): p. 2959-2961.

[18] Morones, J.R., et al., *The bactericidal effect of silver nanoparticles.* Nanotechnology, 2005. **16**(10): p. 2346-2353.

[19] Pal, S., Y.K. Tak, and J.M. Song, *Does the antibacterial activity of silver nanoparticles depend on the shape of the nanoparticle? A study of the gram-negative bacterium Escherichia coli.* Applied and Environmental Microbiology, 2007. **73**(6): p. 1712-1720.

[20] Panacek, A., et al., *Silver colloid nanoparticles: Synthesis, characterization, and their antibacterial activity.* Journal of Physical Chemistry B, 2006. **110**(33): p. 16248-16253.

[21] Shahverdi, A.R., et al., *Synthesis and effect of silver nanoparticles on the antibacterial activity of different antibiotics against Staphylococcus aureus and Escherichia coli.* Nanomedicine-Nanotechnology Biology and Medicine, 2007. **3**(2): p. 168-171.

[22] Sondi, I. and B. Salopek-Sondi, *Silver nanoparticles as antimicrobial agent: a case study on E-coli as a model for Gram-negative bacteria.* Journal of Colloid and Interface Science, 2004. **275**(1): p. 177-182.

[23] Fortin, C. and P.G.C. Campbell, *Silver uptake by the green alga Chlamydomonas reinhardtii in relation to chemical speciation: Influence of chloride.* Environmental Toxicology and Chemistry, 2000. **19**(11): p. 2769-2778.

[24] Lee, D.Y., C. Fortin, and P.G.C. Campbell, *Influence of chloride on silver uptake by two green algae, Pseudokirchneriella subcapitata and Chlorella pyrenoidosa.* Environmental Toxicology and Chemistry, 2004. **23**(4): p. 1012-1018.

[25] Lecoanet, H.F., J.Y. Bottero, and M.R. Wiesner, *Laboratory assessment of the mobility of nanomaterials in porous media.* Environmental Science & Technology, 2004. **38**(19): p. 5164-5169.

[26] Lecoanet, H.F. and M.R. Wiesner, *Velocity effects on fullerene and oxide nanoparticle deposition in porous media.* Environmental Science & Technology, 2004. **38**(16): p. 4377-4382.

[27] Brant, J., H. Lecoanet, and M.R. Wiesner, *Aggregation and deposition characteristics of fullerene nanoparticles in aqueous systems.* Journal of Nanoparticle Research, 2005. **7**(4-5): p. 545-553.

[28] Chen, K.L., S.E. Mylon, and M. Elimelech, *Aggregation kinetics of alginate-coated hematite nanoparticles in monovalent and divalent electrolytes.* Environmental Science & Technology, 2006. **40**(5): p. 1516-1523.

[29] Chen, K.L. and M. Elimelech, *Influence of humic acid on the aggregation kinetics of fullerene (C-60) nanoparticles in monovalent and divalent electrolyte solutions.* Journal of Colloid and Interface Science, 2007. **309**(1): p. 126-134.

[30] Hyung, H., et al., *Natural organic matter stabilizes carbon nanotubes in the aqueous phase.* Environmental Science & Technology, 2007. **41**(1): p. 179-184.

[31] Derjaguin B. V., L., L. D., *Theory of the stability of strongly charged lyophobic sols and of the adhesion of strongly charged particles in solutions of electrolytes.* Acta Physiconchim, 1941. **14**: p. 733-762.

[32] Verwey E. J. W., O.J.T.G., *Theory of the stability of lyophobic colloids*. 1948, Amsterdam: Elsevier.

[33] Elimelech, M.G., J.; Jia, X.; Williams, R. J., *Particle Deposition & Aggregation: Measurement, Modelling and Simulation*. 1995, Oxford: Butterworth-Heinemann.

[34] Chen, K.L., S.E. Mylon, and M. Elimelech, *Enhanced aggregation of alginate-coated iron oxide (hematite) nanoparticles in the presence of calcium, strontium, and barium cations.* Langmuir, 2007. **23**(11): p. 5920-5928.

[35] Mylon, S.E., K.L. Chen, and M. Elimelech, *Influence of natural organic matter and ionic composition on the kinetics and structure of hematite colloid aggregation: Implications to iron depletion in estuaries.* Langmuir, 2004. **20**(21): p. 9000-9006.

[36] El Badawy, A., et al., *Impact of Environmental Conditions (pH, Ionic Strength, and Electrolyte Type) on the Surface Charge and Aggregation of Silver Nanoparticles Suspensions.* Environmental Science & Technology, 2010: p. 1260-1266.

[37] Liu, J.Y. and R.H. Hurt, *Ion Release Kinetics and Particle Persistence in Aqueous Nano-Silver Colloids.* Environmental Science & Technology, 2010. **44**(6): p. 2169-2175.

[38] Buffle, J., *Complexation reactions in aquatic systems--an analytical approach*. 1990, Chichester Ellis Horwood.

[39] Kvitek, L., et al., *Effect of surfactants and polymers on stability and antibacterial activity of silver nanoparticles (NPs).* Journal of Physical Chemistry C, 2008. **112**(15): p. 5825-5834.

[40] Virden, J.W. and J.C. Berg, *The Use of Photon-Correlation Spectroscopy for Estimating the Rate-Constant for Doublet Formation in an Aggregating Colloidal Dispersion.* Journal of Colloid and Interface Science, 1992. **149**(2): p. 528-535.

[41] Mulvaney, P., T. Linnert, and A. Henglein, *Surface-Chemistry of Collodial Silver in Aqueous-Solution - Observations on Chemisorption and Reactivity. Journal of Physical Chemistry*, 1991. **95**(20): p. 7843-7846.

[42] Linnert, T., P. Mulvaney, and A. Henglein, *Surface-Chemistry of Colloidal Silver - Surface-Plasmon Damping by Chemisorbed I-, Sh-, and C6h5s-.* Journal of Physical Chemistry, 1993. **97**(3): p. 679-682.

[43] Henglein, A., *Colloidal silver nanoparticles: Photochemical preparation and interaction with O-2, CCl4, and some metal ions.* Chemistry of Materials, 1998. **10**(1): p. 444-450.

[44] Sukhov, N.L., et al., *Absorption spectra of large colloidal silver particles in aqueous solution.* Russian Chemical Bulletin, 1997. **46**(1): p. 197-199.

[45] in, Y.D., et al., *Synthesis and characterization of stable aqueous dispersions of silver nanoparticles through the Tollens process.* Journal of Materials Chemistry, 2002. **12**(3): p. 522-527.

[46] Henglein, A., T. Linnert, and P. Mulvaney, *Reduction of Ag+ in Aqueous Polyanion Solution - Some Properties and Reactions of Long-Lived Loigomeric Silver Clusters and*

Metallic Silver Particles. Berichte der Bunsen-Gesellschaft-Physical Chemistry Chemical Physics, 1990. **94**(12): p. 1449-1457.

[47] Kapoor, S., *Preparation, characterization, and surface modification of silver particles.* Langmuir, 1998. **14**(5): p. 1021-1025.

[48] Chen, M., et al., *Preparation and study of polyacryamide-stabilized silver nanoparticles through a one-pot process.* Journal of Physical Chemistry B, 2006. **110**(23): p. 11224-11231.

[49] Mie, G., Ann. Phys., 1908. **25**: p. 377.

[50] Hulst, V.d., *Light Scattering by Small Particles*. 1957, New York: Wiley.

[51] Kumar, R. and H. Munstedt, *Silver ion release from antimicrobial polyamide/silver composites.* Biomaterials, 2005. **26**(14): p. 2081-2088.

[52] *CRC handbook of chemistry and physics*. 89th ed. 2008, United Kingdom: Taylor & Francis Group.

[53] Weitz, D.A., et al., *Limits of the Fractal Dimension for Irreversible Kinetic Aggregation of Gold Colloids.* Physical Review Letters, 1985. **54**(13): p. 1416-1419.

[54] Hunter, R.J., *Foundations of Colloid Science*. Vol. 1. 1986, Oxford: Clarendon Press.

[55] Stumm, W., *Reactivity at the mineral-water interface: Dissolution and inhibition.* Colloids and Surfaces a-Physicochemical and Engineering Aspects, 1997. **120**(1-3): p. 143-166.

[56] Merga, G., et al., *Redox catalysis on "Naked" silver nanoparticles.* Journal of Physical Chemistry C, 2007. **111**(33): p. 12220-12226.

[57] Dougherty, G., et al., *The zeta potential of suirface-functionalized metallic nanorod particles in aqueous solution.* Electrophoresis, 2008. **29**(5): p. 1131-1139.

[58] Patrito, E.M. and P. Paredes-Olivera, *Adsorption of hydrated hydroxide and hydronium ions on Ag(111). A quantum mechanical investigation.* Surface Science, 2003. **527**(1-3): p. 149-162.

[59] Kvitek, L., et al., *Initial Study on the Toxicity of Silver Nanoparticles (NPs) against Paramecium caudatum.* Journal of Physical Chemistry C, 2009. **113**(11): p. 4296-4300.

[60] Chen, K.L. and M. Elimelech, *Aggregation and deposition kinetics of fullerene (C-60) nanoparticles.* Langmuir, 2006. **22**(26): p. 10994-11001.

[61] Hem, J.D., *Study and Interpretation of the Chemical Characteristics of Natural Water*. 1989, United States Geological Survey: Washington DC. p. 263.

[62] Baalousha, M., *Aggregation and disaggregation of iron oxide nanoparticles: Influence of particle concentration, pH and natural organic matter.* Science of the Total Environment, 2009. **407**(6): p. 2093-2101.

[63] Domingos, R.F., N. Tufenkji, and K.J. Wilkinson, *Aggregation of Titanium Dioxide Nanoparticles: Role of a Fulvic Acid.* Environmental Science & Technology, 2009. **43**(5): p. 1282-1286.

[64] Illes, E. and E. Tombacz, *The role of variable surface charge and surface complexation in the adsorption of humic acid on magnetite.* Colloids and Surfaces a-Physicochemical and Engineering Aspects, 2003. **230**(1-3): p. 99-109.

[65] Jegatheesan, V. and S. Vigneswaran, *Interaction between organic substances and submicron particles in deep bed filtration.* Separation and Purification Technology, 1997. **12**(1): p. 61-66.

[66] Au, K.K., et al., *Natural organic matter at oxide/water interfaces: Complexation and conformation.* Geochimica Et Cosmochimica Acta, 1999. **63**(19-20): p. 2903-2917.

[67] Stevenson, F.J., *Humus chemistry : genesis, composition, reactions*. 2nd ed ed. 1994, New York ; Chichester: Wiley. xiii, 496 p.

[68] Kulovaara, M., S. Metsamuuronen, and M. Nystrom, *Effects of aquatic humic substances on a hydrophobic ultrafiltration membrane.* Chemosphere, 1999. **38**(15): p. 3485-3496.

[69] Pelley, A.J. and N. Tufenkji, *Effect of particle size and natural organic matter on the migration of nano- and microscale latex particles in saturated porous media.* Journal of Colloid and Interface Science, 2008. **321**(1): p. 74-83.

[70] Beckett, R. and N.P. Le, *The Role of Organic-Matter and Ionic Composition in Determining the Surface-Charge of Suspended Particles in Natural-Waters.* Colloids and Surfaces, 1990. **44**: p. 35-49.

[71] Amirbahman, A. and T.M. Olson, *The Role of Surface Conformations in the Deposition Kinetics of Humic Matter-Coated Colloids in Porous-Media.* Colloids and Surfaces a-Physicochemical and Engineering Aspects, 1995. **95**(2-3): p. 249-259.

[72] Tiller, C.L. and C.R. Omelia, *Natural Organic-Matter and Colloidal Stability - Models and Measurements.* Colloids and Surfaces a-Physicochemical and Engineering Aspects, 1993. **73**: p. 89-102.

Tables and Figures

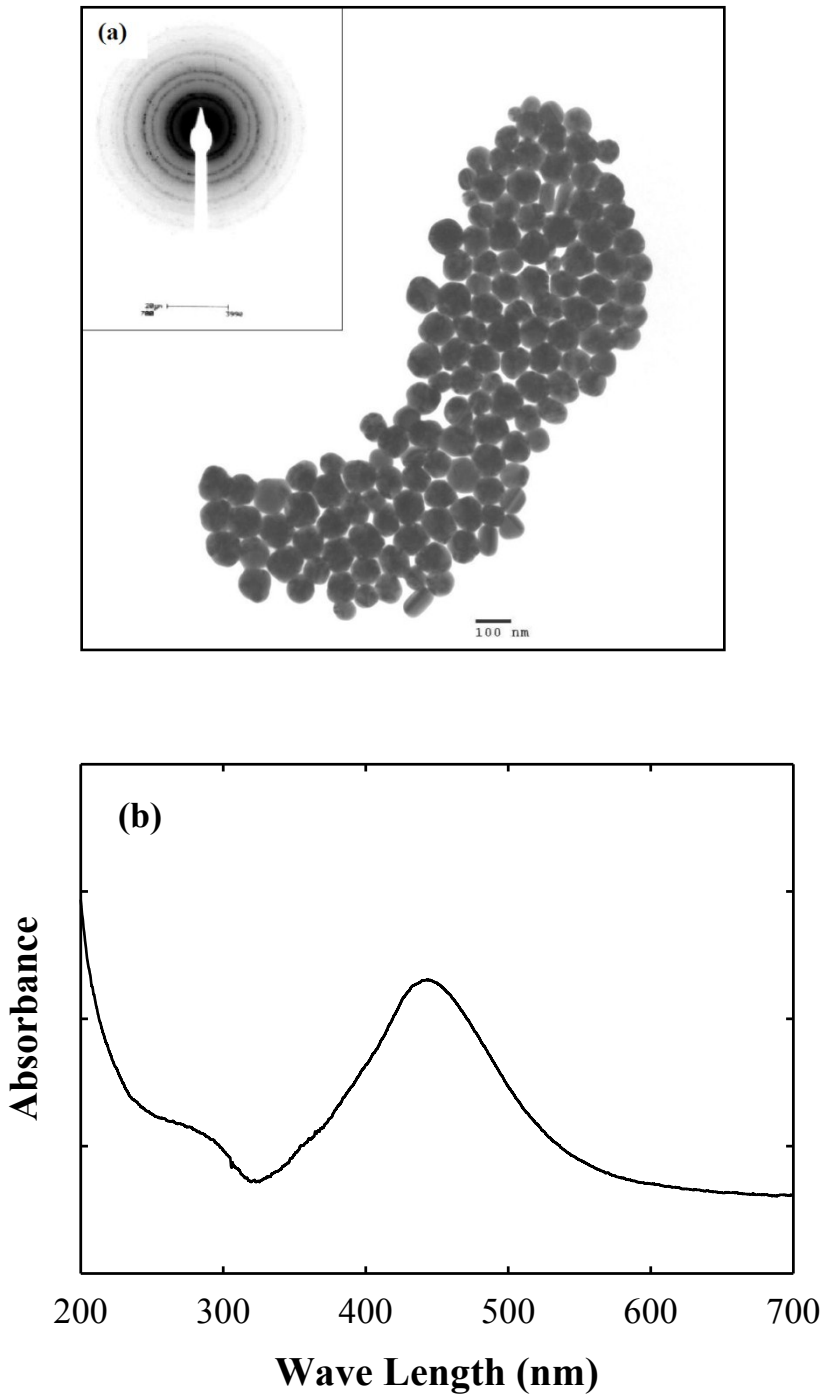

Figure 2.1 (a) TEM image and electron diffraction pattern (insert), and (b) UV-vis absorption spectrum of the silver nanoparticles.

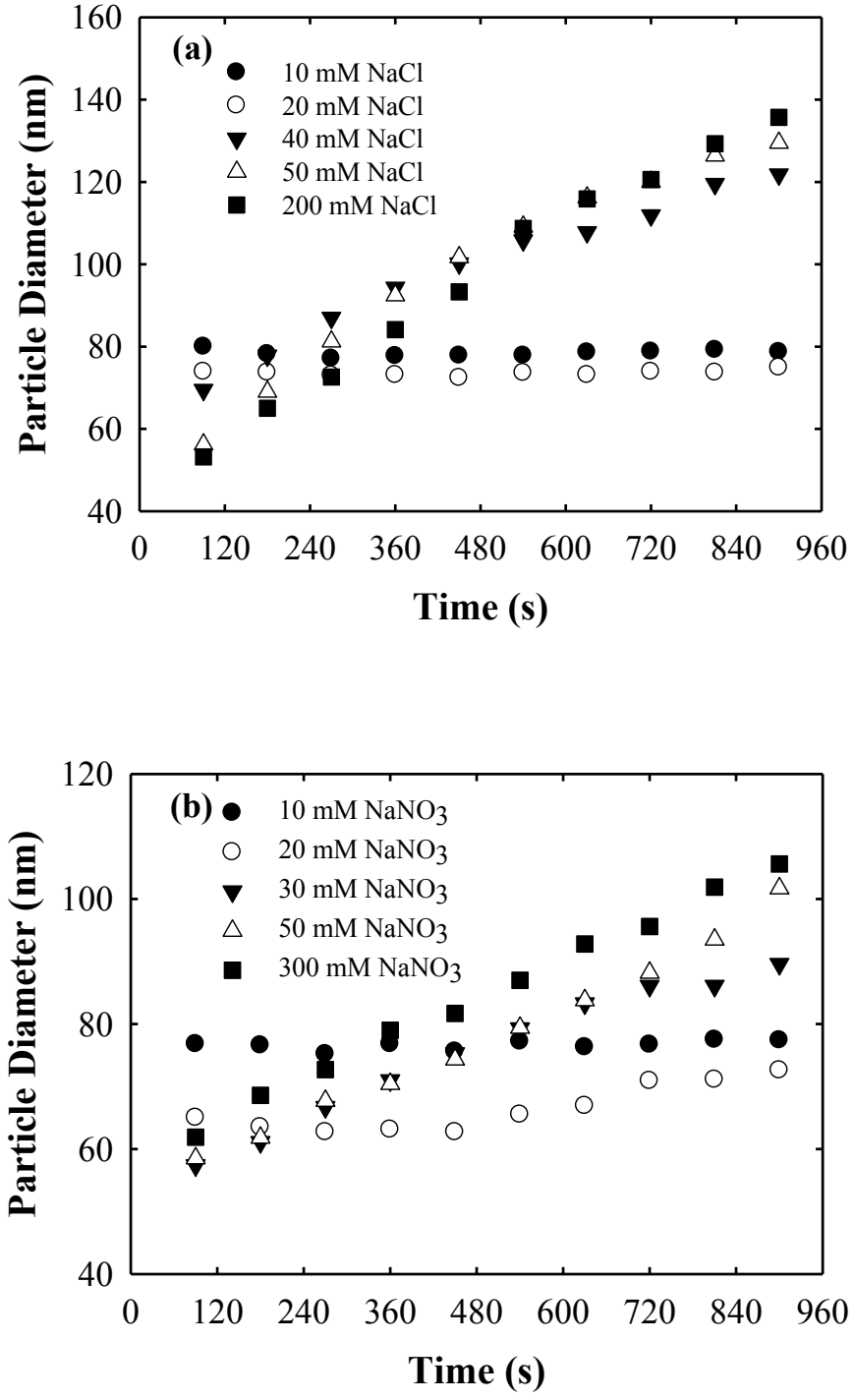

Figure 2.2 Aggregation profiles of silver nanoparticles in the absence of fulvic acid at pH 7.0 as a function of (a) NaCl concentration, and (b) $NaNO_3$ concentrations.

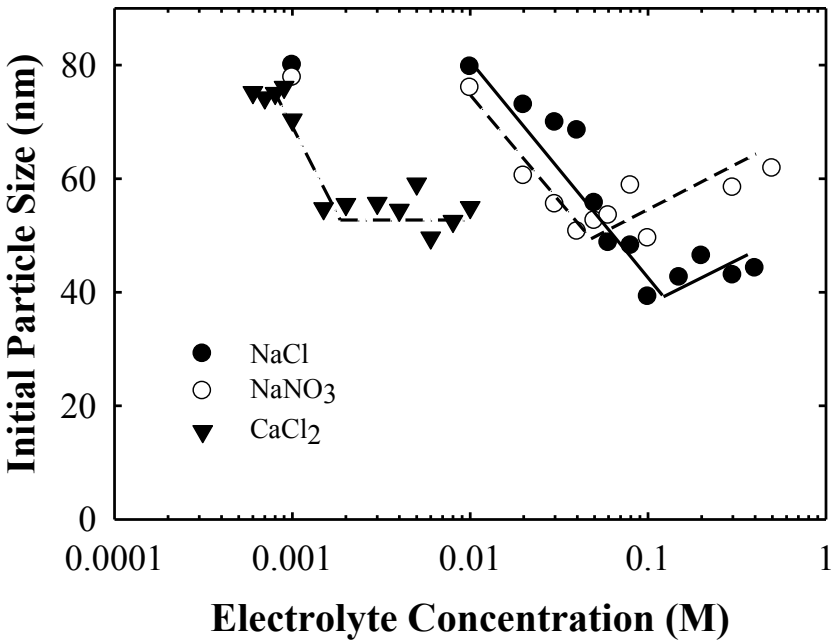

Figure 2.3 Initial hydrodynamic diameter of silver nanoparticles as a function of NaCl and $NaNO_3$ concentrations.

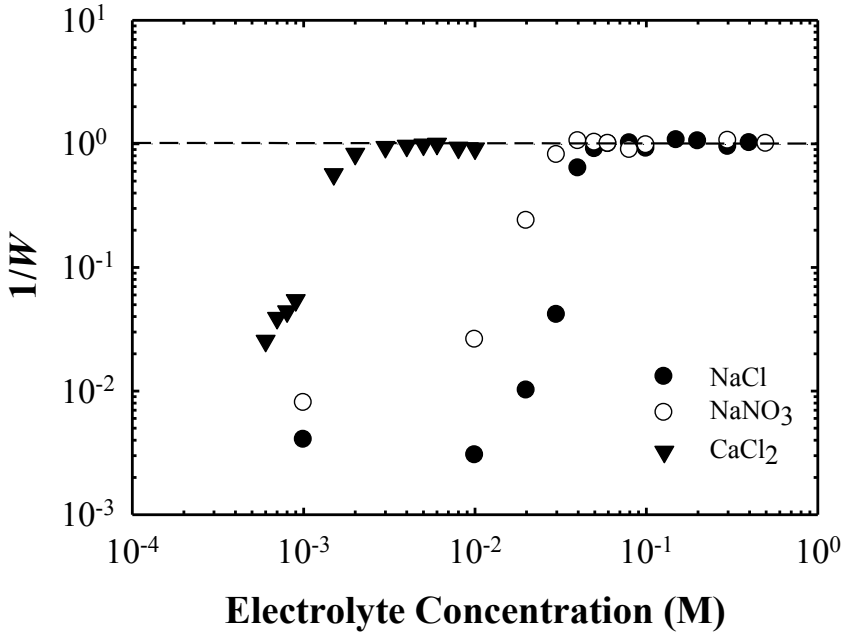

Figure 2.4 Inverse stability ratio ($1/W$) of silver nanoparticles as a function of NaCl, $NaNO_3$ and $CaCl_2$ concentrations.

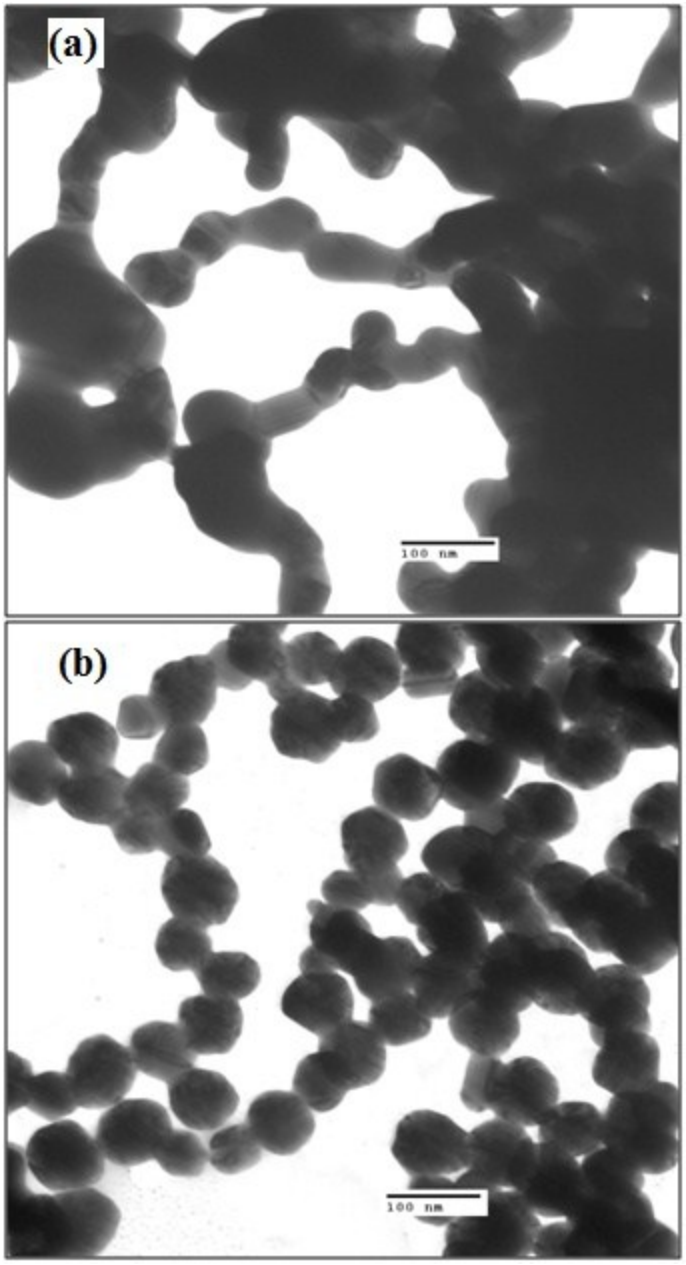

Figure 2.5 TEM images of silver nanoparticles in the absence of fulvic acid after the addition of 100 mM of (a) NaCl and (b) $NaNO_3$.

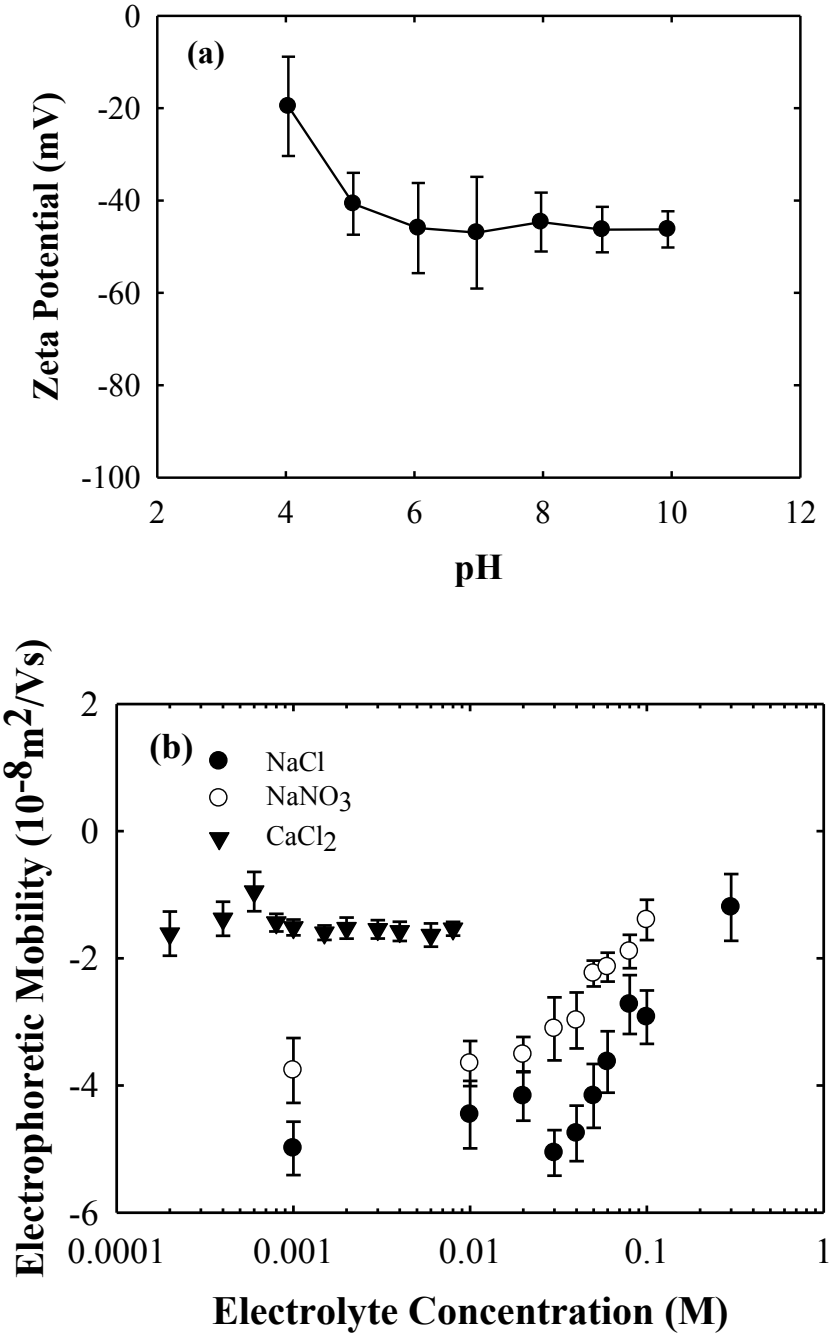

Figure 2.6 (a) Zeta potentials of silver nanoparticles at pH 4.0 - 10.0 in the presence of 1 mM NaCl, and (b) Electrophoretic mobilities of silver nanoparticles at pH 7.0 as a function of NaCl, $NaNO_3$ and $CaCl_2$ concentration

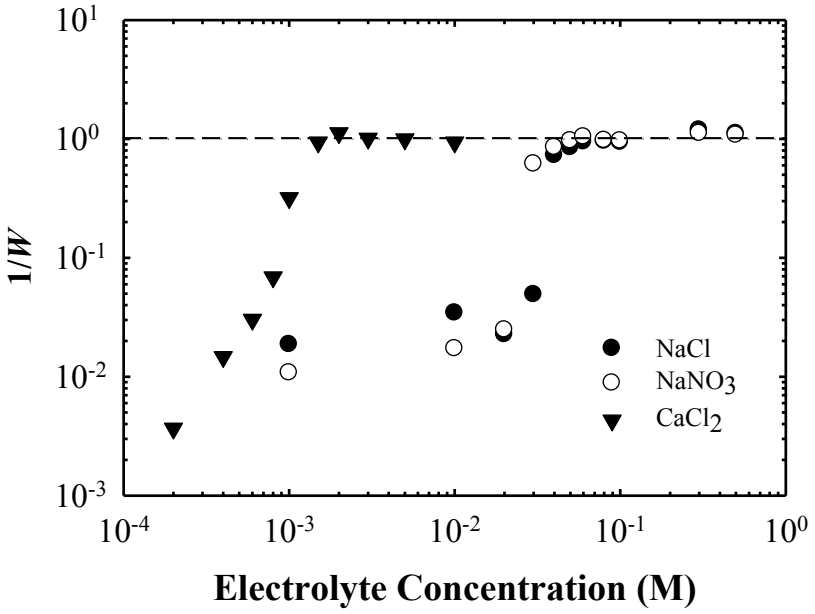

Figure 2.7 Inverse stability ratio ($1/W$) of silver nanoparticles in the presence of fulvic acid as a function of NaCl, $NaNO_3$ and $CaCl_2$ concentration.

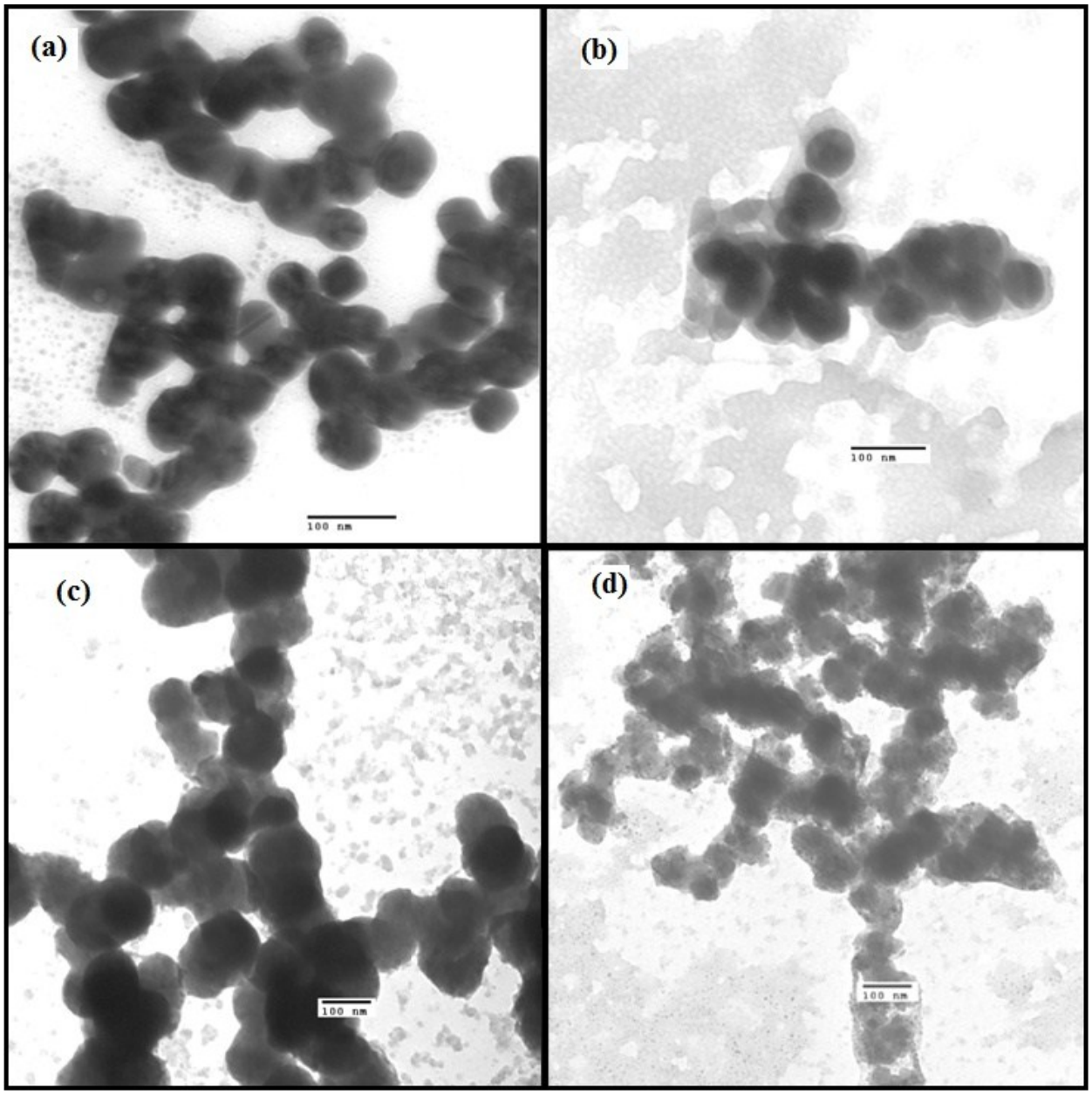

Figure 2.8 TEM images of silver nanoparticles in the presence of fulvic acid after the addition of (a) 1 mM, (b) 10 mM, (c) 100 mM and (d) 200 mM NaCl.

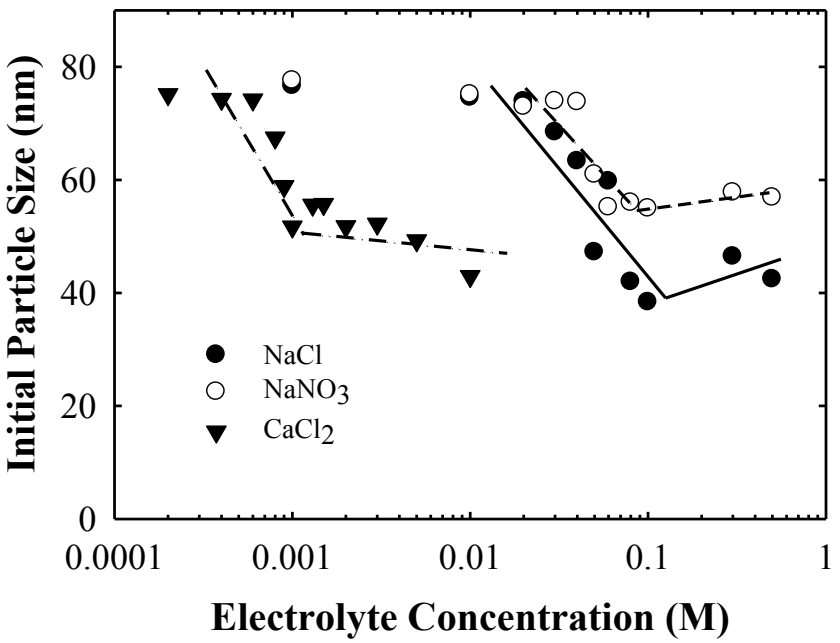

Figure 2.9 Initial particle hydrodynamic diameter of silver nanoparticles in the presence of fulvic acid as a function of of NaCl, $NaNO_3$ and $CaCl_2$ concentration.

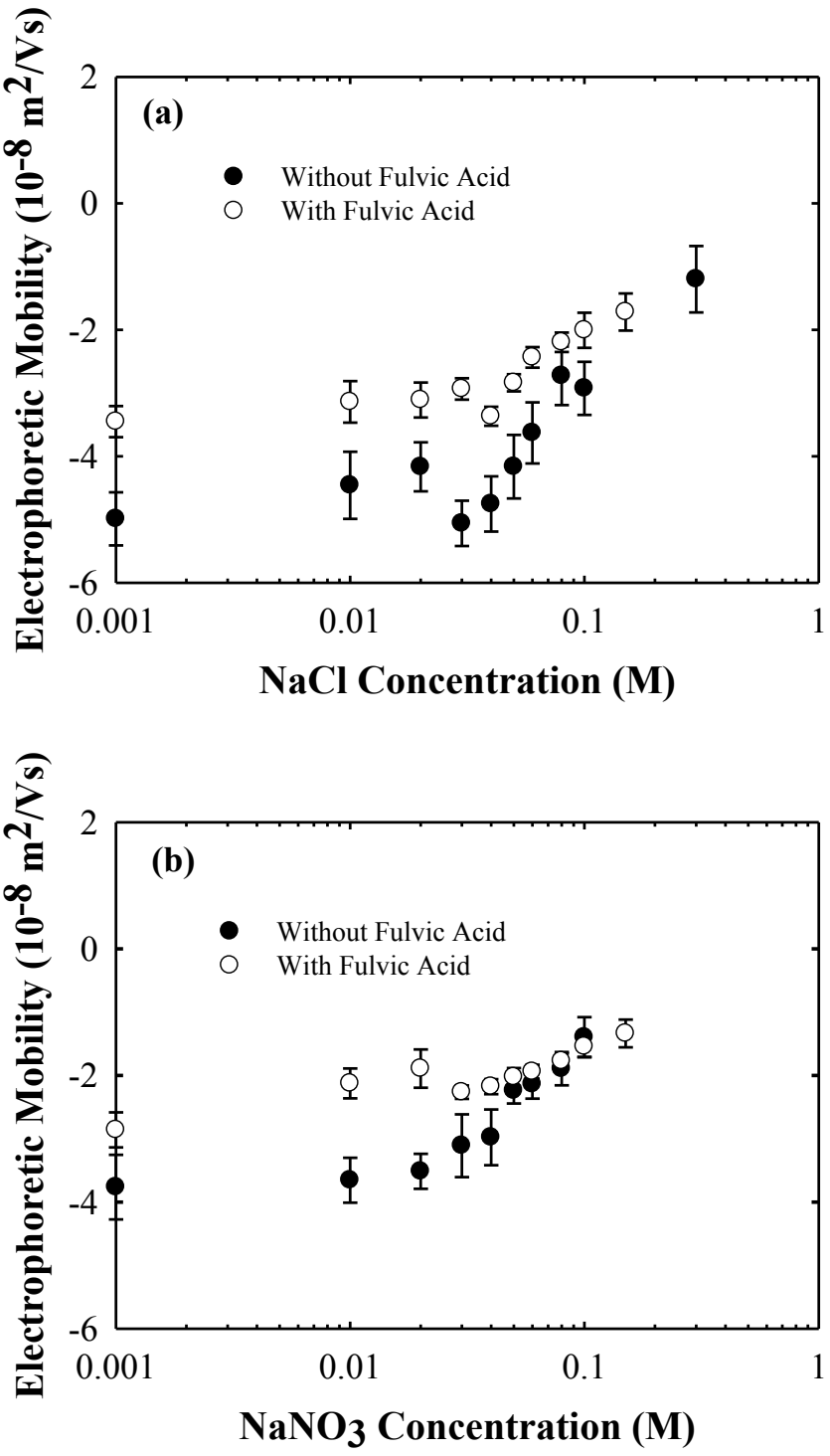

Figure 2.10 Electrophoretic mobility of silver nanoparticles in the presence and absence of fulvic acid as a function of (a) NaCl, (b) $NaNO_3$, and (c) $CaCl_2$ concentration.(Continued)

Figure 2.10: (Continued)

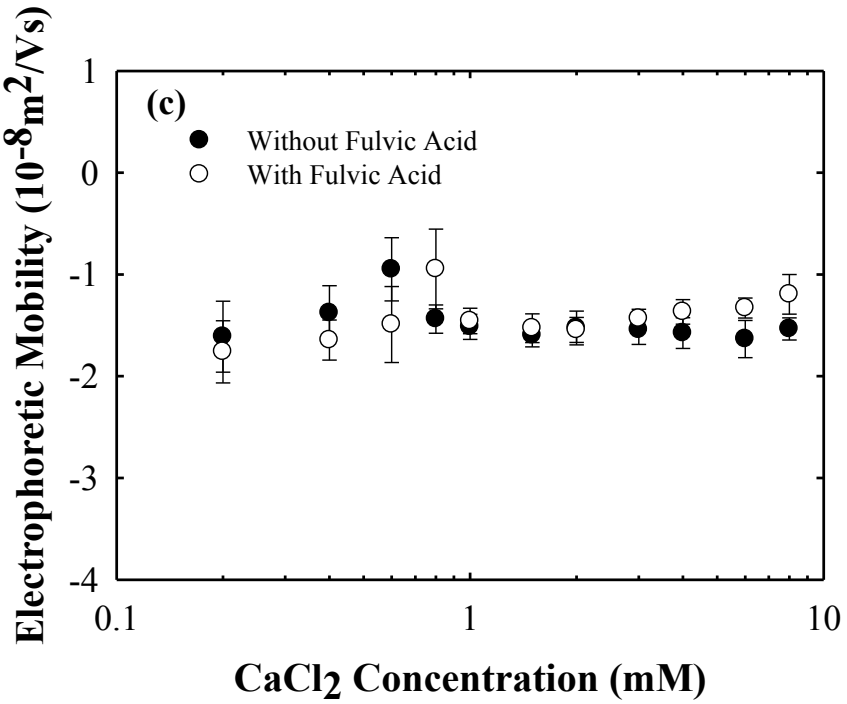

Chapter 3. Aggregation Kinetics and Dissolution of Coated Silver Nanoparticles

(Langmuir, In Press)

Abstract.

Determining the fate of manufactured nanomaterials in the environment is contingent upon understanding how stabilizing agents influence the stability of nanoparticles in aqueous systems. In this study, the aggregation and dissolution tendencies of uncoated silver nanoparticles and the same particles coated with three common coating agents, trisodium citrate, sodium dodecyl sulfate (SDS), and Tween 80 (Tween), were evaluated. Early stage aggregation kinetics of the uncoated and coated silver nanoparticles were assessed by dynamic light scattering over a range of electrolyte types (NaCl, $NaNO_3$, and $CaCl_2$) and concentrations that span those observed in natural waters. Although particle dissolution was observed, aggregation of all particle types was still consistent with classical Derjaguin-Landau-Verwey-Overbeek (DLVO) theory. The aggregation of citrate-coated particles and SDS-coated particles were very similar to that for the uncoated particles, as the critical coagulation concentrations (CCC) of the particles in different electrolytes were all approximately the same (40 mM NaCl, 30 mM $NaNO_3$ and 2 mM $CaCl_2$). The Tween-stabilized particles were significantly more stable than the other particles, however, and in $NaNO_3$ aggregation was not observed up to an electrolyte concentration of 1M. Differences in the rate of aggregation under diffusion-limited aggregation conditions at high electrolyte concentrations for the SDS and Tween-coated

particles in combination with the moderation of their electrophoretic mobilities suggest SDS and Tween imparted steric interactions to the particles. The dissolution of the silver nanoparticles was inhibited by the SDS and Tween coatings, but not by the citrate coating, and in chloride-containing electrolytes a secondary precipitate of AgCl was observed bridging the individual particles. These results indicate that coating agents could significant influence the fate of silver nanoparticles in aquatic systems and in some cases these stabilizers may completely prevent particle aggregation.

3.1. Introduction

Owing to their antimicrobial properties, silver nanoparticles are mass-produced and utilized in hundreds of commercially available products [1-2]. The release of silver nanoparticles from these products during use is certain, particularly during washing [3], and thus the potential for silver nanoparticles subsequently to be introduced into surface waters at concentrations that pose a risk is real [4-5]. The toxicity of silver nanoparticles to bacteria and algae in freshwater environments is primarily linked to ionic silver released by the dissolving silver nanoparticles [1]; however, there exists uncertainty over whether the toxicity can be attributed simply to the effects of the Ag^{+} ions or an additional mechanism specific to the silver nanoparticles [6-12]. Critical to determining the potential adverse effects of nanoparticles upon introduction to aqueous systems is knowledge regarding whether the particles remain stable in solution or whether they aggregate and subsequently deposit.

The aggregation and deposition behavior of a variety of nanoparticles have been extensively studied in systems with monovalent electrolytes, divalent electrolytes, and natural organic matter [13-19]. While these studies illustrate the importance of many factors, including solution chemistry (e.g., pH, ionic strength, electrolyte composition, and presence of natural organic matter) and coating layer, with few exceptions [20-23] they have not done so in similar comprehensive manner with silver nanoparticles. In general, the classic Derjaguin-Landau-Verwey-Overbeek (DLVO) theory of colloid stability [24-25] satisfactorily explains aggregation behavior of nanoparticles in the presence of simple electrolytes [14-16, 26], which induce aggregation by screening the

surface charge [27]. Studies with silver nanoparticles are no different [20, 23], despite the fact that dissolution of silver nanoparticles incurred by electrolytes and dissolved oxygen accompanies aggregation [20].

One essential problem that not only influences the manufacturing of silver nanoparticles and their application in commercial products, but also their fate in the environment, is the limited stability of the particles in aqueous suspensions under certain chemistries [28-30]. Aggregation during synthesis hinders the production of silver nanoparticle suspensions of small and uniform size [30]. For antibacterial applications, the generation of aggregates leads to a reduction in the antibacterial activity of silver nanoparticles [28-30]. To address these issues, various coating agents, like surfactants and polymers, are commonly introduced during or after synthesis to increase particle stability. Adsorption of the coating agent molecules onto the particle surface depends on the molecular weight, ionization and charge density of the stabilizer molecules, the charge density and polarity of the particle surface, and solution chemistry [31-32]. The mass and configuration of the adsorbed layer plays a major role in controlling particle stability and depends on the affinity of coating molecules to the particle surface, repulsion from neighboring molecules, loss of chain entropy upon adsorption, and also nonspecific dipole interactions between the macromolecule, the solvent and the surface [31-32].

Coating layers may enhance electrostatic and steric repulsion thereby increasing the stability of the particle suspension. Ionic molecules form a charged layer that hinders particle aggregation and adhesion by increasing repulsive electrostatic interactions. Sodium dodecyl sulfate (SDS) is one such molecule and it is widely used as a dispersant

in many industries [33]. Citrate, which is often adopted as a reducing reagent in the synthesis of silver nanoparticles, is also believed to enhance electrostatic repulsion since a certain amount of it remains adsorbed on the particle surface after synthesis [21]. Steric repulsion nearly always involves the adsorption of polymers or non-ionic surfactants, with the magnitude of the steric repulsion depending primarily upon the thickness of the adsorbed layer [34]. The non-ionic surfactant Tween is among the most frequently used stabilizers in the food industry [35]. Stabilizing agents (e.g., citrate, SDS and Tween) enhance antibacterial activity mainly through stabilizing the silver nanoparticle dispersions [30, 36-37]. Very little is known, however, regarding how these stabilizers influence particle aggregation, and hence silver nanoparticle fate, across a range of conditions that parallel those often encountered in natural aquatic systems [21].

In this study, we evaluate the aggregation kinetics of silver nanoparticles coated with stabilizing agents commonly used for commercial applications, with the objective of determining how these agents impact nanoparticle fate in aquatic systems. Silver nanoparticles, with a diameter of 82 nm, were synthesized and coated with citrate, SDS and Tween 80. The time-rate of change of the particle hydrodynamic radius was measured using Dynamic Light Scattering (DLS) over a range of electrolyte types (NaCl, $NaNO_3$ and $CaCl_2$) and concentrations to obtain the early stage aggregation kinetics. The electrophoretic mobility of the particles over the same range of electrolyte types was also determined. Morphologies of particles and aggregates were evaluated using transmission electron microscopy (TEM). Our results indicate that coating agents not only induced

varying degrees of stabilization, but also differ in their ability to prevent particle dissolution.

3.2. Experimental Section

3.2.1 Materials.

$AgNO_3$ (99.8%), D-maltose (99%), sodium dodecyl sulfate (SDS, BioUltra, ≥99.0%) and trisodium citrate (ACS reagent, ≥99.0%) were purchased in powdered form from Sigma-Aldrich and were used without further purification. Tween 80 (Tween), in the form of a viscous liquid (BioXtra), was also purchased from Sigma-Aldrich and also used without further purification. Ammonium hydroxide (trace metal grade) was purchased from Fisher Scientific. All other reagents were analytical grade or higher. The 18.2 MΩ cm water used in the experiments was supplied from a deionized water system (Milli-Q, Millipore). Prior to use, all solutions were filtered through 0.1 μm cellulose ester membranes (Millipore). The labware and glassware used in the experiments were acid-washed using 10% nitric acid, rinsed thoroughly with deionized water and oven-dried under dust-free conditions.

3.2.2 Synthesis and characterization of the silver nanoparticles.

Monodisperse suspensions of silver nanoparticles were synthesized after Li et al. [20] by chemically reducing the $[Ag(NH_3)_2]^+$ complex with D-maltose. Further details of the synthesis, dialysis, characterization and storage of these particles are described in Li et al. [20]. The average, intensity weighted, hydrodynamic diameter of the particles was measured as 82.0 ± 1.6 nm by Dynamic Light Scattering (DLS) (90Plus, Brookhaven Instruments Corp., Holtsville, NY), matching that previously determined [20]. The total

silver concentration of the stock suspension was measured using an inductively coupled plasma optical emission spectrometer (ICP-OES; Varian Vista AX) as 31.6 mg/L.

The size and morphology of the uncoated silver nanoparticles was observed by transmission electron microscopy (TEM) using a Technai G2 Spirit TEM at 120 kV. Images were collected using a digital camera at magnifications that ranged from 71,000 to 144,000. Suspensions for imaging were prepared and equilibrated for 15 min in a 2 mL glass vial protected from light. One drop of the resulting suspension was transferred onto a 100 mesh carbon-covered copper grid and the extra water was quickly removed by filter paper. The sample was dried under nitrogen and placed into the TEM chamber. TEM images of the uncoated particles (Figure B.S-1a) confirmed the spherical and monodisperse nature of particles synthesized in this manner [20]. The particle concentration of the silver nanoparticle stock suspension was calculated as 1.1×10^{10} particles mL^{-1} based on the density of metallic silver (10.5 g/cm^3), total silver concentration in the stock of 31.6 mg/L, and 82 nm diameter.

Silver nanoparticle suspensions with coating layers were prepared by introducing pre-calculated volumes of the uncoated silver nanoparticle stock solution and either trisodium citrate, SDS or Tween into 50 mL polycarbonate ultracentrifuge tubes in order to achieve 1 mM trisodium citrate, 10 mM trisodium citrate, 1 mM SDS, 10 mM SDS or 10 mM Tween concentrations, reflecting concentrations observed to provide stabilizing effects in similar systems [30, 33, 38-39]. The coated silver nanoparticles are noted as Citrate-nAg-1, Citrate-nAg-10, SDS-nAg-1, SDS-nAg-10 and Tween-nAg hereafter, respectively. In a similar manner we refer to the uncoated particles as Bare-nAg. The dilution of the silver

nanoparticle suspensions resulting from the introduction of the coating agents was less than 3%. Sodium chloride, sodium bicarbonate and sodium hydroxide were added as needed to achieve an ionic strength of 1 mM and maintain the pH at 7.0 ± 0.3, respectively. The tubes were sealed and slowly shaken for 24 hours in the dark at room temperature which as reported by Kvitek et al. [30] is sufficient time for the system to reach equilibrium. The silver nanoparticle suspensions were subsequently dialyzed against deionized water over a period of 24 hours in order to remove residual coating agents using cellulose ester membranes (Spectra/Pro® Biotech) with a molecular weight cut off of 8-10 kDa for systems with trisodium citrate and SDS and 50 kDa for systems with Tween. The deionized water dialysate was changed a minimum of 4 times and its conductivity and total organic carbon (TOC) content were measured to ensure that residual coating molecules were removed. Except for Tween-nAg, the conductivity and TOC of the dialysate at the conclusion of the dialysis matched that of fresh DI. The final TOC for Tween-nAg was *ca.* 8.6 mg/L, which was roughly 0.1 % of the starting TOC of 7600 mg/L estimated on the basis molecular weight (1310 g/mol) and molecular formula ($C_{64}H_{124}O_{26}$) of Tween 80. This indicates the majority of the Tween molecules were removed during the dialysis. The TOC concentration was measured using a TOC analyzer (TOC-5000A, Shimadzu Corp.) and the conductivity was measured using a zeta potential analyzer (ZetaPALS, Brookhaven Instruments Corp.). The size of the coated particles was determined in the same manner using TEM as previously described for the uncoated particles.

The electrophoretic mobility of the silver nanoparticles was measured at a temperature of 22 ± 0.5 °C across the range of electrolyte concentrations employed in the aggregation experiments for the uncoated and coated silver nanoparticles with a ZetaPALS (Brookhaven Instrument Corp.). Error estimates were based on ten measurements conducted on five separate samples for each experimental condition.

3.2.3 Aggregation Kinetics.

The aggregation experiments were conducted on suspensions of the coated silver nanoparticles diluted 25 times in a 5.0×10^{-2} mM sodium bicarbonate solution that buffered the pH at 7.0 ± 0.3. Based on the 25 times dilution, the resulting suspensions had a particle concentration of 4.4×10^{8} particles mL^{-1} matching that for the uncoated particle suspensions studied by Li et al.[20]. The resulting suspension was briefly sonicated in an ultrasonic water bath in order to disrupt any possible aggregates before the aggregation experiments. 3.0 mL of the silver nanoparticle solution and a specific volume of electrolyte solution were pipetted into a 4 mL acrylic cuvette in order to obtain the desired particle and electrolyte concentrations. The electrolytes tested were NaCl, $NaNO_3$ and $CaCl_2$. The first two electrolytes allow us to evaluate whether differences induced by the potential formation of AgCl observed for Bare-nAg by Li et al.[20] in systems with NaCl translate to coated particles, while the last allows us to evaluate the impact of a divalent cation. A plastic lid was placed on the cuvette and it was briefly shaken by hand before being inserted into the DLS sample holder. Measurements recording the change in the average hydrodynamic diameter over time were immediately started. The total time of

each aggregation experiment was 15 minutes and data were collected at a time interval of 90 seconds. The temperature for all aggregation experiments was fixed at 22 ± 0.5 °C.

For a colloid system where aggregation is governed by DLVO theory, the inverse stability ratio ($1/W$) versus electrolyte concentration at given experimental conditions can be used to characterize the aggregation kinetics [27]. This ratio, also termed the attachment efficiency (α), is determined by dividing the value of the experimental aggregation rate constant (k_{exp}) by the value of the rapid aggregation rate constant (k_{rapid}):

$$\frac{1}{W} = \frac{k_{exp}}{k_{rapid}} \quad (1)$$

where k_{rapid} represents the aggregation rate constant under diffusion-limited conditions. This occurs at electrolyte concentrations higher than the critical coagulation concentration (CCC) where the excess electrolyte ions completely screen surface energy barriers. To determine k_{exp}, the time-rate of change in the average hydrodynamic radius of the silver nanoparticles (dr/dt) was measured during early-stage aggregation and used to estimate k_{exp} based on the following expression [40]:

$$k_{exp} = \frac{1}{oNr_0} \cdot \frac{dr}{dt} \quad (2)$$

where N is the initial particle concentration, r_0 is the initial particle radius, and o is an optical factor [40]. The value of dr/dt under a given experimental condition (electrolyte type and concentration) was calculated by conducting a linear least squares regression analysis to the data across a time change corresponding to the necessary increase in the hydrodynamic radius of 30% [15]. The initial values for N and r_0 were nearly constant

across the given experimental conditions and thus cancel out when calculating $1/W$ with equation (1) based on k_{exp} and k_{rapid} determined using equation (2).

Values of $1/W$ based solely on DLVO theory invoke only van der Waals and electrostatic forces as a means to evaluate particle interactions [24-25, 40]. Within a system dominated by electrostatic interactions, the aggregation rate under favorable conditions, k_{rapid}, is in theory - and often the case experimentally - constant and independent of electrolyte concentration and type [15-16, 41]. When other aggregation mechanisms are present, values of k_{rapid} are not constant, but instead increase or decrease depending upon whether the extra mechanisms enhance or hinder aggregation [15-16]. For nanoparticles coated with stabilizing agents, steric repulsion represents one such mechanism. In such instances, an apparent aggregation rate constant, k_{app}, instead of k_{exp} can be used [15-16]. Thus, we determined $1/W$ values of the coated silver nanoparticles using measured values of k_{app} for each coated-particle system and k_{rapid} for uncoated particles.

$$\frac{1}{W} = \frac{k_{app}}{k_{rapid}} \tag{3}$$

In each case, the values for the aggregation rate constants were specific to each electrolyte type and k_{rapid} was determined by averaging k_{exp} values for the uncoated particles in the diffusion-limited regime. The application of this approach was predicated upon maintaining constant values for N and r_0 in equation (2) across all systems studied.

3.3. Results and Discussions

3.3.1 Characterization of Silver Nanoparticles

The coated and uncoated silver nanoparticles were characterized by DLS and TEM as mono-dispersed and spherical. The hydrodynamic size of the coated silver nanoparticles matched that of the uncoated particles (82 nm) except that Tween-nAg showed an increase in size to *ca*. 88 nm and Citrate-nAg-10 increased in size to *ca.* 170.5 nm. The TEM images of all of the particles, except Citrate-nAg-10, under low ionic strength conditions indicated the particles were initially dispersed (Figure B.S1b - d) and thus the increase in the size of Tween-nAg was not the result of the particles being aggregated. The UV-vis absorption spectrum of the uncoated particles was broad with a maximum absorption peak at a wavelength of *ca*. 450 nm (Figure 3.1), consistent with the reported location of the surface plasmon absorption band of silver nanoparticles synthesized in this manner [20, 30]. According to Li et al. [20] the electron diffraction pattern of particles made in this manner is consistent with metallic silver; however, the observed red-shift and broadening of the absorption band relative to metallic silver nanoparticles of the same size [42] suggests the presence of an oxidized layer on the particle surface [20, 43-47]. Thus, the uncoated silver nanoparticles exhibit a "core-shell structure" with metallic silver as the core and the surface oxide layer as the outer shell (Figure 3.2). After coating with 1 mM citrate, the absorption band blue-shifted by *ca.* 5 nm to 445.5 nm. Silver nanoparticles coated by 10 mM citrate showed a more obvious blue-shift of the absorption peak to 429.5 nm as well as the formation of a more pronounced peak. These results were consistent with citrate reducing the oxide layer at the surface of silver nanoparticles to Ag(0) [46-50]. Conversely, silver nanoparticles coated by 1 mM SDS, 10 mM SDS and 10 mM Tween showed slight red-shifts of the adsorption peak to 453,

457.5 and 458.5 nm, respectively, which as will be discussed later suggested a slightly more oxidized surface (Figure 3.1).

The coated particle electrophoretic mobility values were less negative than those for the uncoated particles (Figure 3.3). For example, the average value for Citrate-nAg-1 at NaCl concentrations below 40 mM was -2.0×10^{-8} m^2/V-s, relative to that for Bare-nAg of -4.7×10^{-8} m^2/V-s. For SDS-nAg-1 and SDS-nAg-10, the corresponding values were -2.6×10^{-8} m^2/V-s and -1.7×10^{-8} m^2/V-s, respectively (Figure 3.3a). The values were not constant across this range of NaCl concentrations, however, as they became more negative as the NaCl concentration increased above 20 mM. At a NaCl concentration of 40 - 60 mM, the decreasing trend in the mobility values of Citrate-nAg-1 and SDS-nAg-1 stopped and as the NaCl concentration increased the mobility values became less negative. At high NaCl concentrations the values approached neutral.

The observed shift in the mobility values for Tween-nAg was larger, with values near -1.3×10^{-8} m^2/V-s at concentrations of NaCl below 40 mM. Above this NaCl concentration, the mobility values approached zero (Figure 3.3a). For SDS and Tween, the less negative electrophoretic mobility values likely reflect moderation of the highly negative charge of the oxide-coated particles due to the adsorption of more moderately (or neutrally) charged molecules, similar to that observed for natural organic matter coated particles [20, 51]. For citrate, however, which is often used as a reductant in certain nano-silver synthesis methods [52-54], the less negative mobility could also reflect the reduction of the surface oxide to Ag(0). Such a reaction would not only reduce the magnitude of the negative surface potential, it would also produce a blue-shift in the surface plasmon band.

A small blue-shift was observed for the Citrate-nAg-1, but it paled in comparison to that observed for Citrate-nAg-10. Unfortunately, the particle size of the Citrate-nAg-10 increased during the coating process to 170.5 nm as the 10 mM trisodium citrate induced particle aggregation. This inhibited further characterization of these particles. During this process, however, a fine layer of metallic silver was deposited on the inner wall of the reaction vessel. This, in combination with the obvious blue-shift in the surface plasmon band suggests a portion of the decrease in the negative surface potential of Citrate-nAg-1 resulted from the reduction of the surface oxide layer to metallic silver.

The electrophoretic mobility of the silver nanoparticles in $NaNO_3$ were very similar to those in NaCl, with the citrate- and SDS-coated particles exhibiting an overall increase compared to Bare-nAg at electrolyte concentrations below 40 mM $NaNO_3$ (Figure 3.3b). The trends for the SDS-, citrate- and uncoated-particles observed in intermediate concentrations of NaCl were also evident at similar concentrations of $NaNO_3$, albeit to a lesser extent. The electrophoretic mobility values for Tween-nAg maintained a slightly negative value that averaged -0.53×10^{-8} m^2/V-s across the range of $NaNO_3$ concentrations tested and showed no obvious trend with increasing electrolyte concentration.

Substituting $CaCl_2$ for NaCl resulted in a net increase in the electrophoretic mobility of the coated silver nanoparticles (Figure 3.3c). Unlike systems with monovalent electrolytes, values for citrate and SDS-coated particles in $CaCl_2$ showed no obvious increase with increasing electrolyte concentration as they were relatively constant at approximately -1×10^{-8} m^2/V-s (Figure 3.3c). These results were similar to those measured for Bare-nAg (Figure 3.3c) as well as for fulvic-acid-coated particles [20] and likely

result from the neutralization of the negative surface charge upon the adsorption of calcium ions [55]. The already near-neutral electrophoretic mobilities for Tween-nAg were little changed in the presence of $CaCl_2$, compared to systems with NaCl or $NaNO_3$, with the exception being that values were slightly more variable and slightly positive at select electrolyte concentrations.

3.3.2 Aggregation of Silver Nanoparticles in the Presence of Sodium Chloride

The aggregation kinetics of silver nanoparticles in NaCl varied with the type and concentration of coating agent (Figure 3.4a). Results for Bare-nAg from Li et al. [20] reproduced in Figure 3.4a were consistent with DLVO-type behavior and resulted in an estimated CCC of 40 mM NaCl. However, dissolution of these particles occurs in conjunction with the aggregation as the initial particle size, determined by reverse extrapolation of the time rate of change in the hydrodynamic particle size to time zero, decreased soon after electrolyte addition [20]. This decrease in particle size, which exhibited a dependence on NaCl concentration (Figure 3.5a), reflects a perturbation in the equilibrium status of the oxide layer at the particle surface and subsequent erosion of the underlying metallic particle [20]. It was also coincident with trends noted in the electrophoretic mobility values (see Figure 3.3a). In ion-free oxygenated systems, dissolution of the oxide layer at the particle surface is hindered by Ag^+ adsorption [48-50]. As schematically described in Figure 3.2, introducing an electrolyte such as NaCl results in the dissolution of the surface oxide layer due to an increase in the solubility of the surface oxide with increasing ionic strength as well as a redistribution and/or replacement of sorbed Ag^+ by the electrolyte ions [20]. This process could also expose

the metallic Ag core of the particle which is readily oxidized leading to further particle dissolution [48-50, 56]. Such changes in the physicochemical nature of the particle's surface were consistent with the previously mentioned changes observed in the electrophoretic mobility values (Figure 3.3a)

Differences in $1/W$ and the initial particle size of Citrate-nAg-1 with changing NaCl concentration showed no obvious differences with Bare-nAg, with a CCC of *ca*. 40 mM (Figure 3.4a), comparable to that observed for similar citrate-coated particles by Huynh and Chen [23]. Nearly identical trends in initial particle size with changing NaCl concentration for Citrate-nAg-1 and Bare-nAg were also observed (Figure 3.5a), indicating the citrate-coated silver nanoparticles readily dissolved. Huynh and Chen [23] did not make a similar observation as slight differences in particle preparation (e.g., application of ultrasound and centrifugation) seemed to produce particles that resisted dissolution. The value for the normalized $1/W$ under diffusion-limited conditions was less than one, however, as the rate at which Citrate-nAg-1 aggregated at high ionic strength conditions never reached that for Bare-nAg. The inability of citrate to significantly alter the stability of the silver nanoparticles was similar to that observed by Li et al. [20] for Nordic fulvic acid and reflects that any decrease in stability due to the moderation of the negative electrophoretic mobility of the Citrate-nAg-1 compared to Bare-nAg was potentially countered by an increase in steric interactions. While steric interactions are primarily thought to arise from the presence of larger molecules at the particle surface, Lenhart et al. [57] recently noted that even relatively small dicarboxylic organic acids

provide for some steric effects. These results suggest that citrate imparts some steric effects as well.

Particles coated with SDS exhibited aggregation behavior quite similar to that for Bare-nAg and Citrate-nAg-1 (Figure 3.4a). Although there was no obvious increase in the CCC for SDS-nAg-1 compared to Bare-nAg or Citrate-nAg-1, there was a slight increase in the CCC from 40 mM to 50 mM NaCl for SDS-nAg-10. As noted for Citrate-nAg-1, the normalized $1/W$ values for both SDS-nAg-1 and SDS-nAg-10 in the diffusion-limited regime were smaller than that for Bare-nAg. The normalized $1/W$ value for SDS-nAg-1 was 0.93 and that for SDS-nAg-10 was 0.78 (Table 1). These values were approximately 7 % and 22 % lower than Bare-nAg ($1/W$=1).

SDS may enhance particle stability by promoting electrosteric repulsion [58-60] as the negatively charged dodecyl sulfate molecules enhance electrostatic repulsion, and the compact coating layer enhances steric repulsion. The critical micelle concentration (CMC) for SDS in DI water is 8.3 mM [61]. When introduced to a particle suspension above the CMC, SDS is thought to assume a double-layer adsorption configuration [33, 38-39]. The first layer is comprised of SDS molecules oriented with the hydrophilic head groups attached to the particle surface and the hydrophobic tails directed outward. The second layer is oriented in the opposite manner, thereby directing the hydrophilic groups away from the particle surface. This double-layer coating structure, which similar surfactants do not assume, is thought to provide enhanced steric repulsion of SDS-coated silver nanoparticles when compared to particles coated with surfactants that do not form a similar structure [33, 38-39]. Particle suspensions coated at SDS concentrations less than

the CMC are less stable than those coated at SDS concentrations above the CMC as the double-layer structure is not formed and the corresponding steric repulsion it enhances is reduced [33, 38-39]. Since the SDS-nAg-10 particles were coated with SDS in excess of the CMC, it seems possible that a similar structure could have formed. Such a structure could have produced the slight increase in the stability of SDS-nAg-10 compared to SDS-nAg-1, because the SDS concentration used in coating the latter particle was below the CMC.

Similar to that for the citrate-coated nanoparticles, the measured electrophoretic mobility values of the SDS-coated nanoparticles were less negative than those for the uncoated particles (Figure 3.3a). This increase suggests, like citrate, that the moderately-charged SDS molecules mask the highly negative mobility imparted on the uncoated particles by the presence of the oxide layer. Values for SDS-nAg-10 were shifted slightly more than were those for SDS-nAg-1, perhaps reflecting the different configuration of the coating layers. Kvitek et al. [30] observed the opposite trend, however, differences in the particle synthesis, coating, and sample preparation methods used by Kvitek et al. [30] and us make comparisons of the results difficult. Since the SDS coating reduced electrostatic repulsion, the fact that stability was little changed and the normalized $1/W$ values were lower than unity suggests the coating layer of adsorbed SDS molecules induced steric repulsion [16, 38]. This effect was slightly more prominent for SDS-nAg-10 than SDS-nAg-1, again perhaps reflecting a difference in the configuration of the SDS coating layer for the two particle types.

The SDS coating reduced particle dissolution, as the initial particle sizes of SDS-nAg-1 and SDS-nAg-10 were consistently larger than Bare-nAg across the entire range of NaCl concentrations evaluated (Figure 3.5a). On average, the initial particle sizes of SDS-nAg-10 and SDS-nAg-1 were 21% and 14% larger than that of Bare-nAg, respectively. In neither case did the initial particle size exceed that measured for the uncoated particles of *ca*. 82 nm. The conformation of the SDS coating was not visible under TEM interrogation and thus we cannot provide a specific explanation for how SDS inhibited dissolution. From the literature, however, we suspect the adsorbed SDS provided a physical barrier near the particle surface [31] thereby hindering the approach of electrolyte ions responsible for disturbing surface equilibrium and initiating particle dissolution.

Unlike the subtle effects observed for particles coated with SDS or citrate, the effect of Tween on enhancing the stability and preventing the dissolution of the silver nanoparticles was pronounced. As shown in Figure 3.4a, the CCC for Tween-nAg in NaCl increased by approximately one order of magnitude from 40 mM to 500 mM. This was despite the nearly complete masking of the particle surface charge (see Figure 3.3a). As was observed for the SDS-coated particles, the average normalized $1/W$ value for Tween-nAg in the diffusion-limited aggregation regime of 0.74 was significantly less than that for Bare-nAg. Thus, the near neutral electrophoretic mobility of Tween-nAg together with the increased CCC and the lower normalized $1/W$ values implies the adsorbed Tween molecules imparted significant steric repulsion.

Similar to the stabilizing effects of polyethyleneglycol or polyvinylpyrrolidone [21, 30], the nonionic Tween molecules likely stabilized the silver nanoparticles through the formation of a coating layer that imparted sterically repulsive interactions. The magnitude and range of the steric repulsion resulting from such a coating layer depends upon the thickness and density of the adsorbed layer, which is a function of the underlying surface as well as the system conditions (e.g., pH, ionic strength and electrolyte type) [31-32]. The increase in the hydrodynamic diameter of Tween-nAg as measured by DLS to 88 nm from 82 nm provides evidence of the formation of an approximately 3 nm thick Tween coating layer. The depth and density of the coating layer is a function of the adsorbed concentration as well as the molecular weight of the stabilizing reagents [18, 31-32, 58, 62-64]. We did not quantify the adsorbed concentration of the coating agents onto the silver nanoparticles, but since the molecular weight of Tween (Tween 80: 1310 g/mol) is much greater than that for SDS (236 g/mol) or citrate (189 g/mol) we believe it reasonable to assume that Tween forms a thicker and denser coating layer than citrate or SDS and thus enhanced particle stability more so than did the other coating agents.

The initial particle size of Tween-nAg did not decrease until the concentration of NaCl reached 300 mM, thereby suggesting the Tween coating prevented dissolution as well as enhanced stability. As noted previously, the decrease in the initial size of the silver nanoparticles reflects a combination of dissolution and oxidative erosion reactions catalyzed by the addition of electrolytes such as NaCl [20, 56]. Coatings comprised of synthetic stabilizing agents or natural organic matter suppress electron transfer reactions because they reduce accessibility of the surface of the underlying particle to reactants

[65-70]. Scheutjens and Fleer [31] introduced a train-loop-tail model to describe the orientation of adsorbed polymers and how the orientation influenced particle behavior. Based on this theoretical framework, two mechanisms that could prevent particle dissolution can be identified. The first mechanism reflects inhibition of diffusion and interaction of electrolyte ions and other reagents with the particle surfaces due to the presence of the coating layer. The second mechanism entails a reduction in the reaction rate due to the coating layer directly blocking access to reactive sites at the particle surface. Layer thickness and density are the main factors affecting the decreasing surface reactivity [31, 70]. For example, Phenrat et al. [70] observed a decrease in the rate of TCE dechlorination by nanoscale zerovalent iron as the amount of polyelectrolyte coating increased. Consistent with the stabilizing effects of SDS and Tween, it seems reasonable to assume that the Tween coating layer was thicker and more rigid than was the SDS layer allowing Tween-nAg to resist dissolution better than the SDS-coated particles.

Dissolution of the uncoated silver nanoparticles occurred soon after the addition of electrolytes and even though the initial particle size decreased, the aggregation profiles under diffusion-limited conditions showed a linear increase with time at the beginning of the aggregation process [20]. The coated particles, however, exhibited less dissolution and this decrease in the initial particle sizes became less obvious with the increase in the protecting abilities of the stabilizing reagents. For example, SDS-nAg-10 and Tween-nAg showed a smaller decrease in the initial particle size, with the initial sizes being 21 % and 32 % larger, respectively, than that of Bare-nAg (see Figure 3.6a). A “sag” in the in the aggregation profile was also observed for the Tween-nAg at NaCl concentrations in

excess of 300 mM (See Figure 3.6b), implying the nearly instantaneous dissolution observed for Bare-nAg was slowed by the protective Tween coating layer.

As previously noted, TEM images of the coated silver nanoparticles suspended in DI water did not provide evidence of any obvious changes in the shape, morphology or size of the particles (Figure B.S-1). To compare morphologies of the Bare-nAg aggregates to those with coatings, images were collected of samples prepared at the conclusion of 15 minutes of aggregation at 100 mM electrolyte concentration. Images of Citrate-nAg-1 aggregates showed a secondary deposit connecting the single particles to one another (Figure 3.7a), similar to that for the uncoated silver particles observed by Li et al. [20]. Consistent with the presence of similar features in images of uncoated particle aggregates, these deposits likely represent an AgCl deposit formed as the Cl^- ions reacted with the Ag^+ ions released from the dissolving silver nanoparticles. Like the Bare-nAg and Citrate-nAg-1 aggregates, the SDS-nAg-10 aggregates also appeared to be connected by the AgCl deposit in systems with 100 mM NaCl (Figure 3.7b); however, the individual particles were more readily apparent in this system. An image for SDS-nAg-1 was not collected, since its aggregation and dissolution behavior were quite similar to Bare-nAg and Citrate-nAg-1 no obvious morphological differences were expected. Thus, consistent with the SDS coating present on the SDS-nAg-10 particles hindering their dissolution, the formation of the AgCl deposit was slightly decreased. For Tween-nAg, neither aggregates nor AgCl deposit was observed in 100 mM NaCl as the imaged nanoparticles were still dispersed and looked identical to those in DI water (see Figure B.S-1d). We attempted to collect TEM images of Tween-nAg in 1M NaCl, corresponding

to the concentration where aggregation occurred, but salt crystals formed during sample preparation under such high electrolyte concentrations completely obscured the nanoparticles.

3.3.3 Aggregation of Silver Nanoparticles in the Presence of Sodium Nitrate

The aggregation behavior of the uncoated and coated nanosilver in $NaNO_3$ generally followed trends observed in NaCl. The CCC for citrate-coated nanoparticles in $NaNO_3$ was approximately 30 mM (Figure 3.4b), which was similar to the value for Bare-nAg and slightly less than the value measured in NaCl. The CCC for SDS-nAg-1 was also close to 30 mM $NaNO_3$, but that for SDS-nAg-10 was slightly increased to 40 mM $NaNO_3$. The average of the uncoated-particle normalized $1/W$ values under diffusion-limited conditions for SDS-nAg-1 and SDS-nAg-10 were 0.92 and 0.69, respectively and that for Citrate-nAg-1 was 0.94 (Table 1). Thus, similar to what was observed in NaCl, the SDS and citrate coatings appear to provide a modicum of steric stability to the particles in $NaNO_3$.

The initial particle size of the citrate-coated particles in $NaNO_3$, like in NaCl, followed a decreasing trend with increasing electrolyte concentration similar to that observed with the uncoated particles (Figure 3.5b). Unlike in NaCl, particles covered with 1 mM SDS readily dissolved; the average initial particle size of SDS-nAg-1 was 65 nm compared with that of Bare-nAg of 63 nm and Citrate-nAg-1 of 64 nm. The SDS-nAg-10 particles, however, did resist dissolution and had an average initial particle size of 76 nm, which was similar to that observed in NaCl. Comparing the initial particle size of the citrate and SDS-coated particles, we note the sizes were bigger in elevated concentrations of $NaNO_3$

than in similar concentrations of NaCl (Figure 3.8a - c), suggesting the stabilizing agents inhibit dissolution better in $NaNO_3$ than in NaCl. Consistent with this result were the smaller shifts observed in the electrophoretic mobility values (Figure 3.3b). Similar to the uncoated particles, no secondary deposit was observed for the Citrate-nAg-1 or SDS-nAg-10 aggregates in $NaNO_3$, where the TEM images showed aggregates composed of distinct particles with little evidence of a secondary deposit (Figure 3.7c, d).

Differences in the magnitude of stabilization and extent of particle dissolution in NaCl or $NaNO_3$ suggest the electrolyte anion plays more of a role in particle behavior than simply providing a ligand to form insoluble complexes. This was further supported by distinct differences in the aggregation of Tween-nAg in NaCl and $NaNO_3$. Even though the concentration of $NaNO_3$ was increased to 1 M, the Tween-nAg particles did not aggregate as the hydrodynamic diameter remained at *ca.* 90 nm across the entire 15 min experiment. In NaCl, the same particles had a CCC of 500 mM and exhibited an obvious decrease in initial particle size (see Figures 4b and 5b). Thus, the marked differences in the systems suggest that Tween-nAg interacts with NO_3^- differently than Cl^-. The difference was not believed to reflect ion size, since the hydrated radius of Cl^- at 3.32 Å and NO_3^- at 3.35 Å are quite close [71] and thus not likely to produce much of an effect. Also, there is no mention of any specific affinity for NO_3^- by Tween documented in the literature and thus it was unlikely that the lack of dissolution or aggregation was due to NO_3^- ions being complexed by the Tween layers.

Oxidative dissolution of metallic silver nanoparticles in the presence of an electron accepter is catalyzed by nucleophilic reagents which change the chemical potential or

Fermi level at the particle surface [48-50, 72]. This oxidation is controlled by the difference in the chemical potential between a silver nanoparticle (with adsorbed Ag^+, nucleophilic agent, or stabilizing agents) and an electron acceptor [50]. For uncoated silver nanoparticles, the oxidation of Ag(0) to Ag^+ at the particle surface shifts the chemical potential of the particle to a more positive value and if it approaches that of the electron acceptor (e.g., O_2) oxidation ceases [49-50]. The opposite shift in the potential occurs for metallic silver nanoparticles with adsorbed nucleophiles (e.g., Cl^- or NO_3^-) resulting in an increase in the oxidation of Ag(0) [48-50]. Evidence of these potential shifts is manifest by changes in the position of the surface plasmon band of the silver nanoparticles [48, 49]. An increase in the potential results in a red-shift, whereas a decrease produces a blue-shift [48-49]. The silver nanoparticles in our system were already coated with an oxide layer, however, shifts in the surface plasmon band could be used to infer changes in surface potential. For example, the plasmon band for citrate-coated particles were blue-shifted, which was most notable at 10 mM citrate (see Figure 3.1), consistent with a reduction of the surface oxide. On the other hand, Tween-coated particles exhibited a slight red-shift and broadening of the plasmon band (see Figure 3.1). As a result, the potential of Tween-nAg likely increased, making these particles less susceptible to further oxidation. This shift may explain, in part, why the dissolution of Tween-nAg was inhibited to such a great extent. It was also consistent with the near complete lack of dissolution in the presence of NO_3^-, which with a nucleophilicity of 1.0 compared to that for Cl^- of 3.0 [73] should be less able to catalyze oxidation and dissolution of the silver nanoparticle [50]. Although exactly why remains unclear, this

difference in nucleophilicity between Cl^- and NO_3^- may also be partly responsible for the differences observed in the aggregation behavior of Tween-nAg in the two electrolyte solutions.

3.3.4 Aggregation of Silver Nanoparticles in the Presence of Calcium Chloride

Except for Tween-nAg, the aggregation behavior observed in $CaCl_2$ was similar to that observed in NaCl. The CCC shifted to lower concentrations as the divalent calcium ion was more effective in screening surface charge (Figure 3.4c), but trends observed with the citrate and SDS-coated particles were similar to those for the same particles in NaCl and were comparable to the uncoated particles. Changes in initial size were also quite similar for these particles (Figure 3.5c). SDS-nAg-10 aggregates appeared to be connected by the AgCl deposit in systems with 10 mM $CaCl_2$, as shown in Figure 3.7e. The stability of the Tween-nAg in $CaCl_2$ was quite different from that in NaCl, however. In $CaCl_2$, the CCC for Tween-nAg increased from 2 mM to ca. 700 mM $CaCl_2$ and the maximum aggregation rate provided a very low normalized $1/W$ value of just 0.23. There was also no decrease in the initial particle size for Tween-nAg in $CaCl_2$. In fact, the initial particle size increased from 90.9 nm at 50 mM $CaCl_2$ to 117.4 nm at 1 M $CaCl_2$. Possible aggregation mechanisms involved were (1) the high charge screening efficiency of divalent Ca^{2+} ions to the ionized groups in the Tween molecules [31], or (2) specific interaction with alkaline-earth metal ions to promote dehydration of both Ca^{2+} ions and the Tween molecules [74]. Both would compress the Tween coating layer, thereby increasing the layer density and/or reducing the steric repulsion force, and inducing aggregation without decreasing the initial particle size.

3.4. Conclusions

To conclude, silver nanoparticles coated with stabilizing agents that provided steric repulsion enhanced stability and reduced dissolution when compared to negatively-charged uncoated particles or particles coated with an electrostatic stabilizing agent. Electrostatic stabilization using a low molecular weight molecule, citrate, showed no obvious effects as the aggregation of the particles and decrease in the initial particle size differed little from those for Bare-nAg. The highly-negative surface potential of the particles as approximated by the electrophoretic mobility became less negative in the presence of all of the coating agents, including those that carry a negative charge (citrate and SDS). For the electrosteric coating reagent, SDS, increasing the initial coating concentration from 1 mM to 10 mM, which was above the CMC of SDS, caused a slight increase in the CCC reflective of an increase in steric repulsion. SDS inhibited particle dissolution, particularly at a coating concentration of 10 mM, whereas citrate did not. The non-ionic steric stabilizer, Tween, significantly enhanced stability. This stabilizer also physically protected the integrity of particles as dissolution was significantly reduced. The behavior of the Tween-coated silver nanoparticles also exhibited a dependence on electrolyte type, as its stability was greater and dissolution was lower in $NaNO_3$ than in NaCl. While the specific mechanism for this difference was not determined, it appears to relate to differences in the nucleophilicities of Cl^- and NO_3^- ions. Results of this study indicate that silver nanoparticles coated with molecules stabilizers that enhance steric repulsion may possess greater stabilities and hence greater mobility, than uncoated particles in natural water systems. Since toxicity is related to aggregation state, sterically-

stabilized particles such as those coated with Tween could present a greater risk to aquatic organisms.

Acknowledgements

This research has been supported by the U.S. National Oceanic and Atmospheric Administration through its Ohio Sea Grant College Program. The authors would like to acknowledge the Nanotech West Laboratory at The Ohio State University for assistance with DLS measurements. Images presented were generated using the instruments and services at the Campus Microscopy and Imaging Facility, The Ohio State University.

Supporting Information Available: Figure B.S1. This material is available free of charge via the Internet at http://pubs.acs.org.

References

[1] Navarro, E., et al., *Toxicity of Silver Nanoparticles to Chlamydomonas reinhardtii.* Environmental Science & Technology, 2008. **42**(23): p. 8959-8964.

[2] Maynard, A., et al., *Safe handling of nanotechnology.* Nature, 2006. **444**(7117): p. 267-269.

[3] Benn, T.M. and P. Westerhoff, *Nanoparticle silver released into water from commercially available sock fabrics.* Environmental Science & Technology, 2008. **42**(11): p. 4133-4139.

[4] Mueller, N.C. and B. Nowack, *Exposure modeling of engineered nanoparticles in the environment.* Environmental Science & Technology, 2008. **42**(12): p. 4447-4453.

[5] Gottschalk, F., et al., *Modeled Environmental Concentrations of Engineered Nanomaterials (TiO2, ZnO, Ag, CNT, Fullerenes) for Different Regions.* Environmental Science & Technology, 2009. **43**(24): p. 9216-9222.

[6] Kim, J.S., et al., *Antimicrobial effects of silver nanoparticles.* Nanomedicine-Nanotechnology Biology and Medicine, 2007. **3**(1): p. 95-101.

[7] Lee, H.Y., et al., *A practical procedure for producing silver nanocoated fabric and its antibacterial evaluation for biomedical applications.* Chemical Communications, 2007(28): p. 2959-2961.

[8] Pal, S., Y.K. Tak, and J.M. Song, *Does the antibacterial activity of silver nanoparticles depend on the shape of the nanoparticle? A study of the gram-negative bacterium Escherichia coli.* Applied and Environmental Microbiology, 2007. **73**(6): p. 1712-1720.

[9] Panacek, A., et al., *Silver colloid nanoparticles: Synthesis, characterization, and their antibacterial activity.* Journal of Physical Chemistry B, 2006. **110**(33): p. 16248-16253.

[10] Shahverdi, A.R., et al., *Synthesis and effect of silver nanoparticles on the antibacterial activity of different antibiotics against Staphylococcus aureus and Escherichia coli.* Nanomedicine-Nanotechnology Biology and Medicine, 2007. **3**(2): p. 168-171.

[11] Sondi, I. and B. Salopek-Sondi, *Silver nanoparticles as antimicrobial agent: a case study on E-coli as a model for Gram-negative bacteria.* Journal of Colloid and Interface Science, 2004. **275**(1): p. 177-182.

[12] Morones, J.R., et al., *The bactericidal effect of silver nanoparticles.* Nanotechnology, 2005. **16**(10): p. 2346-2353.

[13] Lecoanet, H.F. and M.R. Wiesner, *Velocity effects on fullerene and oxide nanoparticle deposition in porous media.* Environmental Science & Technology, 2004. **38**(16): p. 4377-4382.

[14] Brant, J., H. Lecoanet, and M.R. Wiesner, *Aggregation and deposition characteristics of fullerene nanoparticles in aqueous systems.* Journal of Nanoparticle Research, 2005. **7**(4-5): p. 545-553.

[15] Chen, K.L., S.E. Mylon, and M. Elimelech, *Aggregation kinetics of alginate-coated hematite nanoparticles in monovalent and divalent electrolytes.* Environmental Science & Technology, 2006. **40**(5): p. 1516-1523.

[16] Chen, K.L. and M. Elimelech, *Influence of humic acid on the aggregation kinetics of fullerene (C-60) nanoparticles in monovalent and divalent electrolyte solutions.* Journal of Colloid and Interface Science, 2007. **309**(1): p. 126-134.

[17] Hyung, H., et al., *Natural organic matter stabilizes carbon nanotubes in the aqueous phase.* Environmental Science & Technology, 2007. **41**(1): p. 179-184.

[18] Phenrat, T., et al., *Stabilization of aqueous nanoscale zerovalent iron dispersions by anionic polyelectrolytes: adsorbed anionic polyelectrolyte layer properties and their effect on aggregation and sedimentation.* Journal of Nanoparticle Research, 2008. **10**(5): p. 795-814.

[19] Saleh, N., et al., *Ionic strength and composition affect the mobility of surface-modified Fe-0 nanoparticles in water-saturated sand columns.* Environmental Science & Technology, 2008. **42**(9): p. 3349-3355.

[20] Li, X.A., J.J. Lenhart, and H.W. Walker, *Dissolution-Accompanied Aggregation Kinetics of Silver Nanoparticles.* Langmuir, 2010. **26**(22): p. 16690-16698.

[21] El Badawy, A., et al., *Impact of Environmental Conditions (pH, Ionic Strength, and Electrolyte Type) on the Surface Charge and Aggregation of Silver Nanoparticles Suspensions.* Environmental Science & Technology, 2010: p. 1260-1266.

[22] Jin, X., et al., *High-Throughput Screening of Silver Nanoparticle Stability and Bacterial Inactivation in Aquatic Media: Influence of Specific Ions.* Environmental Science & Technology, 2010. **44**(19): p. 7321-7328.

[23] Huynh, K.A. and K.L. Chen, *Aggregation Kinetics of Citrate and Polyvinylpyrrolidone Coated Silver Nanoparticles in Monovalent and Divalent Electrolyte Solutions.* Environmental Science & Technology, 2011: p. null-null.

[24] Derjaguin B. V., L., L. D., *Theory of the stability of strongly charged lyophobic sols and of the adhesion of strongly charged particles in solutions of electrolytes.* Acta Physiconchim, 1941. **14**: p. 733-762.

[25] Verwey E. J. W., O.J.T.G., *Theory of the stability of lyophobic colloids*. 1948, Amsterdam: Elsevier.

[26] Liu, X., et al., *Influence of Ca(2+) and Suwannee River Humic Acid on aggregation of silicon nanoparticles in aqueous media.* Water Research, 2011. **45**(1): p. 105-12.

[27] Elimelech, M.G., J.; Jia, X.; Williams, R. J., *Particle Deposition & Aggregation: Measurement, Modelling and Simulation*. 1995, Oxford: Butterworth-Heinemann.

[28] Shrivastava, S., et al., *Characterization of enhanced antibacterial effects of novel silver nanoparticles.* Nanotechnology, 2007. **18**(22): p. -.

[29] Teeguarden, J.G., et al., *Particokinetics in vitro: Dosimetry considerations for in vitro nanoparticle toxicity assessments.* Toxicological Sciences, 2007. **95**(2): p. 300-312.

[30] Kvitek, L., et al., *Effect of surfactants and polymers on stability and antibacterial activity of silver nanoparticles (NPs).* Journal of Physical Chemistry C, 2008. **112**(15): p. 5825-5834.

[31] Fleer, G.J., *Polymers at interfaces*. 1993, London: Chapman & Hall. xviii, 502 p.

[32] Holmberg, K., *Surfactants and polymers in aqueous solution*. 2nd ed. 2003, Chichester: Wiley. xvi, 545 p.

[33] Mafune, F., et al., *Structure and stability of silver nanoparticles in aqueous solution produced by laser ablation.* Journal of Physical Chemistry B, 2000. **104**(35): p. 8333-8337.

[34] Chou, K.S. and Y.S. Lai, *Effect of polyvinyl pyrrolidone molecular weights on the formation of nanosized silver colloids.* Materials Chemistry and Physics, 2004. **83**(1): p. 82-88.

[35] Goff, H.D., *Colloidal aspects of ice cream - A review.* International Dairy Journal, 1997. **7**(6-7): p. 363-373.

[36] Dorjnamjin, D., M. Ariunaa, and Y.K. Shim, *Synthesis of silver nanoparticles using hydroxyl functionalized ionic liquids and their antimicrobial activity.* International Journal of Molecular Sciences, 2008. **9**(5): p. 807-819.

[37] Yu, D.G., *Formation of colloidal silver nanoparticles stabilized by Na+-poly(gamma-glutamic acid)-silver nitrate complex via chemical reduction process.* Colloids and Surfaces B-Biointerfaces, 2007. **59**(2): p. 171-178.

[38] Chen, Y.H. and C.S. Yeh, *Laser ablation method: use of surfactants to form the dispersed Ag nanoparticles.* Colloids and Surfaces a-Physicochemical and Engineering Aspects, 2002. **197**(1-3): p. 133-139.

[39] Mafune, F., et al., *Formation and size control of sliver nanoparticles by laser ablation in aqueous solution.* Journal of Physical Chemistry B, 2000. **104**(39): p. 9111-9117.

[40] Virden, J.W. and J.C. Berg, *The Use of Photon-Correlation Spectroscopy for Estimating the Rate-Constant for Doublet Formation in an Aggregating Colloidal Dispersion.* Journal of Colloid and Interface Science, 1992. **149**(2): p. 528-535.

[41] Holthoff, H., et al., *Coagulation rate measurements of colloidal particles by simultaneous static and dynamic light scattering.* Langmuir, 1996. **12**(23): p. 5541-5549.

[42] Sukhov, N.L., et al., *Absorption spectra of large colloidal silver particles in aqueous solution.* Russian Chemical Bulletin, 1997. **46**(1): p. 197-199.

[43] Kapoor, S., *Preparation, characterization, and surface modification of silver particles.* Langmuir, 1998. **14**(5): p. 1021-1025.

[44] Mie, G., Ann. Phys., 1908. **25**: p. 377.

[45] Hulst, V.d., *Light Scattering by Small Particles*. 1957, New York: Wiley.

[46] Yin, Y.D., et al., *Synthesis and characterization of stable aqueous dispersions of silver nanoparticles through the Tollens process.* Journal of Materials Chemistry, 2002. **12**(3): p. 522-527.

[47] Chen, M., et al., *Preparation and study of polyacryamide-stabilized silver nanoparticles through a one-pot process.* Journal of Physical Chemistry B, 2006. **110**(23): p. 11224-11231.

[48] Mulvaney, P., T. Linnert, and A. Henglein, *Surface-Chemistry of Collodial Silver in Aqueous-Solution - Observations on Chemisorption and Reactivity. Journal of Physical Chemistry*, 1991. **95**(20): p. 7843-7846.

[49] Henglein, A., *Colloidal silver nanoparticles: Photochemical preparation and interaction with O-2, CCl4, and some metal ions.* Chemistry of Materials, 1998. **10**(1): p. 444-450.

[50] Henglein, A., T. Linnert, and P. Mulvaney, *Reduction of Ag+ in Aqueous Polyanion Solution - Some Properties and Reactions of Long-Lived Loigomeric Silver Clusters and Metallic Silver Particles.* Berichte der Bunsen-Gesellschaft-Physical Chemistry Chemical Physics, 1990. **94**(12): p. 1449-1457.

[51] Pelley, A.J. and N. Tufenkji, *Effect of particle size and natural organic matter on the migration of nano- and microscale latex particles in saturated porous media.* Journal of Colloid and Interface Science, 2008. **321**(1): p. 74-83.

[52] J. Turkevich, P.C.S., J. Hillier,, *A study of the nucleation and growth processes in the synthesis of colloidal gold.* Discuss. Faraday. Soc. , 1951. **11**: p. 55-75.

[53] Sarkar, P., et al., *Aqueous-Phase Synthesis of Silver Nanodiscs and Nanorods in Methyl Cellulose Matrix: Photophysical Study and Simulation of UV-Vis Extinction Spectra Using DDA Method.* Nanoscale Research Letters, 2010. **5**(10): p. 1611-1618.

[54] Pillai, Z.S. and P.V. Kamat, *What factors control the size and shape of silver nanoparticles in the citrate ion reduction method?* Journal of Physical Chemistry B, 2004. **108**(3): p. 945-951.

[55] Stumm, W., *Reactivity at the mineral-water interface: Dissolution and inhibition.* Colloids and Surfaces a-Physicochemical and Engineering Aspects, 1997. **120**(1-3): p. 143-166.

[56] Liu, J.Y. and R.H. Hurt, *Ion Release Kinetics and Particle Persistence in Aqueous Nano-Silver Colloids.* Environmental Science & Technology, 2010. **44**(6): p. 2169-2175.

[57] Lenhart, J.J., et al., *The influence of dicarboxylic acid structure on the stability of colloidal hematite.* Journal of Colloid and Interface Science, 2010. **345**(2): p. 556-560.

[58] Napper, D.H., *Polymeric stabilization of colloidal dispersions*. Colloid science. 1983, San Diego ; London: Academic Press. xvi, 428 p.

[59] Romero-Cano, M.S., A. Martin-Rodriguez, and F.J. de las Nieves, *Electrosteric stabilization of polymer colloids with different functionality.* Langmuir, 2001. **17**(11): p. 3505-3511.

[60] Fritz, G., et al., *Electrosteric stabilization of colloidal dispersions.* Langmuir, 2002. **18**(16): p. 6381-6390.

[61] Cifuentes, A., J.L. Bernal, and J.C. DiezMasa, *Determination of critical micelle concentration values using capillary electrophoresis instrumentation.* Analytical Chemistry, 1997. **69**(20): p. 4271-4274.

[62] Chodanowski, P. and S. Stoll, *Polyelectrolyte adsorption on charged particles in the Debye-Huckel approximation. A Monte Carlo approach.* Macromolecules, 2001. **34**(7): p. 2320-2328.

[63] Cesarano, J., I.A. Aksay, and A. Bleier, *Stability of Aqueous Alpha-Al2o3 Suspensions with Poly(Methacrylic Acid) Poly-Electrolyte.* Journal of the American Ceramic Society, 1988. **71**(4): p. 250-255.

[64] Kirby, G.H., et al., *Poly(acrylic acid)-poly(ethylene oxide) comb polymer effects on BaTiO3 nanoparticle suspension stability.* Journal of the American Ceramic Society, 2004. **87**(2): p. 181-186.

[65] Fabrega, J., et al., *Silver Nanoparticle Impact on Bacterial Growth: Effect of pH, Concentration, and Organic Matter.* Environmental Science & Technology, 2009. **43**(19): p. 7285-7290.

[66] Ho, C.M., et al., *Oxidative Dissolution of Silver Nanoparticles by Biologically Relevant Oxidants: A Kinetic and Mechanistic Study.* Chemistry-an Asian Journal, 2010. **5**(2): p. 285-293.

[67] Saleh, N., et al., *Surface modifications enhance nanoiron transport and NAPL targeting in saturated porous media.* Environmental Engineering Science, 2007. **24**(1): p. 45-57.

[68] Tratnyek, P.G., et al., *Effects of natural organic matter, anthropogenic surfactants, and model quinones on the reduction of contaminants by zero-valent iron.* Water Research, 2001. **35**(18): p. 4435-4443.

[69] Xu, J., A. Dozier, and D. Bhattacharyya, *Synthesis of nanoscale bimetallic particles in polyelectrolyte membrane matrix for reductive transformation of halogenated organic compounds.* Journal of Nanoparticle Research, 2005. **7**(4-5): p. 449-467.

[70] Phenrat, T., et al., *Adsorbed Polyelectrolyte Coatings Decrease Fe-0 Nanoparticle Reactivity with TCE in Water: Conceptual Model and Mechanisms.* Environmental Science & Technology, 2009. **43**(5): p. 1507-1514.

[71] Nightingale, E.R., *Phenomenological Theory of Ion Solvation. Effective Radii of Hydrated Ions.* The Journal of Physical Chemistry, 1959. **63**(9): p. 1381-1387.

[72] Kittel, C. and H. Kroemer, *Thermal physics*. 2d ed. 1980, San Francisco: W. H. Freeman. xvii, 473 p.

[73] Swain, C.G. and C.B. Scott, *Quantitative Correlation of Relative Rates. Comparison of Hydroxide Ion with Other Nucleophilic Reagents toward Alkyl Halides, Esters, Epoxides and Acyl Halides1.* Journal of the American Chemical Society, 1953. **75**(1): p. 141-147.

[74] Konradi, R. and J. Ruhe, *Interaction of poly(methacrylic acid) brushes with metal ions: Swelling properties.* Macromolecules, 2005. **38**(10): p. 4345-4354.

Tables and Figures

Table 3.1 Normalized $1/W$ values under diffusion-limited conditions for the coated silver nanoparticles.

	Bare-nAg	Citrate-nAg-1	SDS-nAg-1	SDS-nAg-10	Tween-nAg
NaCl	1	0.95	0.93	0.78	0.74
$NaNO_3$	1	0.94	0.92	0.69	N/A
$CaCl_2$	1	0.89	0.93	0.67	0.23

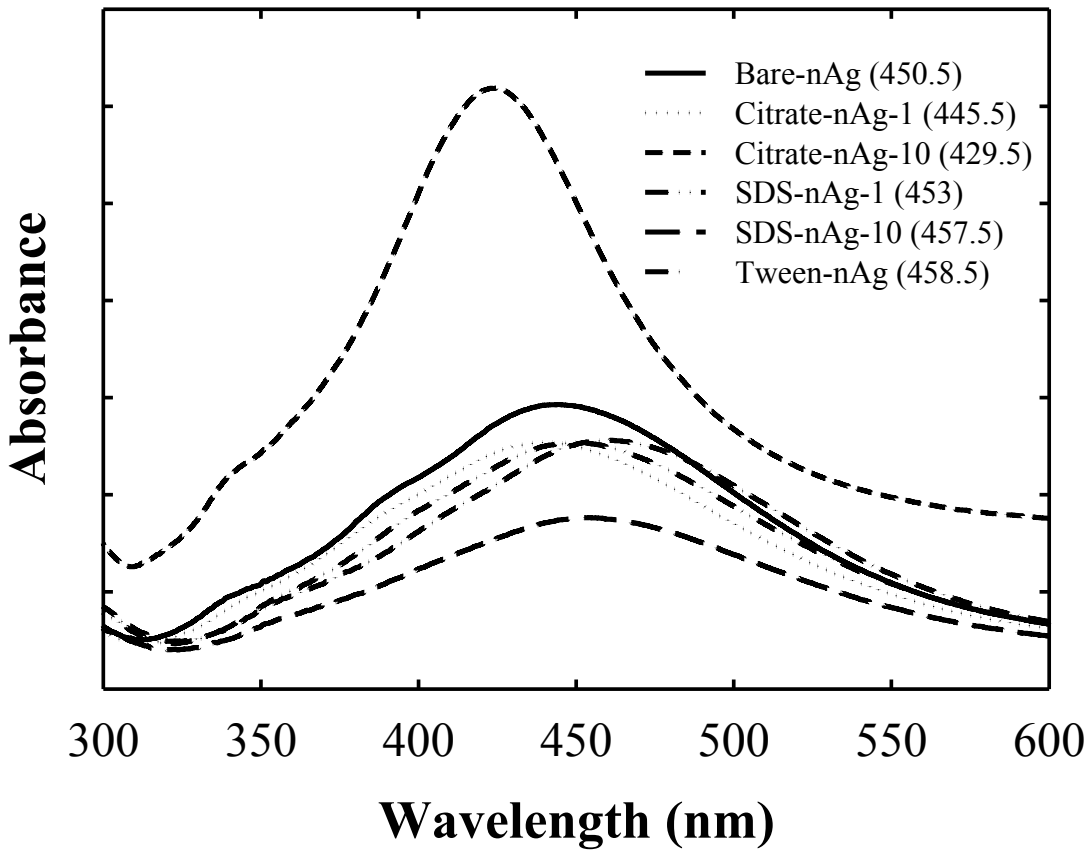

Figure 3.1 UV-vis absorption spectrum of Bare-nAg, Citrate-nAg-1, Citrate-nAg-10, SDS-nAg-1, SDS-nAg-10 and Tween-nAg. The wavelength for each peak are noted in parenthesis.

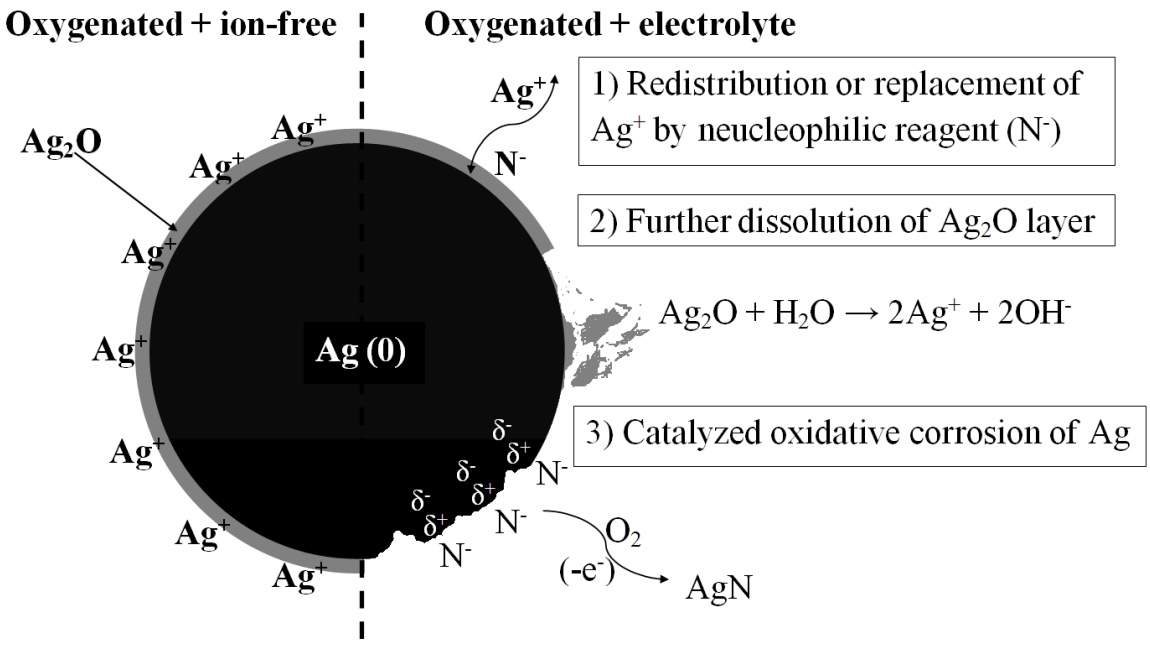

Figure 3.2 Schematic illustration of surface oxidation and dissolution of the oxide-layer coated silver nanoparticles.

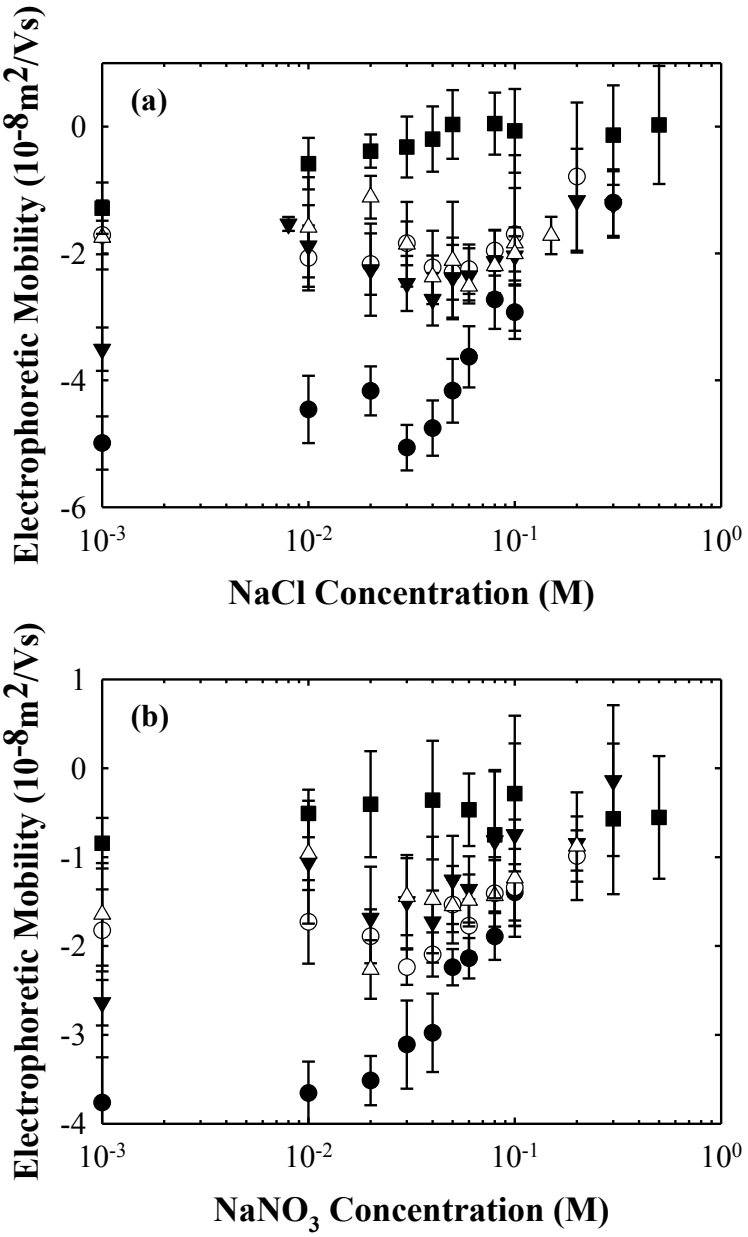

Figure 3.3 Electrophoretic mobilities of Bare-nAg (●), Citrate-nAg-1 (○), SDS-nAg-1 (▼), SDS-nAg-10 (△), and Tween-nAg (■) at pH 7.0 as a function of (a) NaCl, (b) $NaNO_3$ and (c) $CaCl_2$ concentration. The data for Bare-nAg is from Li et al. [20]. (Continued)

Figure 3.3: (Continued)

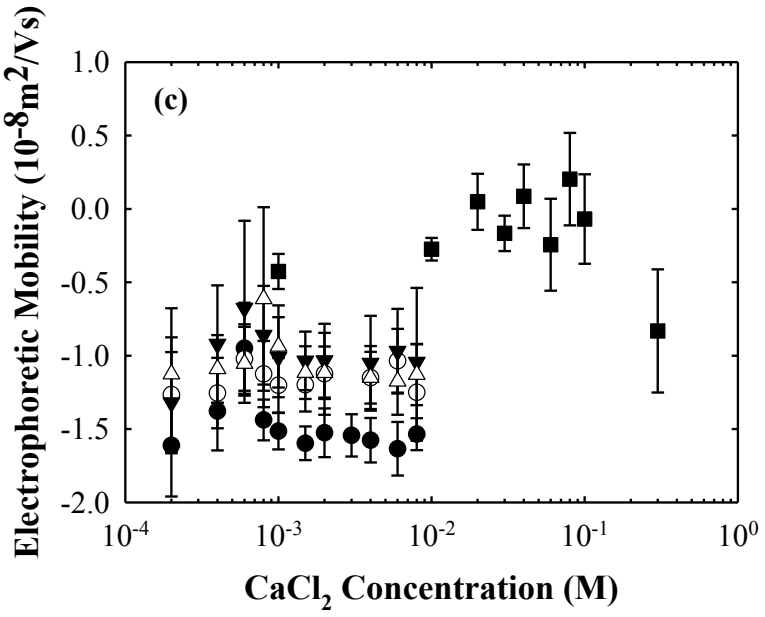

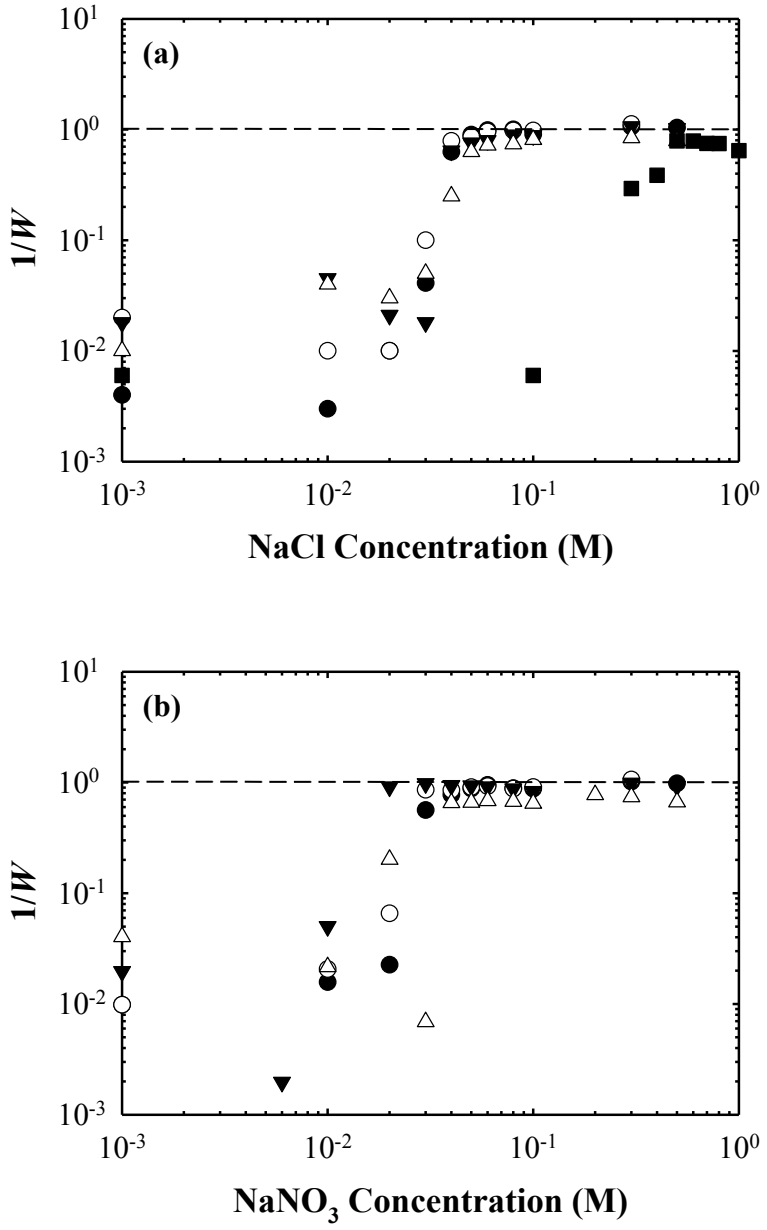

Figure 3.4 Inverse stability ratio ($1/W$) of Bare-nAg (●), Citrate-nAg-1 (○), SDS-nAg-1 (▼), SDS-nAg-10 (△), and Tween-nAg (■) as a function of (a) NaCl, (b) $NaNO_3$ and (c) $CaCl_2$ concentrations. The data for Bare-nAg is from Li et al. [20]. (Continued)

Figure 3.4: (Continued)

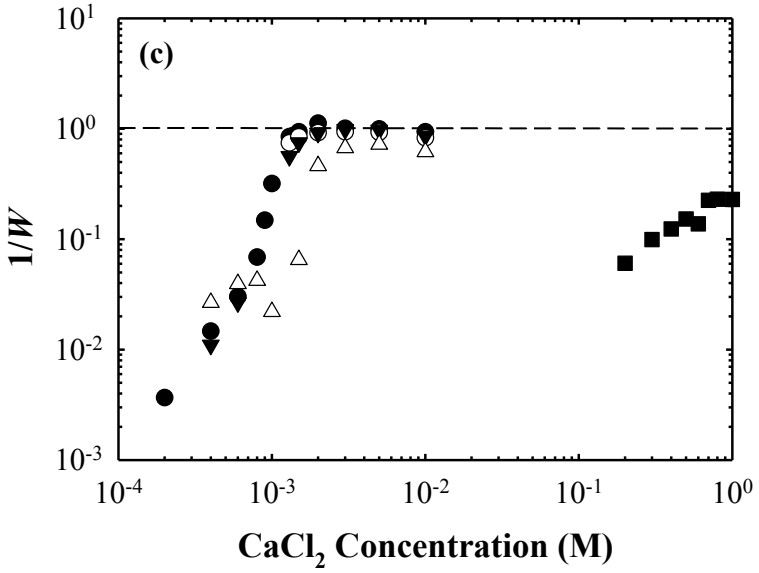

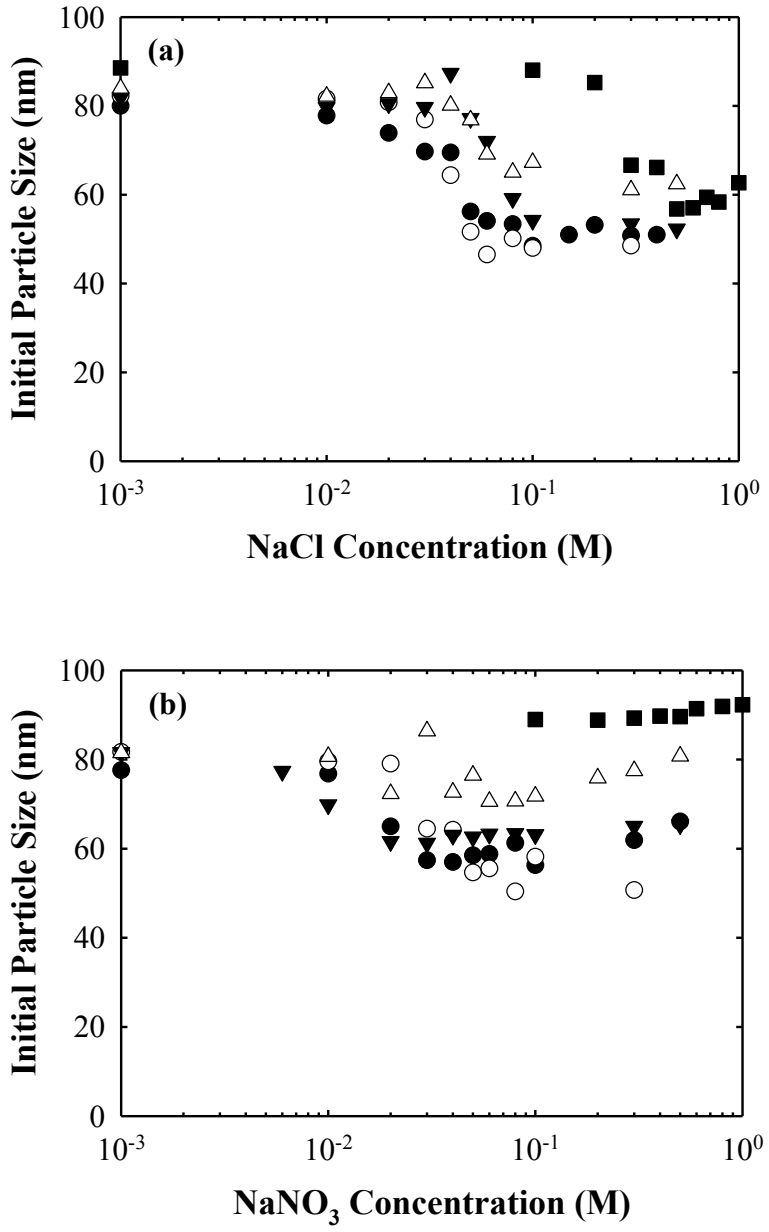

Figure 3.5 Initial hydrodynamic diameter of Bare-nAg (●), Citrate-nAg-1 (○), SDS-nAg-1 (▼), SDS-nAg-10 (△), and Tween-nAg (■) as a function of (a) NaCl, (b) $NaNO_3$ and (c) $CaCl_2$ concentrations. The data for Bare-nAg is from Li et al. [20]. (Continued)

Figure 3.5: (Continued)

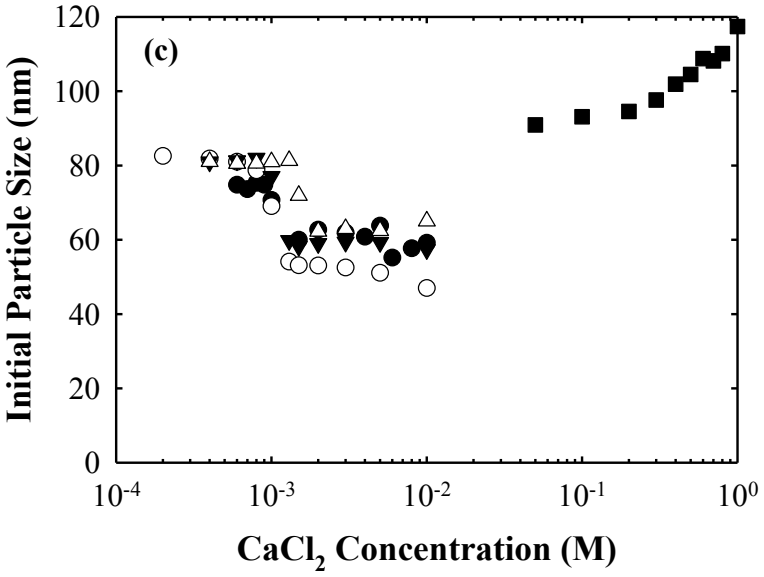

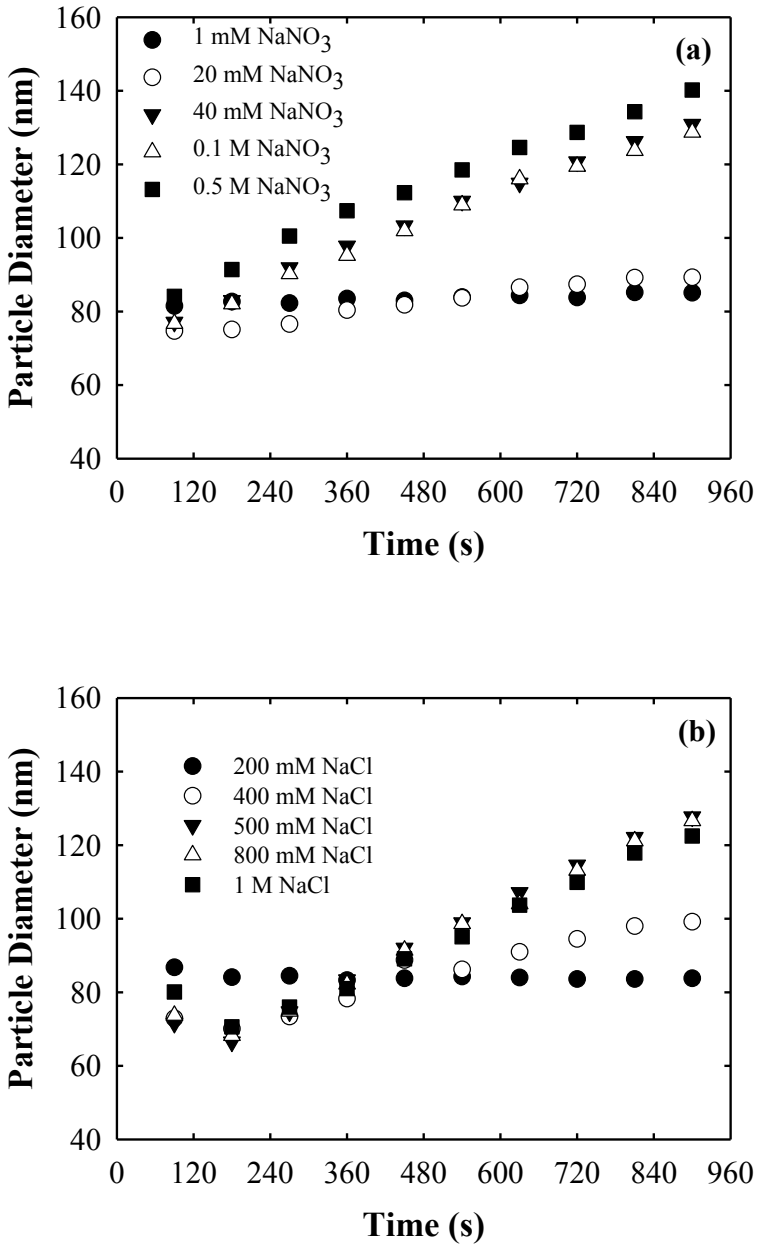

Figure 3.6 Aggregation profiles of (a) SDS-nAg-10 as a function of $NaNO_3$ concentration and (b) Tween-nAg as a function of NaCl concentration.

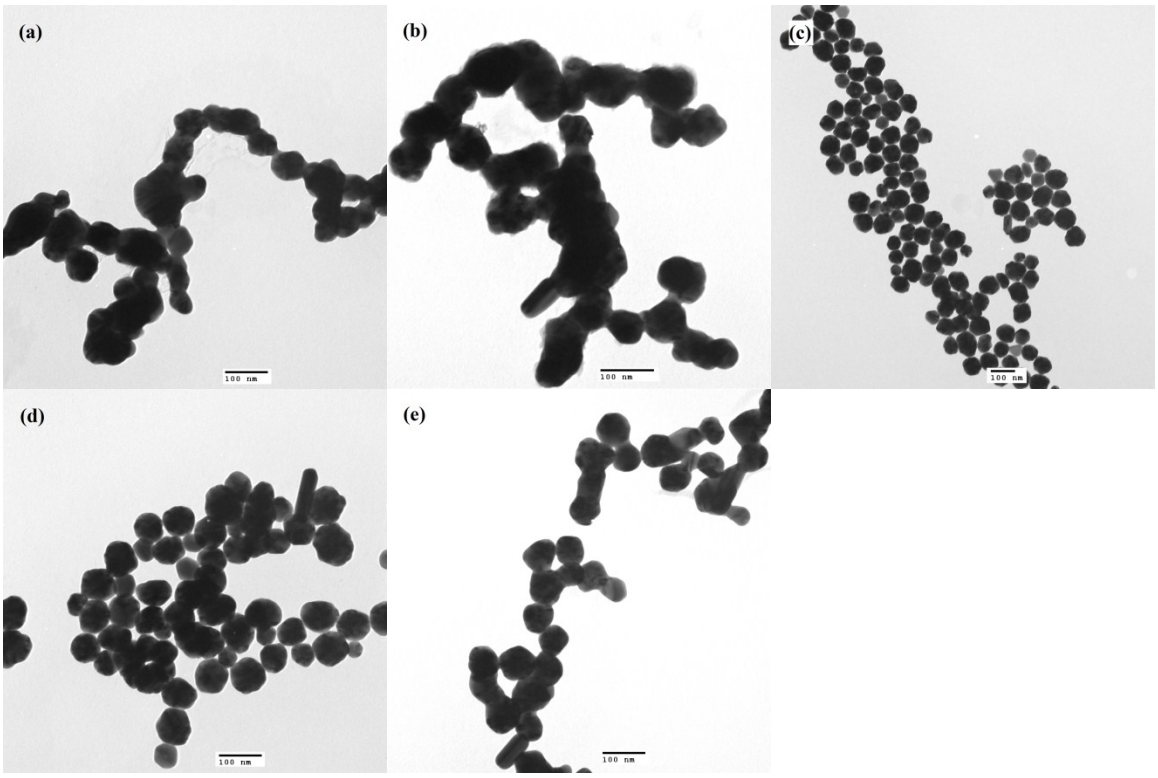

Figure 3.7 TEM images of (a) Citrate-nAg-1 and (b) SDS-nAg-1 after addition of 100 mM of NaCl, (c) Citrate-nAg-1 after addition of 100 mM $NaNO_3$, (d) SDS-nAg-10 after addition of 100 mM $NaNO_3$ and (e) SDS-nAg-10 after addition of 10 mM $CaCl_2$.

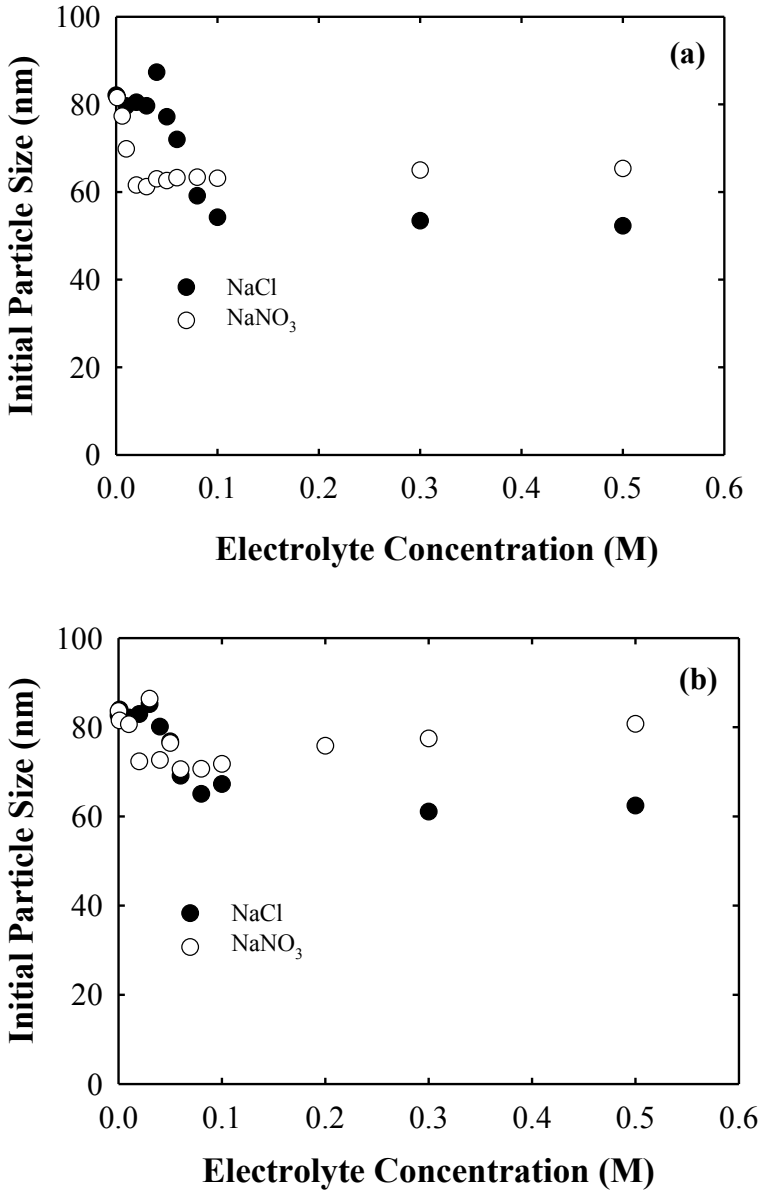

Figure 3.8 Initial particle size of (a) SDS-nAg-1, (b) SDS-nAg-10, and (c) Tween-nAg as a function of NaCl or $NaNO_3$ concentration. (Continued)

Figure 3.8: (Continued)

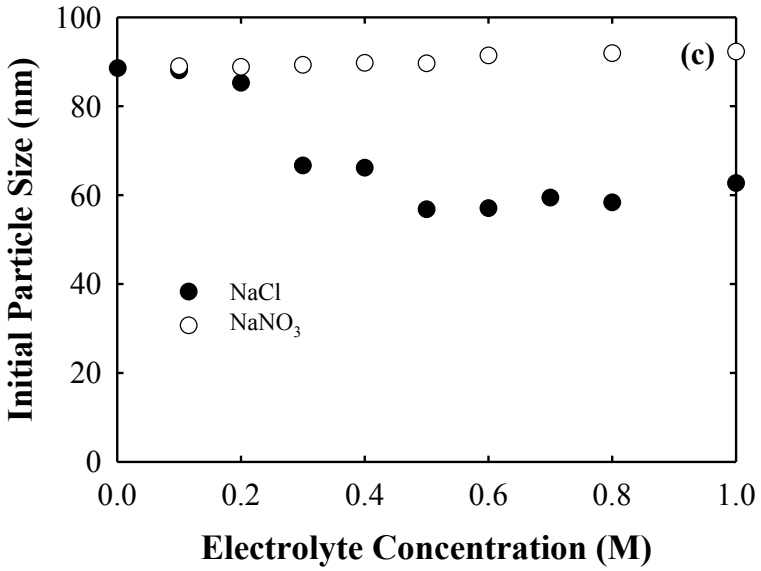

Chapter 4. Ion Release Kinetics and Stability of Coated Silver Nanoparticles in Surface Water

(Environmental Science and Technology, manuscript under preparation)

Abstract.

This study investigated the aggregation and silver release of silver nanoparticles in natural water in the absence and presence of light. Uncoated silver nanoparticles with diameters of *ca*. 82 nm were synthesized by the reduction of the $Ag(NH_3)_2^+$ complex with D-maltose. The influences of the capping layer and light exposure to aggregation and silver release in aquatic systems were investigated using uncoated particles and particles coated with citrate or Tween 80 in batch systems prevented or exposed to synthesized sun light. Dynamic light scattering (DLS) and transmission electron microscopy (TEM) were used to track the aggregation state and morphological changes of silver nanoparticles. Silver release was monitored during a period of 15 days. Results indicate sterically dispersed particles coated with Tween released silver quicker than did bare- and citrate-coated particles, which rapidly aggregated. A silver concentration of 40 μg/L was reached after just 6 hours by Tween-coated particles, accounting for *ca*. 3 % of the total silver. The similar levels of silver concentrations were reached in uncoated and Citrate-coated systems at the end of the 15 days. The presence of synthetic sun light and citrate impart significant morphological changes to the particles, however, aggregation seems the controlling process in this study.

4.1. Introduction

Improved production methods have led to more widespread employment of nanomaterials in commercially available products [1-2]. Among these nanomaterials, silver nanoparticles are increasingly being used as a broad-spectrum antimicrobial agent in clothing, food storage containers, pharmaceuticals, cosmetics, electronics, and optical devices [3-4]. The silver nanoparticles are readily released from these products during use, particularly washing [5], and thus it is likely that these materials will eventually be introduced into the environment. Although bactericidal mechanisms specific to silver nanoparticles, such as direct association of the particles with the membrane and subsequent membrane damage resulting from generated reactive oxygen species have been reported, the toxicity of silver nanoparticles is primarily related to the released ionic silver produced as the silver nanoparticles dissolve [1, 3, 6-11]. The known toxicity of silver and silver nanoparticles necessitates their use and fate in the environment be closely scrutinized to avoid compromising environmental or human health.

Aggregation plays an important role in determining the toxicity of silver nanoparticles as dispersed silver nanoparticles provide enhanced bactericidal effects over aggregated particles [12-14]. This presumably reflects an increase in silver release and more effective contact of the nanoparticles with the target bacteria. Factors that affect the silver ion release from silver nanoparticles, such as pH, dissolved oxygen, complexing agents and natural organic matter have been studied under simplified model experimental conditions (e.g., oxygen-saturated deionized water). Silver nanoparticles release silver ions only after they are oxidized by dissolved oxygen, a process that is facilitated by high

proton concentrations at low pH [15-16]. These released silver ions can be re-adsorbed onto the surface of the nanoparticles as well as other reactive surfaces [7, 15] or form a secondary precipitate with complexing species (e.g. Cl^- and SO_4^{2-}) [17-19]. The released silver ions can also be reduced to Ag(0) by chemical reduction in the presence of substances such as fulvic acid or citric acid [20-22]. However, research investigating the link between the aggregation state of silver nanoparticles and silver ion release in complex environmental conditions is limited [15].

After entering a natural water system, the aggregation of silver nanoparticles is primarily controlled by the presence or absence of a capping layer on the silver nanoparticle surfaces, the ionic strength or salinity of the water, and interactions with natural organic matter [23-27]. In simple electrolyte systems, the initial stage aggregation kinetics of silver nanoparticles follows classical Derjaguin-Landau-Verwey-Overbeek (DLVO) theory [23-24, 27-29], even though the particles are dissolving during aggregation. Uncoated silver nanoparticles are rapidly coated with an oxide layer that provides a significant negative potential to the particles allowing them to be stabilized and suspended for months without aggregation and precipitation in dilute systems [24]. Fast aggregation is induced when the negative surface charge is screened by electrolytes [23-24, 27]. Coating with stabilizers such as Tween and polyvinylpyrrolidone (PVP) enhance the stability of the silver nanoparticles, allowing them to remain dispersed at high ionic strength [13, 23-24, 27]. Natural organic matter (NOM) components such as fulvic and humic acids enhances nanoparticle stability either electrostatically or sterically after

being adsorbed to the surface [30-33], however, its effect on silver nanoparticles has so far been shown to be negligible [24].

Although poorly understood, sunlight irradiation is thought to influence the toxicity of nanomaterials in the environment, particularly since both the nanomaterials and ubiquitous NOM are UV light sensitive [34-35]. Sunlight irradiation may also affect the dispersion of silver nanoparticles in the natural water environment by altering particle morphology. Silver ions released during particle dissolution are reduced by the photoreduction of photoreactive species (e.g., citrate) at the surface of the original nanoparticles and subsequently change their shape and morphology. This process occurs under particle irradiation by a variety of light sources including sunlight and thus is anticipated to be particularly important for understanding the fate of silver nanoparticles in the environment [36-41]. Photoinduced particle fragmentation and fusion, which is observed under laser-light radiation at an intensity that matches that of ambient sunlight, may also bring about morphological changes to silver nanoparticles [42-44].

This study investigated the aggregation and silver release of silver nanoparticles in a natural water in the absence and presence of light. Our prior work indicates that aggregation of silver nanoparticles is highly dependent on the capping layer [23]. For example, Tween-coated silver nanoparticles were stable over long periods of time in the electrolyte solutions studied, whereas bare- and citrate-coated particles aggregate. Thus, the influence of the capping layer was investigated using uncoated particles and particles coated with citrate or Tween 80, with the objective of determining how the coating layers and light exposure impact the fate of silver nanoparticles in aquatic systems. To do so we

monitored the aggregation state and morphological changes of the silver nanoparticles suspended in a natural water exposed to synthetic sun light using dynamic light scattering (DLS) and transmission electron microscopy (TEM). Silver release was also monitored and its dependence on the aggregation state and properties of the silver particles was evaluated. Sterically dispersed particles coated with Tween released silver quicker than did bare- and citrate-coated particles, which rapidly aggregated. The presence of synthetic sun light and citrate impart more vigorous morphological changes to the particles, however, aggregation seems the controlling process in this study.

4.2. Materials and Methods

4.2.1. Materials.

Trisodium citrate (ACS reagent, ≥ 99.0%), silver nitrate (99.8%), and D-maltose (99%) were purchased from Sigma-Aldrich as powder and were used without further purification. Tween 80 (Tween) was purchased from Sigma-Aldrich in the form of a viscous liquid (BioXtra) and used as received without further purification. Trace-metal grade ammonium hydroxide was purchased from Fisher Scientific. All other reagents were analytical grade or above. The deionized water used in the experiments was supplied from a deionized water system (Milli-Q, Millipore) with a resistivity of 18.2 MΩ cm. All solutions except trisodium citrate and Tween were filtered through 0.1 μm cellulose ester membranes (Millipore) prior to use. The labware and glassware used in the experiments were washed with 10% nitric acid, rinsed thoroughly with deionized water and oven-dried under dust-free conditions.

4.2.2. Silver Nanoparticles.

This study utilized three types of silver nanoparticles: bare silver nanoparticles (Bare-nAg), citrate-coated silver nanoparticles (Citrate-nAg) and Tween-coated silver nanoparticles (Tween-nAg). Bare silver nanoparticles were synthesized by the reduction of the $[Ag(NH_3)_2]^+$ complex with D-maltose following Kvítek et al. [13] as modified by Li et al. [24]. Details of particle synthesis, purification, characterization and storage are further described by Li et al. [24].

Stock suspensions of silver nanoparticles coated with trisodium citrate or Tween 80 were prepared following Li et al [23]. In short, pre-calculated volumes of the bare silver nanoparticle stock suspension and either trisodium citrate or Tween 80 were introduced into a 50 mL polycarbonate centrifuge tube to achieve 1 mM trisodium citrate or 10 mM Tween 80. To these, sodium chloride, sodium bicarbonate and sodium hydroxide were added to adjust the ionic strength to 1 mM and buffer the pH at 7.0 ± 0.3, respectively. The tubes were sealed and slowly shaken for 24 hours in the dark at room temperature (22°C) to reach equilibrium. Dialysis of the particle suspensions was conducted after this coating procedure to remove residual coating agents and dissolved silver. Cellulose ester membranes (Spectra/Pro® Biotech) with a molecular weight cut off of 8-10 kDa for systems with Bare-nAg and Citrate-nAg and 50 kDa for systems with Tween-nAg were adopted. Over a period of 24 hours, the deionized water dialysate was changed a minimum of 4 times and its conductivity, dissolved silver concentration and total organic carbon (TOC) content were measured to ensure that residual ions and coating molecules were removed.

The hydrodynamic diameter of the three particle types was measured by dynamic light scattering (DLS) using a Brookhaven Instruments 90Plus. The electrophoretic mobility of the particles was measured with a zeta potential analyzer equipped with a palladium electrode (ZetaPALS, Brookhaven Instrument Corp.). Error estimates were based on ten measurements conducted on three separate samples for each experimental condition. UV-vis absorption spectra for the particles were collected using a Shimadzu UV-4201PC UV-vis spectrophotometer. The morphology of the nanoparticles was observed with a transmission electron microscope (TEM) (Technai G2 Spirit, FEI) at 120 kV. Images were collected using a digital camera at magnifications that ranged from 71,000 to 144,000. Samples were prepared by putting one drop of the particle suspension onto a 100 mesh carbon film-covered copper grid. Extra water was quickly removed using filter paper and the sample was dried under flowing nitrogen.

The total silver concentration of the stock suspensions was measured using an inductively coupled plasma optical emission spectrometer (ICP-AES, Vista AX, Varian, Inc.) following sample digestion by HNO_3. Standards for ICP-AES calibration were purchased from Ventures, Inc.

4.2.3. Collection and Characterization of Natural Water Sample.

A five gallon sample of a representative natural fresh water was collected from the Olentangy River which flows through the Ohio State University Campus in Columbus, OH. The sample was collected at a depth of approximately 0.4 m below the water surface and 4 m away from the river bank. The sample was immediately transported to the laboratory, where it was stored at 4°C prior to use. The conductivity, total organic

carbon (TOC), and pH of the Olentangy river water were measured by a conductivity meter (Model 130, Orion), a TOC analyzer (TOC-5000A, Shimadzu Corp.), and pH meter (720A Plus, Orion) respectively. Concentrations of common elements were measured by ICP-AES. Anion concentrations were determined by ion chromatography (DX-120, Dionex Corp.). Total silver concentration was analyzed by Graphite Furnace Atomic Absorption (GFAA) Spectrometer (Spectr AA 880Z, Varian, Inc.). The alkalinity of the Olentangy river was taken from historical data as an average value of 100 mg/L $CaCO_3$.

4.2.4. Characterization of Particle Stability and Silver Release.

The stability and dissolution of the particles suspended in the river water were studied over a period of 15 days in the presence and absence of light. The river water was equilibrated to room temperature (22 °C) and filtered at 0.45 μm (73050004, Geotech) prior to the introduction of the silver nanoparticles. At time zero, six ml of freshly dialyzed particle stock suspension was introduced into transparent 250 mL polycarbonate narrow-mouth bottles (Nalgene, Thermo Scientific) containing 144 ml of filtered Olentangy river water. A particle concentration of *ca*. 5.2×10^8 particles mL^{-1} was estimated based on the density of metallic silver (10.5 g cm^{-3}) and the average particle diameter of 82 nm. The cap of the bottle was modified by inserting multiple layers of glass fiber filter paper (Whatman, 9907-047) between the cap and the bottle body. The cap was loosely mounted to the bottle in order to permit sample equilibration with air while simultaneously preventing the introduction of dust. At the same time, this setup minimizes mass lost via evaporation. The bottles were placed on an orbital shaker at 30

rpm and exposed to light from a 150 W Xe ozone-free lamp (Model 6255, Newport Inc.) from 10:00 a.m. to 6:00 p.m. each day. The light spectrum from the lamp was corrected by a filter (Global filter Air Mass 1.5/Model 81094, Newport Inc.) to provide a spectrum of light that approximated that of real sun light (see Figure C.S 1 for an example of the light spectrum produced by the experimental setup). The light intensity was controlled at 100 mW/cm^2 using a Newport radiant power meter (Model 70260) and probe (Model 70263) [45-46]. Dark controls were conducted by covering an identical suite of sample bottles with aluminum foil. The dark control samples are noted with /Dark (e.g., nAg-Bare/Dark) and those exposed to light are noted with /Light (e.g., nAg-Bare/Light). Temperature changes during the 8-hour light irradiation were less than 2.5 °C. All experiments were run in duplicate. The results presented were for the average measurements of duplicates. For the GFAA, ICP-AES and DLS measurements these differences were negligible. Differences in the electrophoretic mobility measurements averaged *ca*. 10 percent.

At designated time, aliquots were extracted from each sample for analyses. Volumes removed from the bottle depend upon the measurements to be conducted at that time (Refer to Table C.S 1). The total silver concentration was measured by ICP-AES following sample digestion by concentrated HNO_3 in a microwave digestor (ETHOS 1, Milestone S.r.l.). The dissolved silver concentration was determined on 1.5 mL samples treated using centrifugal ultrafiltration using Amicon Ultra-4 centrifugal filtration cartridges with the 10 kDa membrane (Millipore). Samples were centrifuged for 10 min at 7500 g using a LegendRT centrifuge (SORVALL, Inc.). Silver loss to walls of the 250

mL polycarbonate bottles, sampling bottles (30 ml LDPE bottles) and centrifugal filters was negligible. The hydrodynamic particle diameter and electrophoretic mobility of the silver nanoparticles at different stages of the process were monitored using the methods previously discussed. The morphology of silver nanoparticles in the natural water over the experimental period was imaged using TEM.

4.3. Results and Discussion

4.3.1. Silver Nanoparticle Characterization.

The silver nanoparticles were synthesized followed existing methods [23-24] and the properties of the as-synthesized particles showed a high conformance to those previously described. The hydrodynamic diameters of Citrate-nAg and Bare-nAg measured by DLS were nearly the same at *ca*. 82 nm, whereas that for Tween-nAg was *ca*. 88 nm. Li et al. [23] report similar results and attribute the increase in size of Tween-nAg to the formation of an approximately 3 nm thick Tween coating layer. TEM images of the particles before mixing with natural water demonstrate the particles were mono-dispersed and spherical (Figure C.S 2a-c). The UV-vis absorption spectrum of Bare-nAg was broad with a maximum absorption peak at a wavelength of *ca*. 450 nm (Figure C.S 2d), suggesting the presence of an oxidized layer on the particle surface [23-24, 47-51]. The UV-vis absorption spectrum of Citrate-nAg and Tween-nAg blue-shifted to 445 nm and red-shifted to 458 nm relative to the Bare-nAg, respectively, consistent with a reduction in the chemical potential of the surface by citrate and oxidation of the same by Tween [23, 50-54].

All three particles were negatively charged in deionized water with 1 mM NaCl at pH 7. Bare-nAg was charged to a greater extent than the other particles, as the oxide surface layer produced an electrophoretic mobility for these particles at pH 7 of -4.5×10^{-8} m^2/V-s. Citrate- and Tween-nAg were also negatively charged, albeit to a lesser extent, as the adsorption of more moderately (or neutrally) charged molecules increased the electrophoretic mobility of Citrate-nAg to -1.8×10^{-8} m^2/V-s and Tween-nAg to -1.1×10^{-8} m^2/V-s [24, 55]. Citrate is also used as a reductant in many nano-silver synthesis methods [20-22], and thus a portion of the change in the electrophoretic mobility of Citrate-nAg compared to Bare-nAg could be due to a reduction of the surface oxide to Ag(0) [23]. These results were similar to those previously presented for particles synthesized in this manner [23-24]. Despite their varying electrophoretic mobilities, all three types of silver nanoparticles were stable in the presence of 1 mM NaCl for months without aggregation (data not shown).

4.3.2 Characterization of the River Water.

In general, the composition of the river water (Table 1) was consistent with that expected for a natural surface water [56]. It had a pH of 7.7 and TOC concentration of 5.7 mg-C/L. The concentration for the major monovalent cation, Na^+, was 1.85 mM and that for the major divalent cations, Mg^{2+} and Ca^{2+}, was 0.92 and 1.81 mM. The Cl^-, SO_4^{2-} and HCO_3^- concentrations were 2.23, 0.95 and 1.00 mM. The background concentrations of silver was below analytical detection limits (<1.0 μg/L). The concentrations of all other components were very low or not detected. Based on this composition, the ionic strength of the water was calculated as *ca*. 9.9 mM and the eq/L of anions in the water were within

15% of those for the cations. Under this water chemistry condition, Bare-nAg and Citrate-nAg are expected to form aggregates within several hours and dissolve based on the finds stated in previous two chapters.

4.3.3 Particle Aggregation.

Bare-nAg and Citrate-nAg grew from the starting size of 82 nm quickly to 500-800 nm within 6 hours after mixing with the river water. Both particles kept growing and reached sizes of a few to tens of micrometers at 24 hours, quickly exceeding the instrumental limit of 2μm (Figure 4.1a). The Bare- and Citrate-nAg/Light exhibited larger particle sizes than those kept in the dark. TEM images collected for these later times show micrometer-size aggregates of varying density and structure (Figure 4.2, 4.3). For the particles studied, reported values of the critical coagulation concentration (CCC) for monovalent electrolytes (NaCl and $NaNO_3$) are *ca*. 40 mM and for divalent electrolytes ($CaCl_2$) are *ca*. 2 mM [23-24]. This equates to ionic strength values of 40 mM for a monovalent electrolyte and 6 mM for a divalent electrolyte. Although the river water estimated ionic strength of 9.9 mM was below the CCC for monovalent electrolytes, it was above that for divalent electrolytes. In fact, the contribution of the divalent electrolytes (e.g., Ca^{2+}, Mg^{2+} and SO_4^{2-}) to the ionic strength of the water alone exceeded 7 mM, and it correspondingly resulted in Bare-nAg and Citrate-nAg forming aggregates with hydrodynamic diameter of *ca*. 150 nm within 15 min and *ca*. 500-600 nm within 6 hours.

Over the entire course of the study Tween-nAg was not observed to aggregate as the hydrodynamic diameter did not increase above the initial value of 88 nm (Figure 4.1b).

The dispersed nature of the Tween-nAg particles can also be observed in the TEM images (Figure 4.4). This was consistent with the results of Li et al. [23] demonstrating Tween-coated particles are exceptionally stable with a CCC in NaCl of 500 mM and a CCC in $CaCl_2$ of 700 mM due to the steric repulsion effects of the adsorbed Tween layer. Starting from Day 3, the hydrodynamic diameter of both Tween-nAg/Dark and /light began to decrease. After this time, the hydrodynamic diameter of Tween-nAg/Dark decreased from 88 nm to 81 nm. The decrease in the hydrodynamic diameter of Tween-nAg/Light was greater, as the average hydrodynamic diameter decreased from 88 nm to 57 nm. The decrease in the size of Tween-nAg and relative absence of aggregation could indicate a depletion of the Tween layer and further dissolution of the particles under light exposure. If this were the case, the lack of aggregation within the 15-day course could be attributed to steric repulsion effects from the dissolved Tween molecules. Alternatively, the dissolution of silver nanoparticles could proceed with the Tween coating layer remaining intact. In such a case, the underlying particle was oxidized to Ag^+ and released into the solution. The particle size decreased while the dissolution proceeded. Beyond dissolution, the decreased particle size might also be the results of photofragmentation of silver nanoparticles under light exposure [43]. While the specific mechanism for this phenomenon remains unclear, one or more alternative explanations stated above were likely responsible for the size decreasing of silver nanoparticle without aggregation.

The electrophoretic mobilities of all of the particles mixed with the pH 7.7 river water were approximately -1.0 to -1.2 $\times 10^{-8}$ $m^2/V\text{-}s$, for Bare-nAg and Citrate-nAg, respectively. These values were less negative than those in 1 mM NaCl at a similar pH of

7 of -4.5×10^{-8} m^2/V-s for Bare-nAg and -1.8×10^{-8} m^2/V-s for Citrate-nAg (Figure C.S 3), but were comparable to those in *ca*. 0.2 mM $CaCl_2$ (-1.6 and -1.3×10^{-8} m^2/V-s for Bare-nAg and Citrate-nAg, respectively). This was consistent with the divalent species acting as the major contributor to the screening of surface charge observed for these particles in river water [23]. The mobility data of Bare- and Citrate-nAg after the first day were not reported because they were no longer a dispersed colloid system required for the mobility measurement. The mobility of Tween-nAg in the river water showed increased over the first 5 days then remained at *ca*. -0.4×10^{-8} m^2/V-s (Figure C.S 3). This value was also close to that observed by Li et al. [23] in 0.2 mM $CaCl_2$. Despite the decreased electrostatic repulsion, Tween-coated nAg remained dispersed in the natural water over the entire 15 day study.

4.3.4 Silver Release.

Based on the silver content of the stock nanoparticle suspensions, the total silver concentration in the silver nanoparticle amended river water suspensions averaged 1.46 ± 0.06 mg/L. The starting dissolved silver concentrations were not measured. Dissolved silver concentrations at 10 min were low and ranged from 6.1 ± 0.1 μg/L for Bare-nAg to 1.2 ± 0.1 μg/L for Citrate-nAg. There was little difference at this time between samples exposed to light and those in the dark. In general, Tween-nAg released the most silver while Bare-nAg and Citrate-nAg released similar amounts of silver. The temporal dependence in the release for Tween-nAg differed for that observed for Bare-nAg and Citrate-nAg.

The dissolved silver concentrations in both Bare-nAg systems showed a decrease during the initial few hours, followed by a continuous increase. For example, the dissolved silver concentration decreased from 6.1 µg/L to 3.9 µg/L in the dark and from a similar starting value to 1.0 µg/L in the light. Neither Citrate-nAg nor Tween-nAg exhibited this trend. We suspect this was due to re-adsorption of released silver onto the particle surfaces in the Bare-nAg systems based upon results of a parallel experiment conducted with a sample of Bare-nAg that was dialyzed after synthesis, but was allowed to equilibrate for several days prior to being added to the river water. In this case, the initial dissolved silver concentration was 31 µg/L. This value decreased quickly to 12 µg/L within 12 hours after mixing (Figure C.S 4). Similar results were reported by Liu et al. [15-16] in systems where 3 mg/L $AgClO_4$ added as a source of dissolved silver was observed to decrease by *ca*. 1 mg/L within *ca*. 30 min upon mixing with 2 mg/L of silver nanoparticles.

Except for the first few hours, where it seems that Ag re-adsorption occurred, the concentration of dissolved silver in the Bare-nAg systems continued to increase with time. A similar increasing trend with time was observed for the Citrate-nAg systems, with the measured concentrations slightly exceeding those observed in the Bare-nAg systems. The behavior for Tween-nAg, however, was different. Silver release for Tween-nAg was initially high as the silver concentration reached a value of 40 µg/L after just 6 hours. This value was maintained until roughly day 3 after which time the concentration dropped to about 30 µg/L. Concentrations of released silver for Bare- and Citrate-nAg steadily increased over the 15-day course to levels comparable to that for Tween-nAg,

regardless of whether the samples were exposed to light or not. Note that silver concentration of this magnitude and even lower can cause adverse effects to common freshwater organisms [57].

For the systems studied, the amount of silver released was less than 3 % of that initially present. This differs from the complete particle dissolution observed by Liu and Hurt [15] in air-saturated deionized water. Liu and Hurt [15] also evaluated particle dissolution in more complex solutions and determined that dissolution was significantly enhanced as the pH decreased. In heterogeneous natural waters that incorporate multiple electrolyte ions as well as organic matter and in some instances light irradiation, particle dissolution does not go to completion as processes such as aggregation induced by screening of surface charge of particles, or reduction of dissolved Ag to form Ag(0) structures via organic ligands [20-22] or light [40-42, 44] can preserve or precipitate Ag. In addition, electrolyte ions (e.g., Cl^-) can form precipitates with Ag [23-24]. Lastly, of course, Ag concentrations in solution can decrease through sorption to the original nanoparticles or other particles in solution [7, 15].

4.3.4.1. Influence of aggregation on silver release.

As measured by DLS (Figure 4.1b) and confirmed by TEM (see Figure 4.4), Tween-nAg was dispersed in the river water and thereby exposed the complete particle surface area to the bulk water. As a result, the dissolved silver concentration in the Tween-nAg systems rapidly increased to *ca.* 40 μg/l within 6 hours of mixing (Figure 4.5). This relatively high dissolved Ag concentration was consistent with observations that surfactant-stabilized nAg is more effectively dispersed and better able to inhibit bacterial activity [11, 13, 16,

58-59]. For Bare-nAg and Citrate-nAg, the increase in hydrodynamic size (Figure 4.1a) and TEM images (Figure 4.2, 4.3) indicate the particles aggregated. Accordingly, the dissolved silver concentrations in these systems increased at a gradual rate and at the end of 15 days reach the comparable level of the Tween-nAg systems (Figure 4.5). The impact of the aggregation status on silver release from silver nanoparticles is the subject of considerable interest [60] and in general antibacterial activity decreases when aggregates are formed [11, 13, 16, 58-59]. The underlying mechanism for this decrease is usually attributed to decreased contact between the cell membrane and the nanoparticle, however, a decrease in silver ion release during particle aggregation cannot be ruled out.

At day three, the dissolved silver concentration in the Tween-nAg systems started to decrease (Figure 4.5). This also corresponded with a decrease in the particle hydrodynamic size (Figure 4.1b). Possibly this reflects the re-adsorption of Ag^{+} to the particle surface. The *ca*. 7 μg/l concentration drop may also represent the adsorption capacity of the silver nanoparticles to Ag^{+}, which was comparable to the estimated value of 10 μg/l based on a site density on the silver oxide surface of 1×10^{-5} mol/m^2 [61]. Under the light exposure, the hydrodynamic size of Tween-nAg further decreased to *ca*. 57 nm (Figure 4.1b), indicating possible further dissolution. The dissolved silver concentration in the Tween-nAg/Light system also showed a decrease coincident with the further decreasing particle size after Day 11 (Figure 4.5). Note that both the DLS results (Figure 4.1b) and TEM images (Figure 4.4) indicated the particles in the Tween-nAg systems were still dispersed. Therefore it was possible that the decreased silver

concentration was caused by Ag re-adsorption as the surface area of the particles increased during the fragmentation of the original particles, not from further dissolution.

4.3.4.2. The influence of light irradiation.

Among the four systems, Citrate-nAg/Light showed the highest dissolved silver concentration throughout most of the 15-day experiment, followed by Citrate-nAg/Dark and Bare-nAg/Dark. Bare-nAg /Light gave the lowest dissolved silver concentration after the drop at Day-3. Photoinduced fusion and fragmentation of noble metal nanoparticles occurs under laser-light irradiation [42-44]. Silver nanoparticles fragment into smaller particles under laser pulse excitation [43] and their aggregates fuse to form larger spherical particles [62]. The energy levels in these systems ranged from 5 – 10 mW/cm^2, which is lower than that provided by the synthetic sunlight in our system. Thus, purely on the basis of energy input, morphological changes of the silver nanoparticles in our system seem possible. Stabilizer-coated silver nanoparticles undergo aggregation to form chain-like structures under sunlight exposure; however, no settling was observed for the aggregated particles coated by effective stabilizer such as PVP [63]. Photoinduced morphological changes, either fragmentation or fusion, are proposed to occur mainly due to changes in the dipolar oscillation frequency of the free electrons at the surface of the metal nanoparticles imparted by input of thermal energy from the light [43-44, 63]. Either case may change the morphology and the total available surface area in the system and disturb the equilibrium of adsorbed silver ions.

For both Bare-nAg and Citrate-nAg, observed morphological changes likely result from multiple process including aggregation, dissolution, secondary precipitation and

reduction, and possibly photoinduced fragmentation or fusion acting in concert or individually. A typical image illustrating the heterogeneous and complex nature of the particle structures of the Bare-nAg system (Figure 4.3) taken at Day-13 shows large single particles of 100 – 200 nm (possibly formed by secondary precipitation and/or reduction), large aggregates structures of ~500 nm (possibly due to adhesion and particle photofusion) and small particles of 30 nm (perhaps formed by dissolution or photofragmentation of the original particles). Generally, light induced morphological changes of the particles were not distinguishable from a comparison of the TEM images (Figure 4.2, 4.3) as aggregation appeared to be controlling in both systems. Once aggregation occurred, the influence of sunlight on silver release was masked.

TEM images of Tween-nAg/Dark showed dispersed individual particles throughout the course of 15 days (Figure 4.4). For Tween-nAg exposed to light, however, chain-like structures of aggregated particles were occasionally observed (Figure 4.4). There number was not sufficient to result in an increase in particle size as the DLS data showed a slight decrease in the average hydrodynamic particle size (Figure 4.1b). This was not observed for Tween-nAg/Dark. The decrease in the dissolved silver concentration for Tween-nAg/Light was also possibly the result particle aggregation. Similar phenomenon occurs for PVP-coated nAg that although aggregation occurred to nAg under the sunlight exposure, the particles still resisted settling [63].

4.3.4.3. The role of citrate and light.

On average, Citrate-nAg released more silver than did Bare-nAg. In the dark, the final dissolved silver concentrations were 30.5 ± 0.4 and 28.4 ± 0.6 μg/L for Citrate- and Bare-

nAg, separately whereas under light exposure the values were 28.0 ± 0.9 and 24.5 ± 0.5 μg/L, respectively. This trend seems to indicate that citrate can facilitate the release of silver from the nanoparticles.

Photoreduction of Ag^+ by the photoactivity of citrate has been widely adopted to synthesize silver nanoparticles, or to achieve morphological changes to the original silver nanoparticles [40-41]. Upon irradiation by laser-light citrate is oxidized as follows [41, 64]:

$$\text{Citrate} \xrightarrow{h\nu} \text{acetone—1,3-dicarboxylate} + CO_2 + e^-$$

The released electrons are stored by the silver nanoparticles and increase the chemical reactivity at their surface [65]. Silver ions at the particle surface are also more easily reduced to form secondary solid phases [53]. Instead of systems with laser and citrate, Ag^+ can also be reduced photochemically by other photoactive reagents under the irradiation of variety of light sources, such as UV light, xenon arc lamp, sunlight and even conventional fluorescent tubes [36-39]. When this process occurs in an existing silver nanoparticle system, more heterogenous structures (e.g., individual particles connected by secondary solid phases) can be formed, particularly when aggregation exists. Similar to light induced morphological changes, morphological changes from citrate may also affect the dissolved silver concentration. In our systems exposed to 0.1 W/cm^2 synthetic sunlight for eight hour increments, similar morphological changes caused by photoreduction of citrate were also possible, given that photoreduction of silver ions in a similar situation was observed under just 5 min of sunlight exposure with intensity of *ca*. 0.04 W/cm^2 [39]. Meanwhile, reduction of Ag^+ to form new or expand

existing silver nanoparticles solely by citrate without light irradiation is also possible [20-22]. Nevertheless, morphological changes brought about by photoreduction of citrate were not obvious in the TEM images of Citrate/Dark and Bare-nAg/Dark (Figure 4.2), and Citrate-nAg/Dark and Citrate-nAg/Light (Figure 4.2 and 4.3). In these images we observe that newly formed large single particles, large aggregate structures (~500 nm) and the smaller particles coexist. For any aggregated system, a higher degree of morphological change or characteristic could not be explicitly distinguished. Similarly, the silver release level linked to the effects of citrate, as illustrated at the beginning of this section seems to have no reflection on morphological changes induced by photoreduction by citrate.

4.4. Environmental Implications

The structures and morphologies of silver nanoparticles formed in natural waters are the result of multiple factors including aggregation induced by high ionic strength and/or pH, secondary precipitation formed by Ag-complexing ligands (e.g., Cl^-), re-growth of silver nanoparticles by reducing species (e.g., citrate, fulvic acid) and photoreduction and photoinduced fragmentation and fusion. These factors, combined with those factors affecting the partial oxidation of the nanoparticle (e.g., dissolved oxygen), as well as the re-adsorption of released Ag^+ onto particle surfaces, mediate the silver ion release of silver nanoparticles.

In the natural water system examined, aggregation state was the most important factor controlling silver release. Shortly after being mixed with natural water, the bare- and citrate-coated silver nanoparticles formed aggregates of diversified structures, including

large aggregates of the original particles, newly formed large single particles and smaller particles, due to the combined effects of complexation, precipitation, photoreduction and photoinduced fragmentation/fusion. Tween-coated silver nanoparticles, however, were stabilized in the natural water for much longer periods of time without aggregation and exhibited a more marked decrease in size upon sunlight exposure. These well dispersed silver nanoparticles released silver to a greater extent and at a faster rate than did the aggregated particles. Sunlight and photoactive capping agents such as citrate may affect the silver ion release through the photoreduction of citrate and photoinduced morphological changes, however, no explicit connections can be made between these changes and the silver ion concentrations once aggregation occurred.

This study suggests sterically stabilized silver nanoparticles can persist longer as individual particles in natural water systems and thus will release silver ions more quickly and to a greater extent than would particles that aggregate quickly after entering the water. The higher level of silver released and the potential for more effective contact of the stabilized silver nanoparticles to aquatic organisms suggest that these sterically stabilized particles could present more of a hazard to aquatic organisms in the environment.

References

[1] Navarro, E., et al., *Toxicity of Silver Nanoparticles to Chlamydomonas reinhardtii.* Environmental Science & Technology, 2008. **42**(23): p. 8959-8964.

[2] Maynard, A., et al., *Safe handling of nanotechnology.* NATURE, 2006. **444**(7117): p. 267-269.

[3] Kim, J.S., et al., *Antimicrobial effects of silver nanoparticles.* Nanomedicine-Nanotechnology Biology and Medicine, 2007. **3**(1): p. 95-101.

[4] Tolaymat, T.M., et al., *An evidence-based environmental perspective of manufactured silver nanoparticle in syntheses and applications: A systematic review and critical appraisal of peer-reviewed scientific papers.* Science of the Total Environment, 2010. **408**(5): p. 999-1006.

[5] Benn, T.M. and P. Westerhoff, *Nanoparticle silver released into water from commercially available sock fabrics.* Environmental Science & Technology, 2008. **42**(11): p. 4133-4139.

[6] Lee, H.Y., et al., *A practical procedure for producing silver nanocoated fabric and its antibacterial evaluation for biomedical applications.* Chemical Communications, 2007(28): p. 2959-2961.

[7] Morones, J.R., et al., *The bactericidal effect of silver nanoparticles.* Nanotechnology, 2005. **16**(10): p. 2346-2353.

[8] Pal, S., Y.K. Tak, and J.M. Song, *Does the antibacterial activity of silver nanoparticles depend on the shape of the nanoparticle? A study of the gram-negative bacterium Escherichia coli.* Applied and Environmental Microbiology, 2007. **73**(6): p. 1712-1720.

[9] Panacek, A., et al., *Silver colloid nanoparticles: Synthesis, characterization, and their antibacterial activity.* Journal of Physical Chemistry B, 2006. **110**(33): p. 16248-16253.

[10] Shahverdi, A.R., et al., *Synthesis and effect of silver nanoparticles on the antibacterial activity of different antibiotics against Staphylococcus aureus and*

Escherichia coli. Nanomedicine-Nanotechnology Biology and Medicine, 2007. **3**(2): p. 168-171.

[11] Sondi, I. and B. Salopek-Sondi, *Silver nanoparticles as antimicrobial agent: a case study on E-coli as a model for Gram-negative bacteria.* Journal of Colloid and Interface Science, 2004. **275**(1): p. 177-182.

[12] Dorjnamjin, D., M. Ariunaa, and Y.K. Shim, *Synthesis of silver nanoparticles using hydroxyl functionalized ionic liquids and their antimicrobial activity.* International Journal of Molecular Sciences, 2008. **9**(5): p. 807-819.

[13] Kvitek, L., et al., *Effect of surfactants and polymers on stability and antibacterial activity of silver nanoparticles (NPs).* Journal of Physical Chemistry C, 2008. **112**(15): p. 5825-5834.

[14] Yu, D.G., *Formation of colloidal silver nanoparticles stabilized by Na+-poly(gamma-glutamic acid)-silver nitrate complex via chemical reduction process.* Colloids and Surfaces B-Biointerfaces, 2007. **59**(2): p. 171-178.

[15] Liu, J.Y. and R.H. Hurt, *Ion Release Kinetics and Particle Persistence in Aqueous Nano-Silver Colloids.* Environmental Science & Technology, 2010. **44**(6): p. 2169-2175.

[16] Lok, C.N., et al., *Silver nanoparticles: partial oxidation and antibacterial activities.* Journal of Biological Inorganic Chemistry, 2007. **12**(4): p. 527-534.

[17] Choi, O., et al., *The inhibitory effects of silver nanoparticles, silver ions, and silver chloride colloids on microbial growth.* Water Research, 2008. **42**(12): p. 3066-3074.

[18] Choi, O., et al., *Role of sulfide and ligand strength in controlling nanosilver toxicity.* Water Research, 2009. **43**(7): p. 1879-1886.

[19] Gao, J., et al., *Dispersion and Toxicity of Selected Manufactured Nanomaterials in Natural River Water Samples: Effects of Water Chemical Composition.* Environmental Science & Technology, 2009. **43**(9): p. 3322-3328.

[20] J. Turkevich, P.C.S., J. Hillier,, *A study of the nucleation and growth processes in the synthesis of colloidal gold.* Discuss. Faraday. Soc. , 1951. **11**: p. 55-75.

[21] Sarkar, P., et al., *Aqueous-Phase Synthesis of Silver Nanodiscs and Nanorods in Methyl Cellulose Matrix: Photophysical Study and Simulation of UV-Vis Extinction Spectra Using DDA Method.* Nanoscale Research Letters, 2010. **5**(10): p. 1611-1618.

[22] Pillai, Z.S. and P.V. Kamat, *What factors control the size and shape of silver nanoparticles in the citrate ion reduction method?* Journal of Physical Chemistry B, 2004. **108**(3): p. 945-951.

[23] Li, X.A., J.J. Lenhart, and H.W. Walker, *Aggregation Kinetics and Dissolution of Coated Silver Nanoparticles.* Langmuir, (In Press).

[24] Li, X.A., J.J. Lenhart, and H.W. Walker, *Dissolution-Accompanied Aggregation Kinetics of Silver Nanoparticles.* Langmuir, 2010. **26**(22): p. 16690-16698.

[25] El Badawy, A., et al., *Impact of Environmental Conditions (pH, Ionic Strength, and Electrolyte Type) on the Surface Charge and Aggregation of Silver Nanoparticles Suspensions.* Environmental Science & Technology, 2010: p. 1260-1266.

[26] Jin, X., et al., *High-Throughput Screening of Silver Nanoparticle Stability and Bacterial Inactivation in Aquatic Media: Influence of Specific Ions.* Environmental Science & Technology, 2010. **44**(19): p. 7321-7328.

[27] Huynh, K.A. and K.L. Chen, *Aggregation Kinetics of Citrate and Polyvinylpyrrolidone Coated Silver Nanoparticles in Monovalent and Divalent Electrolyte Solutions.* Environmental Science & Technology, 2011: p. null-null.

[28] Derjaguin B. V., L., L. D., *Theory of the stability of strongly charged lyophobic sols and of the adhesion of strongly charged particles in solutions of electrolytes.* Acta Physiconchim, 1941. **14**: p. 733-762.

[29] Verwey E. J. W., O.J.T.G., *Theory of the stability of lyophobic colloids*. 1948, Amsterdam: Elsevier.

[30] Chen, K.L., S.E. Mylon, and M. Elimelech, *Aggregation kinetics of alginate-coated hematite nanoparticles in monovalent and divalent electrolytes.* Environmental Science & Technology, 2006. **40**(5): p. 1516-1523.

[31] Chen, K.L. and M. Elimelech, *Influence of humic acid on the aggregation kinetics of fullerene (C-60) nanoparticles in monovalent and divalent electrolyte solutions.* Journal of Colloid and Interface Science, 2007. **309**(1): p. 126-134.

[32] Chen, K.L., S.E. Mylon, and M. Elimelech, *Enhanced aggregation of alginate-coated iron oxide (hematite) nanoparticles in the presence of calcium, strontium, and barium cations.* Langmuir, 2007. **23**(11): p. 5920-5928.

[33] Mylon, S.E., K.L. Chen, and M. Elimelech, *Influence of natural organic matter and ionic composition on the kinetics and structure of hematite colloid aggregation: Implications to iron depletion in estuaries.* Langmuir, 2004. **20**(21): p. 9000-9006.

[34] Li, Q.L. and Y.S. Hwang, *Characterizing Photochemical Transformation of Aqueous nC(60) under Environmentally Relevant Conditions.* Environmental Science & Technology, 2010. **44**(8): p. 3008-3013.

[35] Li, Q.L., et al., *Kinetics of C(60) Fullerene Dispersion in Water Enhanced by Natural Organic Matter and Sunlight.* Environmental Science & Technology, 2009. **43**(10): p. 3574-3579.

[36] Wodka, D., et al., *Photocatalytic activity of titanium dioxide modified by silver nanoparticles.* ACS Appl Mater Interfaces, 2010. **2**(7): p. 1945-53.

[37] Callegari, A., D. Tonti, and M. Chergui, *Photochemically grown silver nanoparticles with wavelength-controlled size and shape.* Nano Letters, 2003. **3**(11): p. 1565-1568.

[38] Torigoe, K. and K. Esumi, *Preparation of Bimetallic Ag-Pd Colloids from Silver(I) Bis(Oxalato)Palladate(Ii).* Langmuir, 1993. **9**(7): p. 1664-1667.

[39] Shahverdi, A.R., et al., *A sunlight-induced method for rapid biosynthesis of silver nanoparticles using an Andrachnea chordifolia ethanol extract.* Applied Physics a-Materials Science & Processing, 2011. **103**(2): p. 349-353.

[40] Maillard, M., P.R. Huang, and L. Brus, *Silver nanodisk growth by surface plasmon enhanced photoreduction of adsorbed [Ag+].* Nano Letters, 2003. **3**(11): p. 1611-1615.

[41] Ahern, A.M. and R.L. Garrell, *Insitu Photoreduced Silver-Nitrate as a Substrate for Surface-Enhanced Raman-Spectroscopy.* Analytical Chemistry, 1987. **59**(23): p. 2813-2816.

[42] Kamat, P.V., *Photophysical, photochemical and photocatalytic aspects of metal nanoparticles.* Journal of Physical Chemistry B, 2002. **106**(32): p. 7729-7744.

[43] Kamat, P.V., M. Flumiani, and G.V. Hartland, *Picosecond dynamics of silver nanoclusters. Photoejection of electrons and fragmentation.* Journal of Physical Chemistry B, 1998. **102**(17): p. 3123-3128.

[44] Fujiwara, H., S. Yanagida, and P.V. Kamat, *Visible laser induced fusion and fragmentation of thionicotinamide-capped gold nanoparticles.* Journal of Physical Chemistry B, 1999. **103**(14): p. 2589-2591.

[45] Materials, A.S.o.T., *Standard for solar spectral irradiance tables at air mass 1.5 for a 37^0 tilted surface*, in *ASTM Standard E892-82*. 1982: Philadelphia, PA.

[46] Bird, R.E., et al., *Solar spectral measurements in the terrestrial environment.* Appl Opt, 1982. **21**(8): p. 1430-6.

[47] Kapoor, S., *Preparation, characterization, and surface modification of silver particles.* Langmuir, 1998. **14**(5): p. 1021-1025.

[48] Mie, G., Ann. Phys., 1908. **25**: p. 377.

[49] Hulst, V.d., *Light Scattering by Small Particles*. 1957, New York: Wiley.

[50] Yin, Y.D., et al., *Synthesis and characterization of stable aqueous dispersions of silver nanoparticles through the Tollens process.* Journal of Materials Chemistry, 2002. **12**(3): p. 522-527.

[51] Chen, M., et al., *Preparation and study of polyacryamide-stabilized silver nanoparticles through a one-pot process.* Journal of Physical Chemistry B, 2006. **110**(23): p. 11224-11231.

[52] Mulvaney, P., T. Linnert, and A. Henglein, *Surface-Chemistry of Collodial Silver in Aqueous-Solution - Observations on Chemisorption and Reactivity. Journal of Physical Chemistry*,, 1991. **95**(20): p. 7843-7846.

[53] Henglein, A., *Colloidal silver nanoparticles: Photochemical preparation and interaction with O-2, CCl4, and some metal ions.* Chemistry of Materials, 1998. **10**(1): p. 444-450.

[54] Henglein, A., T. Linnert, and P. Mulvaney, *Reduction of Ag+ in Aqueous Polyanion Solution - Some Properties and Reactions of Long-Lived Loigomeric Silver Clusters and Metallic Silver Particles.* Berichte der Bunsen-Gesellschaft-Physical Chemistry Chemical Physics, 1990. **94**(12): p. 1449-1457.

[55] Pelley, A.J. and N. Tufenkji, *Effect of particle size and natural organic matter on the migration of nano- and microscale latex particles in saturated porous media.* Journal of Colloid and Interface Science, 2008. **321**(1): p. 74-83.

[56] Hem, J.D., *Study and Interpretation of the Chemical Characteristics of Natural Water*. 1989, United States Geological Survey: Washington DC. p. 263.

[57] Ratte, H., *Bioaccumulation and toxicity of silver compounds: A review.* Environmental Toxicology and Chemistry, 1999. **18**(1): p. 89-108.

[58] Shrivastava, S., et al., *Characterization of enhanced antibacterial effects of novel silver nanoparticles.* Nanotechnology, 2007. **18**(22): p. -.

[59] Teeguarden, J.G., et al., *Particokinetics in vitro: Dosimetry considerations for in vitro nanoparticle toxicity assessments.* Toxicological Sciences, 2007. **95**(2): p. 300-312.

[60] Marambio-Jones, C. and E.M.V. Hoek, *A review of the antibacterial effects of silver nanomaterials and potential implications for human health and the environment.* Journal of Nanoparticle Research, 2010. **12**(5): p. 1531-1551.

[61] Chau, L.K. and M.D. Porter, *Surface Isoelectric Point of Evaporated Silver Films - Determination by Contact-Angle Titration.* Journal of Colloid and Interface Science, 1991. **145**(1): p. 283-286.

[62] Tripathy, S.K., *Nanophotothermolysis of poly-(vinyl) alcohol capped silver particles.* Nanoscale Research Letters, 2008. **3**(4): p. 164-167.

[63] Liu, J., et al., *Toxicity Reduction of Polymer-Stabilized Silver Nanoparticles by Sunlight.* Journal of Physical Chemistry C, 2011. **115**(11): p. 4425-4432.

[64] Sato, T., et al., *Photochemical Formation of Silver Gold (Ag-Au) Composite Colloids in Solutions Containing Sodium Alginate.* Applied Organometallic Chemistry, 1991. **5**(4): p. 261-268.

[65] Linnert, T., P. Mulvaney, and A. Henglein, *Photochemistry of Collodial Silver Particles – The Effects of N2O and Adsorbed CN-*. Berichte der Bunsen-Gesellschaft-Physical Chemistry Chemical Physics, 1991. **95**(7): p. 838-841.

Tables and Figures

Table 4.1 Characteristics of natural water (Olentangy River) used in this study

Constituent	Concentration (mg/L)*
Calcium (mg/L)	72.4
Magnesium (mg/L)	22.0
Sodium (mg/L)	42.5
Potassium (mg/L)	2.12
Chloride (mg/L)	79.3
Sulfate (mg/L)	91.6
Nitrate (mg/L, as N)	0.360
TOC (mg C/L)	5.70
pH	7.73
Conductivity (μS/cm)	809
Alkalinity (mg $CaCO_3$/L) *	100

*Based on historical data

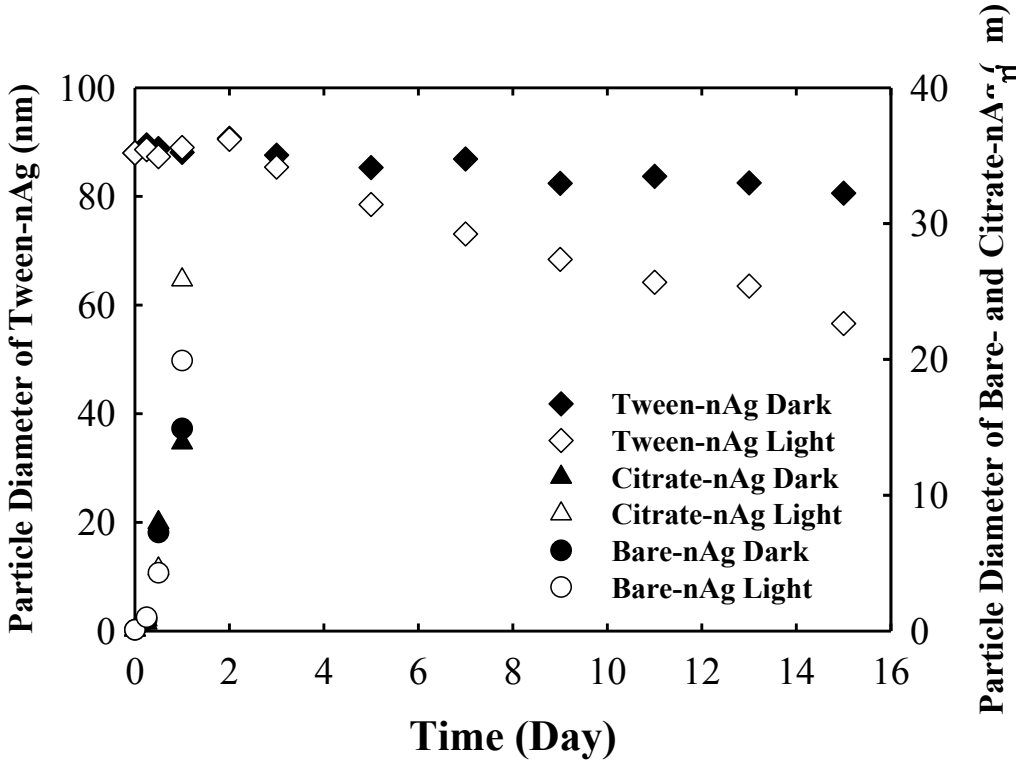

Figure 4.1 Aggregation kinetics of the silver nanoparticles

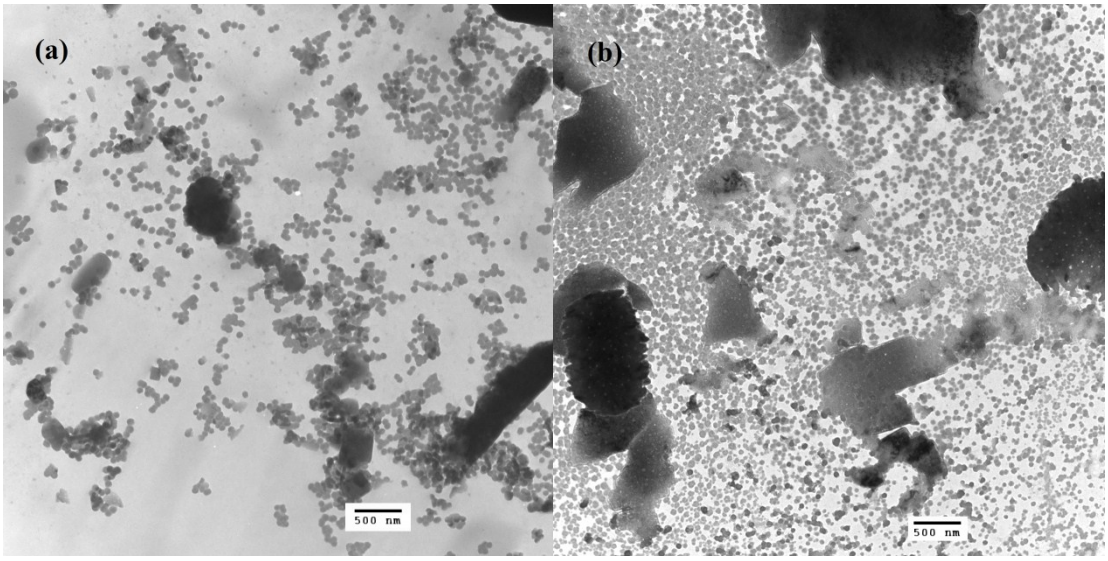

Figure 4.2 TEM images of Bare-nAg taken at Day-11 (a) and Citrate-nAg (b) taken at Day-13 in dark. More TEM images taken at different time are available in supporting information.

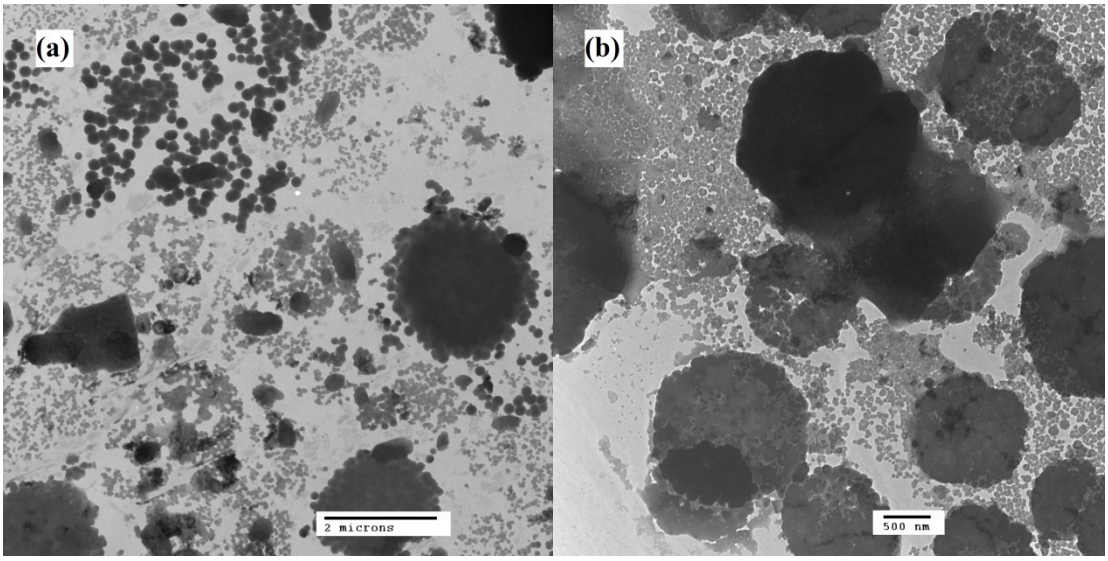

Figure 4.3 TEM images of Bare-nAg taken at Day-13 (a) and Citrate-nAg (b) taken at Day-13 exposed to light. More TEM images taken at different time are available in supporting information.

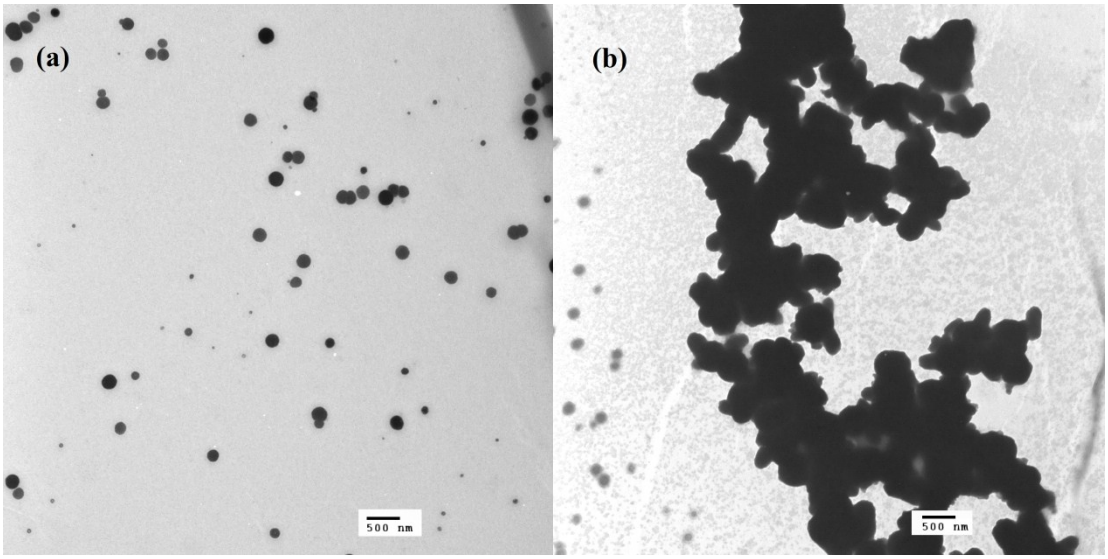

Figure 4.4 TEM images of Tween-nAg taken at Day-11 in the dark (a) and Day-13 exposed to light (b). More TEM images taken at different time are available in supporting information.

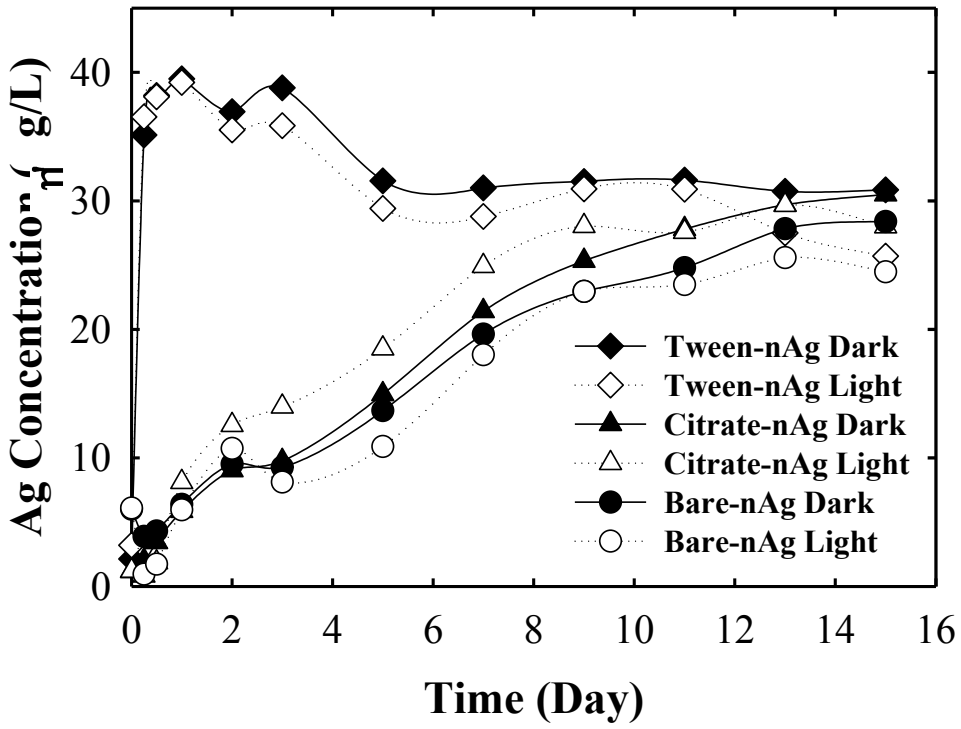

Figure 4.5 Silver release kinetics in the Olentangy River water

Chapter 5. Conclusions

5.1. Conclusions

To elucidate the three objectives described in Chapter 1, a systematic investigation of the aggregation and silver release of uncoated and coated (citrate, SDS, Tween) silver nanoparticles in simple electrolyte solutions or natural river water were conducted. The following are specific conclusions resulting from this study.

1. Objective 1 - Evaluate how water chemistry, mainly concentration and valence of electrolyte, as well as dissolved natural organic matter affect the aggregation of silver nanoparticles (Chapter 2)

Silver nanoparticles with diameters of *ca*. 82 nm were synthesized with a layer of Ag_2O. Dissolution-accompanied aggregation of these silver nanoparticles was observed in the presence of monovalent NaCl, $NaNO_3$ and divalent $CaCl_2$. Nevertheless, the early-stage aggregation behavior of silver nanoparticles was consistent with classical DLVO theory. The CCC for silver nanoparticles was determined as 40 mM NaCl, 30 mM $NaNO_3$ and 2 mM $CaCl_2$. The initial particle size decrease was monitored by DLS immediately after the addition of the electrolyte and attributed to the dissolution of silver nanoparticles.

The dissolution likely results from electrolyte-induced perturbations in the concentration of adsorbed Ag^+ which seems to inhibit dissolution of the surface oxide layer. AgCl precipitates formed within the chloride-containing systems as the particles dissolved during aggregation. The resulting particles and aggregates were characterized by having

smooth continuous surfaces with little evidence of separate particles. The relative absence of a comparable precipitate in systems with $NaNO_3$ resulted in aggregates and particles of a more discrete nature.

The presence of 10 mg L^{-1} fulvic acid was found to have no obvious effects on the aggregation kinetics, as the CCC values were little changed. The dissolution of the silver nanoparticles in systems with fulvic acid and NaCl was somewhat enhanced and a small increase was measured in the electrophoretic mobilities of the particles with fulvic acid. However, neither change was sufficient in magnitude to alter the stability of the particles.

2. Objective 2 - Elucidate how the physical and chemical properties of the silver nanoparticles, altered through the addition of different capping layers, affects their aggregation (Chapter 3)

Silver nanoparticles coated with stabilizing agents that provided steric repulsion enhanced stability and reduced dissolution when compared to negatively-charged uncoated particles or particles coated with an electrostatic stabilizing agent. Electrostatic stabilization using a low molecular weight molecule, citrate, showed no obvious effects as the aggregation of the particles and decrease in the initial particle size differed little from those for uncoated particles. For the electrosteric coating reagent, SDS, increasing the initial coating concentration from 1 mM to 10 mM, which was above the CMC of SDS, caused a slight increase in the CCC reflective of an increase in steric repulsion. SDS inhibited particle dissolution, particularly at a coating concentration of 10 mM, whereas citrate did not. The non-ionic steric stabilizer, Tween, significantly enhanced

stability. This stabilizer also physically protected the integrity of particles as dissolution was significantly reduced.

The behavior of the Tween-coated silver nanoparticles also exhibited a dependence on electrolyte type, as its stability was greater and dissolution was lower in $NaNO_3$ than in NaCl. While the specific mechanism for this difference was not determined, it appears to relate to differences in the nucleophilicities of Cl^- and NO_3^- ions.

3. Objective 3 - Investigate how aggregation, capping layer and environmentally-related factors, mainly sunlight irradiation affect silver release from silver nanoparticles in natural water (Chapter 4)

In the natural water system examined, aggregation state decided by capping layers and ionic strength was the most important factor controlling silver release. The intermediate term change of aggregation states of silver nanoparticles was consistent with the observations and predictions from results of previous chapters. Shortly after being mixed with natural water, the bare- and citrate-coated silver nanoparticles formed aggregates of diversified structures, including large aggregates of the original particles, newly formed large single particles and smaller particles, due to the combined effects of complexation, precipitation, photoreduction and photoinduced fragmentation/fusion. Tween-coated silver nanoparticles, however, were stabilized in the natural water for much longer periods of time without aggregation and exhibited a more marked decrease in size upon sunlight exposure.

Well dispersed silver nanoparticles coated with Tween released silver to a greater extent and at a faster rate than did the aggregated particles. Sunlight and photoactive capping

agents such as citrate may affect the silver ion release through the photoreduction of citrate and photoinduced morphological changes, however, no explicit connections can be made between these changes and the silver ion concentrations once aggregation occurred. For the system investigated here, the observed dissolved silver concentration reached a level that could adverse effects to freshwater organism.

5.2. Recommendations for Future Studies

1. The extent to which silver nanoparticles was oxidized (aged) before the aggregation experiment is suspected to affect the particle size decrease upon mixing with electrolyte solutions. However, aging and oxidation state of the silver nanoparticles were not characterized either directly or quantitatively. Existence of oxidized layer was only confirmed by comparing the UV-Vis adsorption spectrum of documented non-oxidized particles and our aged particles with red-shifted adsorption peak. Either the direct evidence (e.g., X-ray/IR spectrum or morphological images) or the quantified parameters (e.g., the depth or amount of the oxidized layer) were needed in the following research for further characterizations.

2. Oxidation and dissolution are the important processes affecting silver release and toxicity of silver nanoparticles. However, the speciation and affiliation (e.g., released as free Ag^{+}, complexed by Ag^{+} binding ligands, re-adsorbed by silver nanoparticles, adsorbed by natural colloid and organic matter) of the released silver ions in the complicated water matrix were poorly characterized. Meanwhile, qualitative descriptions to the each group listed above would be greatly beneficial for the environmental fate and ecotoxicity studies of silver nanoparticles.

3. The interactions between the bulk silver nanoparticles (including the oxidized layer) and engineered or natural capping layers are mostly unknown. This process is critical in deciding both the transport (e.g., aggregation, precipitation, adsorption) and dissolution of silver nanoparticles in aquatic environments. Molecular spectroscopy (e.g., FT-IR) and nuclear magnetic resonance (NMR) might be applicable to characterize potential chemical bonds formed between molecules of capping agents and surface of particles. How adsorption kinetics, coverage and depletion of the capping agents affect stability and dissolution of silver nanoparticles also needs to be answered.

4. Effects of environmentally-relevant parameters such as sunlight exposure to the aggregation and silver release have been investigated in natural water, though the effect was not distinguishable from the morphological change induced by aggregation. Effects of sunlight exposure to aggregation and silver release of the non-aggregated silver nanoparticles, which requires a deionized environment with no or low electrolyte concentration, need to be evaluated to further understand if and how those environmentally-relevant factors will affect their fate.

5. Besides aggregation, the deposition behavior of silver nanoparticles is another decisive process affecting their environmental fate in surface water. Similarly, deposition attachment efficiencies (α) and the critical deposition concentration (CDC) can be derived from deposition kinetics experiments. The quartz crystal microbalance with dissipation monitoring (QCM-D) is typically employed for nanoparticle deposition studies due to its high sensitivity and small sample volume requirements. The column

filtration experiment can also be conducted to investigate the transport of nanoparticles in porous media.

Appendix A: Supporting Information for Chapter 2

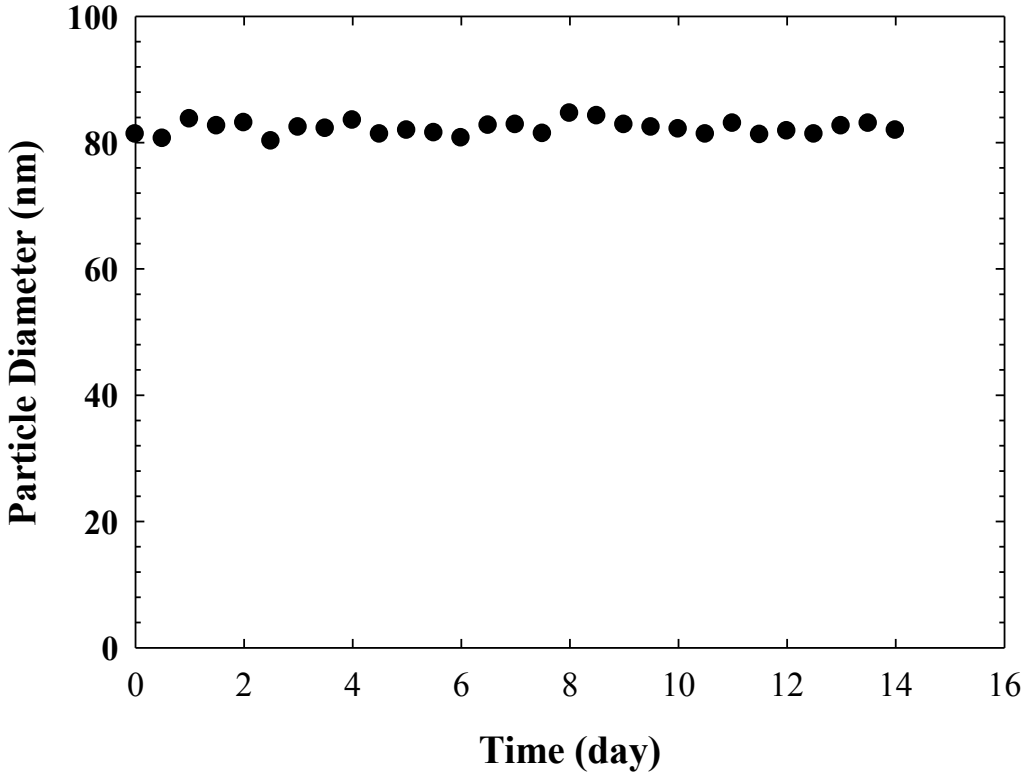

Figure A.S1. Hydrodynamic diameter of the stock silver nanoparticles over time.

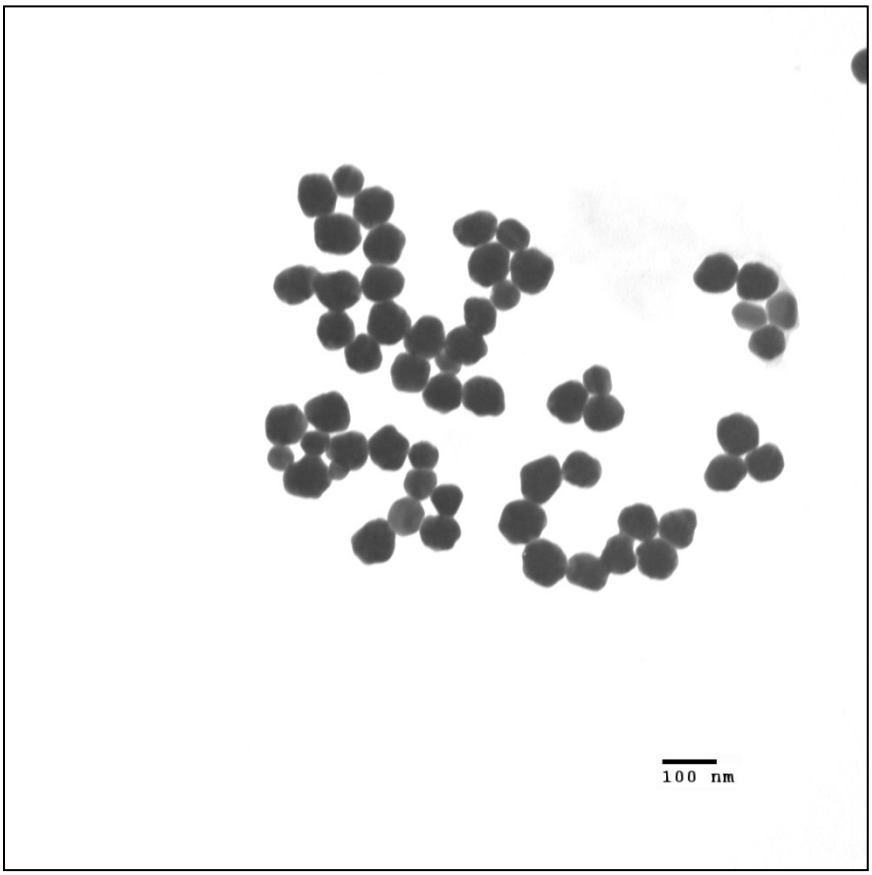

Figure A.S2. TEM image of silver nanoparticles after the addition of 1.5 mM $CaCl_2$.

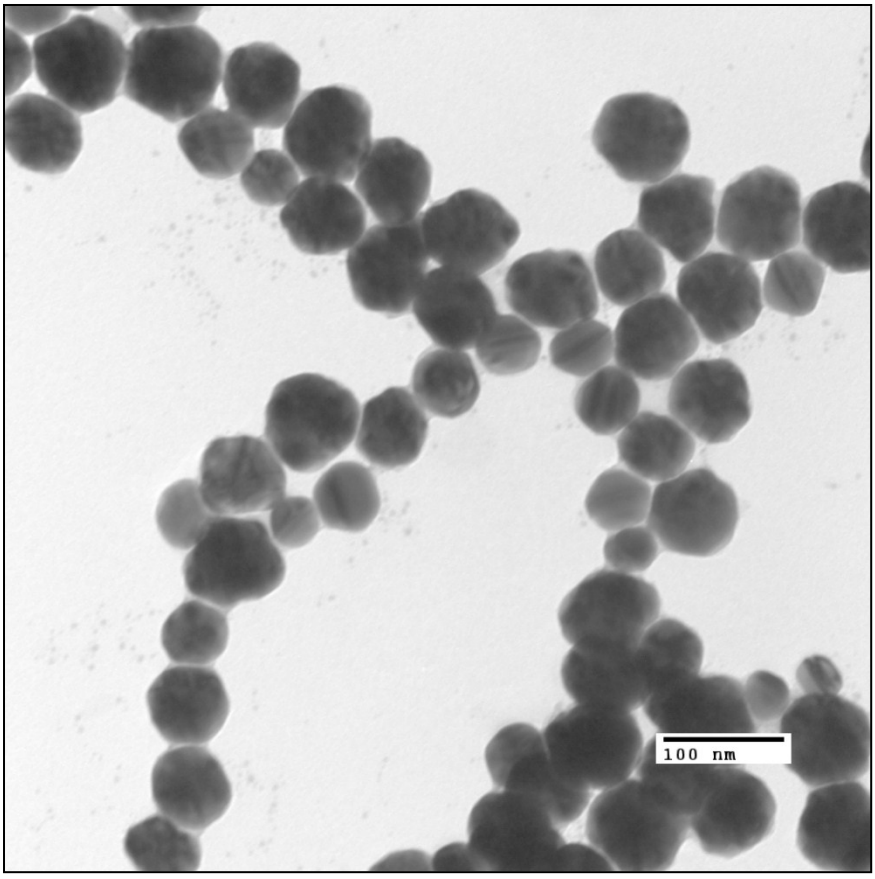

Figure A.S3. TEM image of silver nanoparticles in the presence of fulvic acid after the addition of 10 mM $NaNO_3$.

Appendix B: Supporting Information for Chapter 3

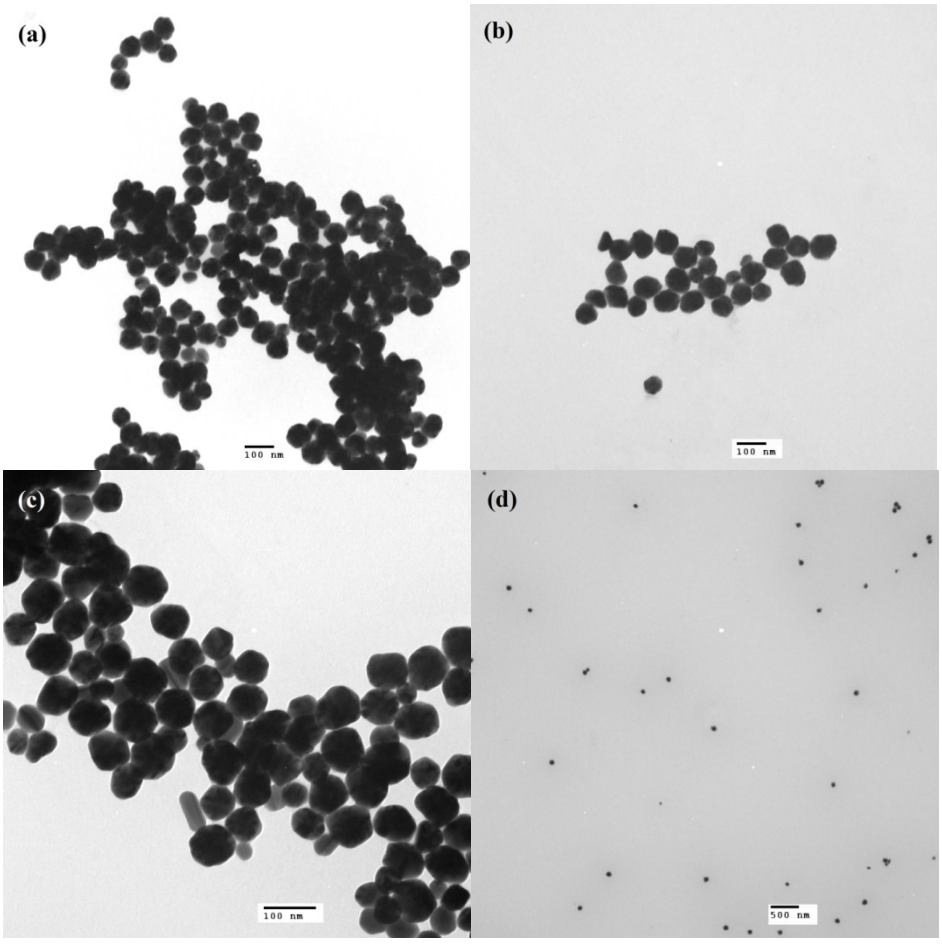

Figure B.S1. TEM images of (a) Bare-nAg, (b) Citrate-nAg-1 and (c) SDS-nAg-10, (d) Tween-nAg in the absence of electrolyte

Appendix C: Supporting Information for Chapter 4

Table C.S 1. Volumes withdrawed of each sampling

Timeline	Sample Volumes Withdrawed for Analysis (mL)				
	DLS	TEM	EPM	AA	Total
10 min	3	0	0	2	5
6 h	3	0	0	2	5
12 h	3	0	0	2	5
1 day	3	0.01	4.5	2	9.51
3 day	3	0.01	4.5	2	9.51
5 day	3	0.01	4.5	2	9.51
7 day	3	0.01	4.5	2	9.51
9 day	3	0.01	0	2	5.01
11 day	3	0.01	4.5	2	9.51
13 day	3	0.01	0	2	5.01
15 day	3	0.01	4.5	2	9.51

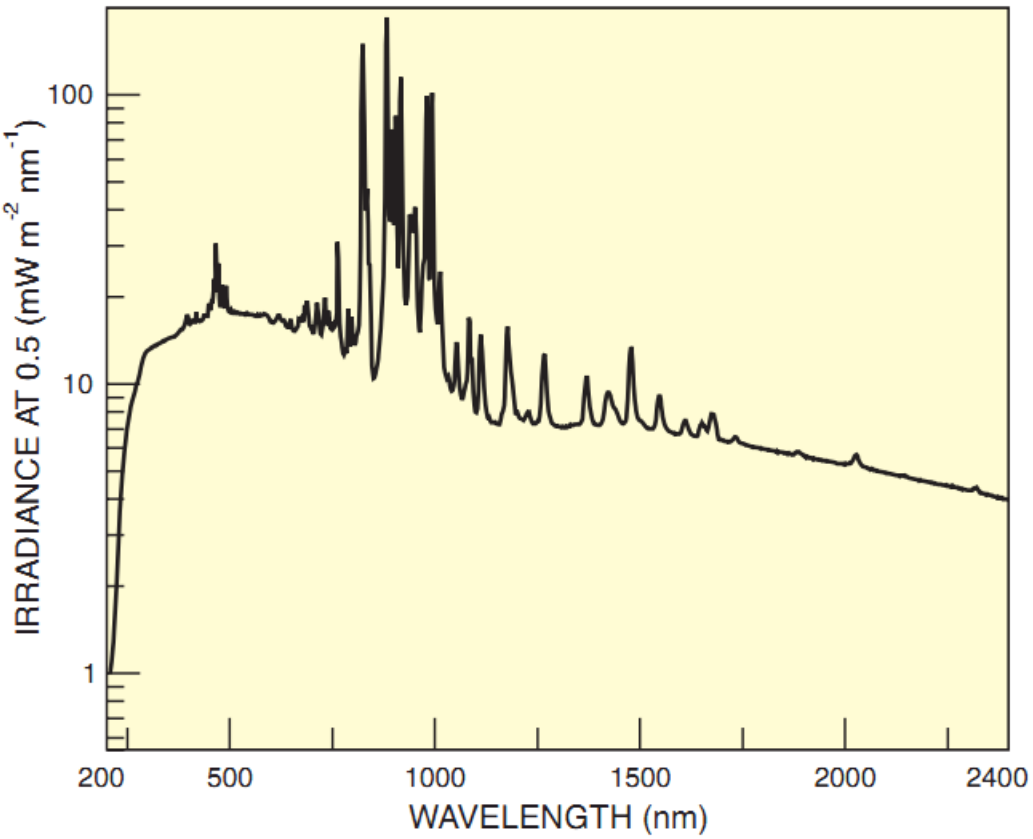

Figure C.S 1. The spectrum of the synthetic sun light system (150 W Xe Ozone Free lamp light source (Model 6255) corrected by a filter (Global filter Air Mass 1.5/Model 81094). Provided by the manufacturer, Newport Inc.

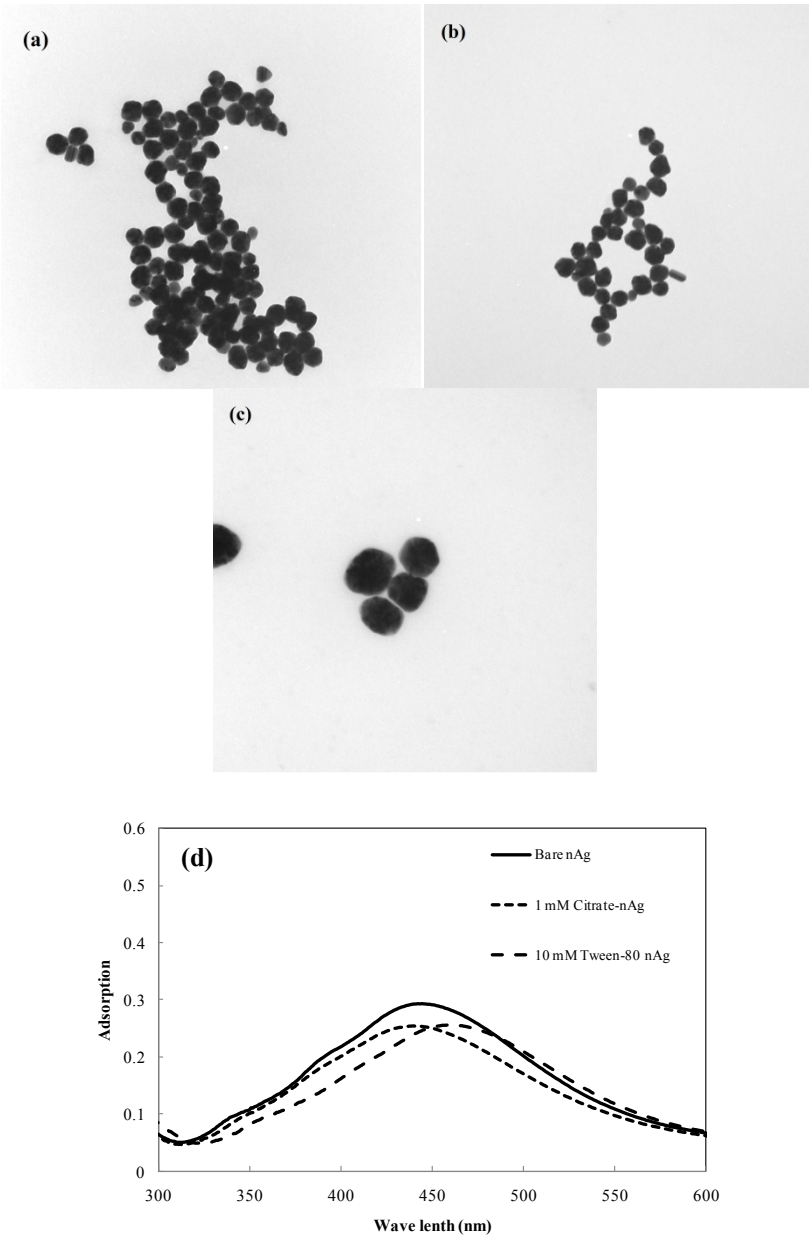

Figure C.S 2. TEM images of (a) Bare-nAg, (b) Citrate-nAg-1 and (c) Tween-nAg in the DI water and (d) the coordinating UV-vis absorption spectrum

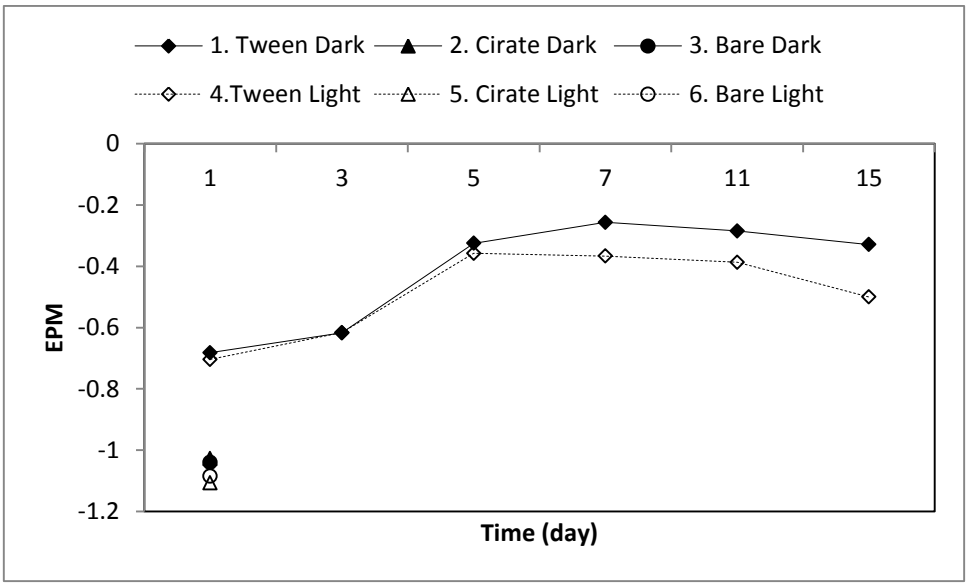

Figure C.S 3. Electrophoretic mobilities of silver nanoparticles in the Olentangy River water

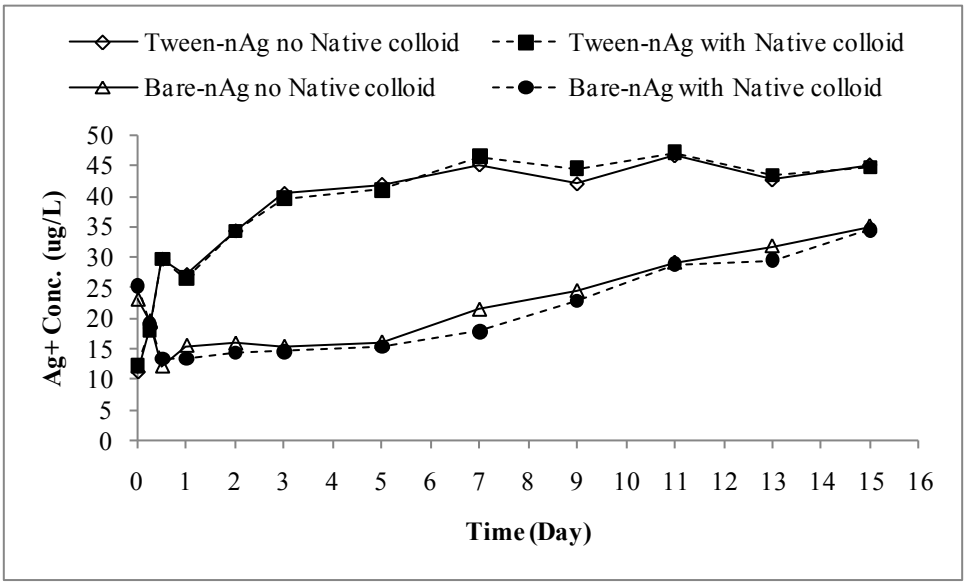

Figure C.S 4. Silver release kinetics in the Olentangy River water (Ag^+ was not removed in the Bare-nAg systems)

Bibliography

Ahern, A. M. and R. L. Garrell (1987). "Insitu Photoreduced Silver-Nitrate as a Substrate for Surface-Enhanced Raman-Spectroscopy." Analytical Chemistry **59**(23): 2813-2816.

Amirbahman, A. and T. M. Olson (1995). "The Role of Surface Conformations in the Deposition Kinetics of Humic Matter-Coated Colloids in Porous-Media." Colloids and Surfaces a-Physicochemical and Engineering Aspects **95**(2-3): 249-259.

Au, K. K., A. C. Penisson, et al. (1999). "Natural organic matter at oxide/water interfaces: Complexation and conformation." Geochimica Et Cosmochimica Acta **63**(19-20): 2903-2917.

Baalousha, M. (2009). "Aggregation and disaggregation of iron oxide nanoparticles: Influence of particle concentration, pH and natural organic matter." Science of the Total Environment **407**(6): 2093-2101.

Banfield, J. F. and H. Z. Zhang (2001). "Nanoparticles in the environment." Nanoparticles and the Environment **44**: 1-58.

Barcelo, D., M. la Farre, et al. (2008). "Fate and toxicity of emerging pollutants, their metabolites and transformation products in the aquatic environment." Trac-Trends in Analytical Chemistry **27**(11): 991-1007.

Beckett, R. and N. P. Le (1990). "The Role of Organic-Matter and Ionic Composition in Determining the Surface-Charge of Suspended Particles in Natural-Waters." Colloids and Surfaces **44**: 35-49.

Benn, T. M. and P. Westerhoff (2008). "Nanoparticle silver released into water from commercially available sock fabrics." Environmental Science & Technology **42**(11): 4133-4139.

Bird, R. E., R. L. Hulstrom, et al. (1982). "Solar spectral measurements in the terrestrial environment." Appl Opt **21**(8): 1430-1436.

Blaser, S. A. (2006). Environmental risk analysis for silver-containing nanofunctionalized products Zurich, Swiss Federal Institute of Technology (ETHZ). Master Thesis

Blaser, S. A., M. Scheringer, et al. (2008). "Estimation of cumulative aquatic exposure and risk due to silver: Contribution of nano-functionalized plastics and textiles." Science of the Total Environment **390**(2-3): 396-409.

Brandt, D., B. Park, et al. (2005). "Argyria secondary to ingestion of homemade silver solution." Journal of the American Academy of Dermatology **53**(2, Supplement): S105-S107.

Brant, J., H. Lecoanet, et al. (2005). "Aggregation and deposition characteristics of fullerene nanoparticles in aqueous systems." Journal of Nanoparticle Research **7**(4-5): 545-553.

Buffle, J. (1990). Complexation reactions in aquatic systems--an analytical approach. Chichester Ellis Horwood.

Buffle, J., K. J. Wilkinson, et al. (1998). "A generalized description of aquatic colloidal interactions: The three-colloidal component approach." Environmental Science & Technology **32**(19): 2887-2899.

Callegari, A., D. Tonti, et al. (2003). "Photochemically grown silver nanoparticles with wavelength-controlled size and shape." Nano Letters **3**(11): 1565-1568.

Cao, G. (2004). Nanostructures & nanomaterials : synthesis, properties & applications. London, Imperial College Press.

Carlson, C., S. M. Hussain, et al. (2008). "Unique Cellular Interaction of Silver Nanoparticles: Size-Dependent Generation of Reactive Oxygen Species." The Journal of Physical Chemistry B **112**(43): 13608-13619.

Cesarano, J., I. A. Aksay, et al. (1988). "Stability of Aqueous Alpha-Al2o3 Suspensions with Poly(Methacrylic Acid) Poly-Electrolyte." Journal of the American Ceramic Society **71**(4): 250-255.

Chau, L. K. and M. D. Porter (1991). "Surface Isoelectric Point of Evaporated Silver Films - Determination by Contact-Angle Titration." Journal of Colloid and Interface Science **145**(1): 283-286.

Chen, K. L. and M. Elimelech (2006). "Aggregation and deposition kinetics of fullerene (C-60) nanoparticles." Langmuir **22**(26): 10994-11001.

Chen, K. L. and M. Elimelech (2007). "Influence of humic acid on the aggregation kinetics of fullerene (C-60) nanoparticles in monovalent and divalent electrolyte solutions." Journal of Colloid and Interface Science **309**(1): 126-134.

Chen, K. L., S. E. Mylon, et al. (2006). "Aggregation kinetics of alginate-coated hematite nanoparticles in monovalent and divalent electrolytes." Environmental Science & Technology **40**(5): 1516-1523.

Chen, K. L., S. E. Mylon, et al. (2007). "Enhanced aggregation of alginate-coated iron oxide (hematite) nanoparticles in the presence of calcium, strontium, and barium cations." Langmuir **23**(11): 5920-5928.

Chen, M., L. Y. Wang, et al. (2006). "Preparation and study of polyacryamide-stabilized silver nanoparticles through a one-pot process." Journal of Physical Chemistry B **110**(23): 11224-11231.

Chen, Y. H. and C. S. Yeh (2002). "Laser ablation method: use of surfactants to form the dispersed Ag nanoparticles." Colloids and Surfaces a-Physicochemical and Engineering Aspects **197**(1-3): 133-139.

Chodanowski, P. and S. Stoll (2001). "Polyelectrolyte adsorption on charged particles in the Debye-Huckel approximation. A Monte Carlo approach." Macromolecules **34**(7): 2320-2328.

Choi, O., T. E. Cleuenger, et al. (2009). "Role of sulfide and ligand strength in controlling nanosilver toxicity." Water Research **43**(7): 1879-1886.

Choi, O., K. K. Deng, et al. (2008). "The inhibitory effects of silver nanoparticles, silver ions, and silver chloride colloids on microbial growth." Water Research **42**(12): 3066-3074.

Choi, O. and Z. Q. Hu (2008). "Size dependent and reactive oxygen species related nanosilver toxicity to nitrifying bacteria." Environmental Science & Technology **42**(12): 4583-4588.

Chou, K. S. and Y. S. Lai (2004). "Effect of polyvinyl pyrrolidone molecular weights on the formation of nanosized silver colloids." Materials Chemistry and Physics **83**(1): 82-88.

Cifuentes, A., J. L. Bernal, et al. (1997). "Determination of critical micelle concentration values using capillary electrophoresis instrumentation." Analytical Chemistry **69**(20): 4271-4274.

Colvin, V. L. (2003). "The potential environmental impact of engineered nanomaterials." Nature Biotechnology **21**(10): 1166-1170.

CRC handbook of chemistry and physics. United Kingdom, (2008). Taylor & Francis Group.

Cushing, B. L., V. L. Kolesnichenko, et al. (2004). "Recent advances in the liquid-phase syntheses of inorganic nanoparticles." Chemical Reviews **104**(9): 3893-3946.

D, R. (2009). "Nanotechnology and consumer products.", from http://www.nanotechproject.org/publications/archive/nanotechnology_consumer_products/.

Damm, C. and H. Munstedt (2008). "Kinetic aspects of the silver ion release from antimicrobial polyamide/silver nanocomposites." Applied Physics a-Materials Science & Processing **91**(3): 479-486.

Derjaguin B. V., L., L. D. (1941). "Theory of the stability of strongly charged lyophobic sols and of the adhesion of strongly charged particles in solutions of electrolytes." Acta Physiconchim **14**: 733-762.

Domingos, R. F., N. Tufenkji, et al. (2009). "Aggregation of Titanium Dioxide Nanoparticles: Role of a Fulvic Acid." Environmental Science & Technology **43**(5): 1282-1286.

Dorjnamjin, D., M. Ariunaa, et al. (2008). "Synthesis of silver nanoparticles using hydroxyl functionalized ionic liquids and their antimicrobial activity." International Journal of Molecular Sciences **9**(5): 807-819.

Dougherty, G., K. Rose, et al. (2008). "The zeta potential of suirface-functionalized metallic nanorod particles in aqueous solution." Electrophoresis **29**(5): 1131-1139.

El Badawy, A., T. Luxton, et al. (2010). "Impact of Environmental Conditions (pH, Ionic Strength, and Electrolyte Type) on the Surface Charge and Aggregation of Silver Nanoparticles Suspensions." Environmental Science & Technology: 1260-1266.

Elimelech, M. G., J.; Jia, X.; Williams, R. J. (1995). Particle Deposition & Aggregation: Measurement, Modelling and Simulation. Oxford, Butterworth-Heinemann.

Fabrega, J., S. R. Fawcett, et al. (2009). "Silver Nanoparticle Impact on Bacterial Growth: Effect of pH, Concentration, and Organic Matter." Environmental Science & Technology **43**(19): 7285-7290.

Fleer, G. J. (1993). Polymers at interfaces. London, Chapman & Hall.

Fortin, C. and P. G. C. Campbell (2000). "Silver uptake by the green alga Chlamydomonas reinhardtii in relation to chemical speciation: Influence of chloride." Environmental Toxicology and Chemistry **19**(11): 2769-2778.

Fritz, G., V. Schadler, et al. (2002). "Electrosteric stabilization of colloidal dispersions." Langmuir **18**(16): 6381-6390.

Fujiwara, H., S. Yanagida, et al. (1999). "Visible laser induced fusion and fragmentation of thionicotinamide-capped gold nanoparticles." Journal of Physical Chemistry B **103**(14): 2589-2591.

Gao, J., S. Youn, et al. (2009). "Dispersion and Toxicity of Selected Manufactured Nanomaterials in Natural River Water Samples: Effects of Water Chemical Composition." Environmental Science & Technology **43**(9): 3322-3328.

Goff, H. D. (1997). "Colloidal aspects of ice cream - A review." International Dairy Journal **7**(6-7): 363-373.

Gottschalk, F., T. Sonderer, et al. (2009). "Modeled Environmental Concentrations of Engineered Nanomaterials (TiO2, ZnO, Ag, CNT, Fullerenes) for Different Regions." Environmental Science & Technology **43**(24): 9216-9222.

Guzman, K. A. D., M. R. Taylor, et al. (2006). "Environmental risks of nanotechnology: National nanotechnology initiative funding, 2000-2004." Environmental Science & Technology **40**(5): 1401-1407.

Hem, J. D. (1989). Study and Interpretation of the Chemical Characteristics of Natural Water. Washington DC, United States Geological Survey**:** 263.

Henglein, A. (1998). "Colloidal silver nanoparticles: Photochemical preparation and interaction with O-2, CCl4, and some metal ions." Chemistry of Materials **10**(1): 444-450.

Henglein, A., T. Linnert, et al. (1990). "Reduction of Ag+ in Aqueous Polyanion Solution - Some Properties and Reactions of Long-Lived Loigomeric Silver Clusters and Metallic Silver Particles." Berichte der Bunsen-Gesellschaft-Physical Chemistry Chemical Physics **94**(12): 1449-1457.

Hiriart-Baer, V. P., C. Fortin, et al. (2006). "Toxicity of silver to two freshwater algae, Chlamydomonas reinhardtii and Pseudokirchneriella subcapitata, grown under continuous culture conditions: Influence of thiosulphate." Aquatic Toxicology **78**(2): 136-148.

Ho, C. M., S. K. W. Yau, et al. (2010). "Oxidative Dissolution of Silver Nanoparticles by Biologically Relevant Oxidants: A Kinetic and Mechanistic Study." Chemistry-an Asian Journal **5**(2): 285-293.

Holmberg, K. (2003). Surfactants and polymers in aqueous solution. Chichester, Wiley.

Holthoff, H., S. U. Egelhaaf, et al. (1996). "Coagulation rate measurements of colloidal particles by simultaneous static and dynamic light scattering." Langmuir **12**(23): 5541-5549.

Hulst, V. d. (1957). Light Scattering by Small Particles. New York, Wiley.

Hunter, R. J. (1986). Foundations of Colloid Science. Oxford, Clarendon Press.

Hussain, S., K. Hess, et al. (2005). "In vitro toxicity of nanoparticles in BRL 3A rat liver cells." Toxicology in Vitro **19**(7): 975-983.

Huynh, K. A. and K. L. Chen (2011). "Aggregation Kinetics of Citrate and Polyvinylpyrrolidone Coated Silver Nanoparticles in Monovalent and Divalent Electrolyte Solutions." Environmental Science & Technology: null-null.

Hwang, E. T., J. H. Lee, et al. (2008). "Analysis of the Toxic Mode of Action of Silver Nanoparticles Using Stress-Specific Bioluminescent Bacteria." Small **4**(6): 746-750.

Hyung, H., J. D. Fortner, et al. (2007). "Natural organic matter stabilizes carbon nanotubes in the aqueous phase." Environmental Science & Technology **41**(1): 179-184.

Illes, E. and E. Tombacz (2003). "The role of variable surface charge and surface complexation in the adsorption of humic acid on magnetite." Colloids and Surfaces a-Physicochemical and Engineering Aspects **230**(1-3): 99-109.

Inoue, Y., M. Hoshino, et al. (2002). "Bactericidal activity of Ag–zeolite mediated by reactive oxygen species under aerated conditions." Journal of Inorganic Biochemistry **92**(1): 37-42.

J. Turkevich, P. C. S., J. Hillier, (1951). "A study of the nucleation and growth processes in the synthesis of colloidal gold." Discuss. Faraday. Soc. **11**: 55-75.

Jegatheesan, V. and S. Vigneswaran (1997). "Interaction between organic substances and submicron particles in deep bed filtration." Separation and Purification Technology **12**(1): 61-66.

Jin, X., M. H. Li, et al. (2010). "High-Throughput Screening of Silver Nanoparticle Stability and Bacterial Inactivation in Aquatic Media: Influence of Specific Ions." Environmental Science & Technology **44**(19): 7321-7328.

Ju-Nam, Y. and J. R. Lead (2008). "Manufactured nanoparticles: An overview of their chemistry, interactions and potential environmental implications." Science of the Total Environment **400**(1-3): 396-414.

Kamat, P. V. (2002). "Photophysical, photochemical and photocatalytic aspects of metal nanoparticles." Journal of Physical Chemistry B **106**(32): 7729-7744.

Kamat, P. V., M. Flumiani, et al. (1998). "Picosecond dynamics of silver nanoclusters. Photoejection of electrons and fragmentation." Journal of Physical Chemistry B **102**(17): 3123-3128.

Kapoor, S. (1998). "Preparation, characterization, and surface modification of silver particles." Langmuir **14**(5): 1021-1025.

Kim, J. S., E. Kuk, et al. (2007). "Antimicrobial effects of silver nanoparticles." Nanomedicine-Nanotechnology Biology and Medicine **3**(1): 95-101.

Kim, S. K., E. Mendis, et al. (2005). "Investigation of jumbo squid (Dosidicus gigas) skin gelatin peptides for their in vitro antioxidant effects." Life Sciences **77**(17): 2166-2178.

Kirby, G. H., D. J. Harris, et al. (2004). "Poly(acrylic acid)-poly(ethylene oxide) comb polymer effects on BaTiO3 nanoparticle suspension stability." Journal of the American Ceramic Society **87**(2): 181-186.

Kittel, C. and H. Kroemer (1980). Thermal physics. San Francisco, W. H. Freeman.

Klaine, S. J., P. J. J. Alvarez, et al. (2008). "Nanomaterials in the environment: Behavior, fate, bioavailability, and effects." Environmental Toxicology and Chemistry **27**(9): 1825-1851.

Konradi, R. and J. Ruhe (2005). "Interaction of poly(methacrylic acid) brushes with metal ions: Swelling properties." Macromolecules **38**(10): 4345-4354.

Kulovaara, M., S. Metsamuuronen, et al. (1999). "Effects of aquatic humic substances on a hydrophobic ultrafiltration membrane." Chemosphere **38**(15): 3485-3496.

Kumar, R., S. Howdle, et al. (2005). "Polyamide/silver antimicrobials: Effect of filler types on the silver ion release." Journal of Biomedical Materials Research Part B-Applied Biomaterials **75B**(2): 311-319.

Kumar, R. and H. Munstedt (2005). "Silver ion release from antimicrobial polyamide/silver composites." Biomaterials **26**(14): 2081-2088.

Kvitek, L., A. Panacek, et al. (2008). "Effect of surfactants and polymers on stability and antibacterial activity of silver nanoparticles (NPs)." Journal of Physical Chemistry C **112**(15): 5825-5834.

Kvitek, L., M. Vanickova, et al. (2009). "Initial Study on the Toxicity of Silver Nanoparticles (NPs) against Paramecium caudatum." Journal of Physical Chemistry C **113**(11): 4296-4300.

Lecoanet, H. F., J. Y. Bottero, et al. (2004). "Laboratory assessment of the mobility of nanomaterials in porous media." Environmental Science & Technology **38**(19): 5164-5169.

Lecoanet, H. F. and M. R. Wiesner (2004). "Velocity effects on fullerene and oxide nanoparticle deposition in porous media." Environmental Science & Technology **38**(16): 4377-4382.

Lee, D. Y., C. Fortin, et al. (2004). "Influence of chloride on silver uptake by two green algae, Pseudokirchneriella subcapitata and Chlorella pyrenoidosa." Environmental Toxicology and Chemistry **23**(4): 1012-1018.

Lee, H. Y., H. K. Park, et al. (2007). "A practical procedure for producing silver nanocoated fabric and its antibacterial evaluation for biomedical applications." Chemical Communications(28): 2959-2961.

Lenhart, J. J., R. Heyler, et al. (2010). "The influence of dicarboxylic acid structure on the stability of colloidal hematite." Journal of Colloid and Interface Science **345**(2): 556-560.

Li, Q. L. and Y. S. Hwang (2010). "Characterizing Photochemical Transformation of Aqueous nC(60) under Environmentally Relevant Conditions." Environmental Science & Technology **44**(8): 3008-3013.

Li, Q. L., B. Xie, et al. (2009). "Kinetics of C(60) Fullerene Dispersion in Water Enhanced by Natural Organic Matter and Sunlight." Environmental Science & Technology **43**(10): 3574-3579.

Li, X. A., J. J. Lenhart, et al. (2010). "Dissolution-Accompanied Aggregation Kinetics of Silver Nanoparticles." Langmuir **26**(22): 16690-16698.

Li, X. A., J. J. Lenhart, et al. (2011). "Aggregation Kinetics and Dissolution of Coated Silver Nanoparticles." Langmuir (In Press).

Liau, S. Y., D. C. Read, et al. (1997). "Interaction of silver nitrate with readily identifiable groups: relationship to the antibacterial action of silver ions." Letters in Applied Microbiology **25**(4): 279-283.

Linnert, T., P. Mulvaney, et al. (1991). "Photochemistry of Collodial Silver Particles – The Effects of N2O and Adsorbed CN-." Berichte der Bunsen-Gesellschaft-Physical Chemistry Chemical Physics **95**(7): 838-841.

Linnert, T., P. Mulvaney, et al. (1993). "Surface-Chemistry of Colloidal Silver - Surface-Plasmon Damping by Chemisorbed I-, Sh-, and C6h5s-." Journal of Physical Chemistry **97**(3): 679-682.

Liu, J., Y. W. Cheng, et al. (2011). "Toxicity Reduction of Polymer-Stabilized Silver Nanoparticles by Sunlight." Journal of Physical Chemistry C **115**(11): 4425-4432.

Liu, J. Y. and R. H. Hurt (2010). "Ion Release Kinetics and Particle Persistence in Aqueous Nano-Silver Colloids." Environmental Science & Technology **44**(6): 2169-2175.

Liu, X., M. Wazne, et al. (2011). "Influence of Ca(2+) and Suwannee River Humic Acid on aggregation of silicon nanoparticles in aqueous media." Water Research **45**(1): 105-112.

Lok, C. N., C. M. Ho, et al. (2007). "Silver nanoparticles: partial oxidation and antibacterial activities." Journal of Biological Inorganic Chemistry **12**(4): 527-534.

Mafune, F., J. Kohno, et al. (2000). "Formation and size control of sliver nanoparticles by laser ablation in aqueous solution." Journal of Physical Chemistry B **104**(39): 9111-9117.

Mafune, F., J. Kohno, et al. (2000). "Structure and stability of silver nanoparticles in aqueous solution produced by laser ablation." Journal of Physical Chemistry B **104**(35): 8333-8337.

Maillard, M., P. R. Huang, et al. (2003). "Silver nanodisk growth by surface plasmon enhanced photoreduction of adsorbed [Ag+]." Nano Letters **3**(11): 1611-1615.

Marambio-Jones, C. and E. M. V. Hoek (2010). "A review of the antibacterial effects of silver nanomaterials and potential implications for human health and the environment." Journal of Nanoparticle Research **12**(5): 1531-1551.

Materials, A. S. o. T. (1982). Standard for solar spectral irradiance tables at air mass 1.5 for a 37^0 tilted surface. ASTM Standard E892-82. Philadelphia, PA.

Maynard, A., R. Aitken, et al. (2006). "Safe handling of nanotechnology." NATURE **444**(7117): 267-269.

Merga, G., R. Wilson, et al. (2007). "Redox catalysis on "Naked" silver nanoparticles." Journal of Physical Chemistry C **111**(33): 12220-12226.

Mie, G. (1908). Ann. Phys. **25**: 377.

Morones, J. R., J. L. Elechiguerra, et al. (2005). "The bactericidal effect of silver nanoparticles." Nanotechnology **16**(10): 2346-2353.

Mueller, N. C. and B. Nowack (2008). "Exposure modeling of engineered nanoparticles in the environment." Environmental Science & Technology **42**(12): 4447-4453.

MULVANEY, P., T. LINNERT, et al. (1991). "Surface-Chemistry of Collodial Silver in Aqueous-Solution - Observations on Chemisorption and Reactivity." Journal of Physical Chemistry **95**(20): 7843-7846.

Mylon, S. E., K. L. Chen, et al. (2004). "Influence of natural organic matter and ionic composition on the kinetics and structure of hematite colloid aggregation: Implications to iron depletion in estuaries." Langmuir **20**(21): 9000-9006.

Napper, D. H. (1983). Polymeric stabilization of colloidal dispersions. San Diego ; London, Academic Press.

Navarro, E., F. Piccapietra, et al. (2008). "Toxicity of Silver Nanoparticles to Chlamydomonas reinhardtii." Environmental Science & Technology **42**(23): 8959-8964.

Niemeyer, C. M. (2001). "Nanoparticles, proteins, and nucleic acids: Biotechnology meets materials science." Angewandte Chemie-International Edition **40**(22): 4128-4158.

Nightingale, E. R. (1959). "Phenomenological Theory of Ion Solvation. Effective Radii of Hydrated Ions." The Journal of Physical Chemistry **63**(9): 1381-1387.

Omelia, C. R. (1989). "Particle Particle Interactions in Aquatic Systems." Colloids and Surfaces **39**(1-3): 255-271.

Pal, S., Y. K. Tak, et al. (2007). "Does the antibacterial activity of silver nanoparticles depend on the shape of the nanoparticle? A study of the gram-negative bacterium Escherichia coli." Applied and Environmental Microbiology **73**(6): 1712-1720.

Pal, T., T. K. Sau, et al. (1997). "Reversible formation and dissolution of silver nanoparticles in aqueous surfactant media." Langmuir **13**(6): 1481-1485.

Panacek, A., L. Kvitek, et al. (2006). "Silver colloid nanoparticles: Synthesis, characterization, and their antibacterial activity." Journal of Physical Chemistry B **110**(33): 16248-16253.

Patrito, E. M. and P. Paredes-Olivera (2003). "Adsorption of hydrated hydroxide and hydronium ions on Ag(111). A quantum mechanical investigation." Surface Science **527**(1-3): 149-162.

Pelley, A. J. and N. Tufenkji (2008). "Effect of particle size and natural organic matter on the migration of nano- and microscale latex particles in saturated porous media." Journal of Colloid and Interface Science **321**(1): 74-83.

Phenrat, T., Y. Q. Liu, et al. (2009). "Adsorbed Polyelectrolyte Coatings Decrease Fe-0 Nanoparticle Reactivity with TCE in Water: Conceptual Model and Mechanisms." Environmental Science & Technology **43**(5): 1507-1514.

Phenrat, T., N. Saleh, et al. (2008). "Stabilization of aqueous nanoscale zerovalent iron dispersions by anionic polyelectrolytes: adsorbed anionic polyelectrolyte layer properties and their effect on aggregation and sedimentation." Journal of Nanoparticle Research **10**(5): 795-814.

Pillai, Z. S. and P. V. Kamat (2004). "What factors control the size and shape of silver nanoparticles in the citrate ion reduction method?" Journal of Physical Chemistry B **108**(3): 945-951.

Poole, C. P. and F. J. Owens (2003). Introduction to nanotechnology. Hoboken, NJ, J. Wiley.

Ratte, H. (1999). "Bioaccumulation and toxicity of silver compounds: A review." Environmental Toxicology and Chemistry **18**(1): 89-108.

Romero-Cano, M. S., A. Martin-Rodriguez, et al. (2001). "Electrosteric stabilization of polymer colloids with different functionality." Langmuir **17**(11): 3505-3511.

Rosi, N. L. and C. A. Mirkin (2005). "Nanostructures in Biodiagnostics." Chemical Reviews **105**(4): 1547-1562.

Rotello, V. M. (2004). Nanoparticles : building blocks for nanotechnology. New York, Kluwer Academic/Plenum Publishers.

Saleh, N., H. J. Kim, et al. (2008). "Ionic strength and composition affect the mobility of surface-modified Fe-0 nanoparticles in water-saturated sand columns." Environmental Science & Technology **42**(9): 3349-3355.

Saleh, N., K. Sirk, et al. (2007). "Surface modifications enhance nanoiron transport and NAPL targeting in saturated porous media." Environmental Engineering Science **24**(1): 45-57.

Sarkar, P., D. K. Bhui, et al. (2010). "Aqueous-Phase Synthesis of Silver Nanodiscs and Nanorods in Methyl Cellulose Matrix: Photophysical Study and Simulation of UV-Vis Extinction Spectra Using DDA Method." Nanoscale Research Letters **5**(10): 1611-1618.

Sato, T., S. Kuroda, et al. (1991). "Photochemical Formation of Silver Gold (Ag-Au) Composite Colloids in Solutions Containing Sodium Alginate." Applied Organometallic Chemistry **5**(4): 261-268.

Scheckel, K. G., T. P. Luxton, et al. (2010). "Synchrotron Speciation of Silver and Zinc Oxide Nanoparticles Aged in a Kaolin Suspension." Environmental Science & Technology **44**(4): 1307-1312.

Schmid, G. (2010). Nanoparticles : from theory to application. Weinheim, Wiley-VCH.

Shahverdi, A. R., A. Fakhimi, et al. (2007). "Synthesis and effect of silver nanoparticles on the antibacterial activity of different antibiotics against Staphylococcus aureus and Escherichia coli." Nanomedicine-Nanotechnology Biology and Medicine **3**(2): 168-171.

Shahverdi, A. R., A. Z. Zarchi, A. A. K., et al. (2011). "A sunlight-induced method for rapid biosynthesis of silver nanoparticles using an Andrachnea chordifolia ethanol extract." Applied Physics a-Materials Science & Processing **103**(2): 349-353.

Shrivastava, S., T. Bera, et al. (2007). "Characterization of enhanced antibacterial effects of novel silver nanoparticles." Nanotechnology **18**(22): -.

Smetana, A. B., K. J. Klabunde, et al. (2008). "Biocidal Activity of Nanocrystalline Silver Powders and Particles." Langmuir **24**(14): 7457-7464.

Sondi, I. and B. Salopek-Sondi (2004). "Silver nanoparticles as antimicrobial agent: a case study on E-coli as a model for Gram-negative bacteria." Journal of Colloid and Interface Science **275**(1): 177-182.

Stevenson, F. J. (1994). Humus chemistry : genesis, composition, reactions. New York ; Chichester, Wiley.

Stumm, W. (1997). "Reactivity at the mineral-water interface: Dissolution and inhibition." Colloids and Surfaces a-Physicochemical and Engineering Aspects **120**(1-3): 143-166.

Stumm, W., L. Sigg, et al. (1992). Chemistry of the solid-water interface : processes at the mineral-water and particle-water interface in natural systems. New York, Wiley.

Sukhov, N. L., N. B. Ershov, et al. (1997). "Absorption spectra of large colloidal silver particles in aqueous solution." Russian Chemical Bulletin **46**(1): 197-199.

Swain, C. G. and C. B. Scott (1953). "Quantitative Correlation of Relative Rates. Comparison of Hydroxide Ion with Other Nucleophilic Reagents toward Alkyl Halides, Esters, Epoxides and Acyl Halides1." Journal of the American Chemical Society **75**(1): 141-147.

Sweet, L. and B. Strohm (2006). "Nanotechnology - Life-cycle risk management." Human and Ecological Risk Assessment **12**(3): 528-551.

Teeguarden, J. G., P. M. Hinderliter, et al. (2007). "Particokinetics in vitro: Dosimetry considerations for in vitro nanoparticle toxicity assessments." Toxicological Sciences **95**(2): 300-312.

Tiller, C. L. and C. R. Omelia (1993). "Natural Organic-Matter and Colloidal Stability - Models and Measurements." Colloids and Surfaces a-Physicochemical and Engineering Aspects **73**: 89-102.

Tolaymat, T. M., A. M. El Badawy, et al. (2010). "An evidence-based environmental perspective of manufactured silver nanoparticle in syntheses and applications: A

systematic review and critical appraisal of peer-reviewed scientific papers." Science of the Total Environment **408**(5): 999-1006.

Torigoe, K. and K. Esumi (1993). "Preparation of Bimetallic Ag-Pd Colloids from Silver(I) Bis(Oxalato)Palladate(Ii)." Langmuir **9**(7): 1664-1667.

Tratnyek, P. G., M. M. Scherer, et al. (2001). "Effects of natural organic matter, anthropogenic surfactants, and model quinones on the reduction of contaminants by zero-valent iron." Water Research **35**(18): 4435-4443.

Tripathy, S. K. (2008). "Nanophotothermolysis of poly-(vinyl) alcohol capped silver particles." Nanoscale Research Letters **3**(4): 164-167.

Verwey E. J. W., O. J. T. G. (1948). Theory of the stability of lyophobic colloids. Amsterdam, Elsevier.

Virden, J. W. and J. C. Berg (1992). "The Use of Photon-Correlation Spectroscopy for Estimating the Rate-Constant for Doublet Formation in an Aggregating Colloidal Dispersion." Journal of Colloid and Interface Science **149**(2): 528-535.

Weitz, D. A., J. S. Huang, et al. (1985). "Limits of the Fractal Dimension for Irreversible Kinetic Aggregation of Gold Colloids." Physical Review Letters **54**(13): 1416-1419.

Wiesner, M., G. Lowry, et al. (2006). "Assessing the risks of manufactured nanomaterials." Environmental Science & Technology **40**(14): 4336-4345.

Wiesner, M. R. (2005). Responsible development of nanotechnologies for water and wastewater treatment. 3rd IWA Leading-Edge Conference Water and Wastewater Treatment Technologies, Sapporo, JAPAN.

Wodka, D., E. Bielanska, et al. (2010). "Photocatalytic activity of titanium dioxide modified by silver nanoparticles." ACS Appl Mater Interfaces **2**(7): 1945-1953.

Wood, C. M., R. C. Playle, et al. (1999). "Physiology and modeling of mechanisms of silver uptake and toxicity in fish." Environmental Toxicology and Chemistry **18**(1): 71-83.

Xu, J., A. Dozier, et al. (2005). "Synthesis of nanoscale bimetallic particles in polyelectrolyte membrane matrix for reductive transformation of halogenated organic compounds." Journal of Nanoparticle Research **7**(4-5): 449-467.

Yin, Y. D., Z. Y. Li, et al. (2002). "Synthesis and characterization of stable aqueous dispersions of silver nanoparticles through the Tollens process." Journal of Materials Chemistry **12**(3): 522-527.

Yoon, J., H. J. Park, et al. (2009). "Silver-ion-mediated reactive oxygen species generation affecting bactericidal activity." Water Research **43**(4): 1027-1032.

Yoon, K. Y., J. H. Byeon, et al. (2008). "Antimicrobial Effect of Silver Particles on Bacterial Contamination of Activated Carbon Fibers." Environmental Science & Technology **42**(4): 1251-1255.

Yu, D. G. (2007). "Formation of colloidal silver nanoparticles stabilized by Na+-poly(gamma-glutamic acid)-silver nitrate complex via chemical reduction process." Colloids and Surfaces B-Biointerfaces **59**(2): 171-178.